สารออกฤทธิ์ทางชีวภาพจากผลและรากคนทา *Harrisonia perforata* (Blanco) Merr.

นางสาวศิวัตรา ชูเดช

วิทยานิพนธ์นี้เป็นส่วนหนึ่งของการศึกษาตามหลักสูตรปริญญาวิทยาศาสตรมหาบัณฑิต
สาขาวิชาเคมี ภาควิชาเคมี
คณะวิทยาศาสตร์ จุฬาลงกรณ์มหาวิทยาลัย
ปีการศึกษา 2555

BIOACTIVE COMPOUNDS FROM FRUITS AND ROOTS OF *Harrisonia perforata* (Blanco) Merr.

Miss Siwattra Choodej

A Thesis Submitted in Partial Fulfillment of the Requirements
for the Degree of Master of Science Program in Chemistry
Faculty of Science
Chulalongkorn University
Academic Year 2012

Thesis Title	BIOACTIVE COMPOUNDS FROM FRUITS AND ROOTS OF *Harrisonia perforata* (Blanco) Merr.
By	Miss Siwattra Choodej
Field of study	Chemistry
Thesis Advisor	Assistant Professor Khanitha Pudhom, Ph.D.

Accepted by the Faculty of Science, Chulalongkorn University in Partial Fulfillment of the Requirements for the Master's Degree

……..…....Dean of the Faculty of Science

(Professor Supot Hannongbua, Dr.rer.nat.)

THESIS COMMITTEE

…….……...Chairman

(Assistant Professor Warinthorn Chavasiri, Ph.D.)

…….…….....Thesis Advisor

(Assistant Professor Khanitha Pudhom, Ph.D.)

……Examiner

(Assistant Professor Pattara Sawasdee, Ph.D.)

……External Examiner

(Damrong Sommit, Ph.D.)

ศิวัตรา ชูเดช: สารออกฤทธิ์ทางชีวภาพจากผลและรากคนทา *Harrisonia perforata* (Blanco) Merr. (BIOACTIVE COMPOUNDS FROM FRUITS AND ROOTS OF *Harrisonia perforata* (Blanco) Merr.) อ. ที่ปรึกษาวิทยานิพนธ์หลัก : ผศ.ดร .ขนิษฐา พุดหอม, 88 หน้า.

งานวิจัยนี้ศึกษาการแยกและพิสูจน์ทราบโครงสร้างของสารที่มีฤทธิ์ต้านการอักเสบจากคนทา *Harrisonia perforata* การแยกสารสกัดหยาบเอทิลแอซิเทตของผลและรากคนทาโดยใช้เทคนิคทางโครมาโทรกราฟี พบว่า ได้สารใหม่กลุ่ม chromone 1 ชนิด คือ harperamone (**8**) และลิโมนอยด์ชนิดที่มีการจัดเรียงตัวใหม่อีก 2 ชนิด คือ harperfolide (**2**) และ harperforatin (**4**) รวมทั้งสารที่มีรายงานมาก่อนหน้านี้ 6 ชนิด คือ harrisonin (**1**), obacunone (**3**), (+)-vouacapenic acid (**5**), harrisonol A (**6**), peucenin-7-methyl ether (**7**) และ braylin I (**9**) จากรายงานการวิจัยพบว่า braylin I (**9**) และ (+)-vouacapenic acid (**5**) แยกได้จากพืชสกุล *Harrisonia* เป็นครั้งแรก โครงสร้างทางเคมีของสารใหม่พิสูจน์ทราบด้วยเทคนิคทางสเปกโทรสโกปีและ single-crystal X-ray diffraction ในขณะที่สารที่มีการรายงานก่อนหน้าได้พิสูจน์ทราบโดยเปรียบเทียบข้อมูลจากรายงานวิจัยก่อนหน้านี้ จากนั้นได้นำสารที่แยกได้มาทดสอบฤทธิ์ต้านการอักเสบโดยวัดการยับยั้งการผลิตไนตริกออกไซด์ในเซลล์แมคโครฟาจ J774.A1 ที่ถูกเหนี่ยวนำให้เกิดการอักเสบด้วยลิโปโพลิแซคคาไรด์ (LPS) ผลที่ได้ คือ harperfolide (**2**) แสดงฤทธิ์ยับยั้งการผลิตไนตริกออกไซด์ได้ดีที่สุด โดยมีค่า IC_{50} เท่ากับ 6.51 μM นอกจากนี้ในงานวิจัยนี้ยังได้ศึกษาการยับยั้งการผลิตไนตริกออกไซด์โดยวัดจากการกดการแสดงออกของโปรตีน iNOS ด้วยเทคนิค Western blot จากผลการทดลองพบว่าการทรีทเซลล์แมคโครฟาจ J774.A1 ที่ถูกกระตุ้นด้วย LPS ด้วยสาร (**2**) ส่งผลให้การแสดงออกของโปรตีน iNOS ลดลง แสดงให้เห็นว่า สาร (**2**) สามารถควบคุมการแสดงออกของโปรตีน iNOS ได้ตั้งแต่ระดับการถอดรหัส

สาขาวิชา……..เคมี.....…..... ลายมือชื่อนิสิต……..……..….....

ปีการศึกษา……2555……... ลายมือชื่ออ.ที่ปรึกษาวิทยานิพนธ์หลัก.....

##5372344423: MAJOR CHEMISTRY
KEYWORDS: *Harrisonia perforata* / limonoid / chromone / anti-inflammatory

SIWATTRA CHOODEJ: BIOACTIVE LIMONOIDS FROM SEEDS AND ROOTS OF *Harrisonia perforata* (Blanco) Merr. THESIS ADVISOR: ASST. PROF. KHANITHA PUDHOM, Ph.D., 88 pp.

This research focused on the isolation and identification of anti-inflammatory compounds from *Harrisonia perforata*. Chromatographic fractionation of the EtOAc crude extracts of *H. perforata* fruits and roots led to the isolation of two new rearranged limonoids, harperfolide (**2**) and harperforatin (**4**), and a new chromone, harperamone (**8**), together with six known compounds including harrisonin (**1**), obacunone (**3**), (+)-vouacapenic acid (**5**), harrisonol A (**6**), peucenin-7-methyl ether (**7**) and braylin I (**9**). Among known compounds, a coumarin braylin I (**9**) and a cassane diterpene (+)-vouacapenic acid (**5**) were first isolated from the genus *Harrisonia*. The structures of new compounds were elucidated on the basis of spectroscopic data and single-crystal X-ray diffraction analysis, whereas those of the known ones were identified by comparison of their spectroscopic data with those in the literature. Isolated compounds were assessed for their anti-inflammatory activity by monitoring the inhibition of nitric oxide (NO) production in lipopolysaccharide (LPS)-induced macrophage J774.A1 cell lines. Harperfolide (**2**), a new rearranged limonoid, displayed the most potent anti-inflammatory activity by suppressing nitric oxide production from activated macrophages with IC_{50} value of 6.51 μM. Furthermore, the inhibitory effect of harperfolide (**2**) on NO production via the inhibition of the corresponding iNOS protein expression, was further investigated by Western blot analysis. Pretreatment of the cells with various concentrations of **2** attenuated LPS-induced iNOS protein expression in a concentration-dependent manners. These data suggested harperfolide (**2**) can down regulate LPS-induced iNOS expression at the transcriptional level.

Field of Study :.....Chemistry……... Student's Signature…….....…….....

Academic Year :.……...2012……..… Advisor's Signature.....

ACKNOWLEDGEMENTS

I would like to express my gratitude, Assistant Professor Dr. Khanitha Pudhom, Department of Chemistry, Faculty of Science, Chulalongkorn University, for contributing a great deal to my research.

Moreover I would to thank the Chairperson: Assistant Professor Dr. Warinthorn Chavasiri, Department of Chemistry, Faculty of Science, Chulalongkorn University; the thesis examiners: Assistant Professor Dr. Pattara Sawasdee, Department of Chemistry, Faculty of Science, Chulalongkorn University and Dr. Damrong Sommit, Mahanakorn University of Technology, for their invaluable discussion and suggestion.

I wish to thank The 90th Anniversary of Chulalongkorn University Fund (Ratchadaphiseksomphot Endowment Fund) for granting in partial financial support to conduct this research.

Special thanks to the member of laboratory (1532) for their help and kind friendship.

Finally, I am deeply grateful to my family for their love and encouragement throughout my M.Sc. study.

CONTENTS

Page

LIST OF TABLES

LIST OF FIGURES

Figure **Page**

Figure **Page**

LIST OF SCHEMES

LIST OF ABBREVIATIONS

J	Coupling constant
δ	Chemical shift
δ_H	Chemical shift of proton
δ_C	Chemical shift of carbon
s	Singlet (for NMR spectra)
d	Doublet (for NMR spectra)
dd	Doublet of doublet (for NMR spectra)
t	Triplet (for NMR spectra)
m	Multiplet (for NMR spectra)
q	Quartet (for NMR spectra)
brs	Broad singlet (for NMR spectra)
brd	Broad doublet (for NMR spectra)
calcd.	Calculated
^{1}H NMR	Proton nuclear magnetic resonance
^{13}C NMR	Carbon-13 nuclear magnetic resonance
2D NMR	Two dimensional nuclear magnetic resonance
^{1}H-^{1}H COSY	Homonuclear (proton-proton) correlation spectroscopy
HSQC	Heteronuclear single quantum coherence
HMBC	Heteronuclear multiple bond correlation
ORTEP	Oak ridge thermal ellipsoid plot
HPLC	High performance liquid chromatography
HRESIMS	High resolution electrospray ionization mass spectrometry
CC	Column chromatography
TLC	Thin layer chromatography
IC_{50}	Half maximal inhibitory concentration
$CDCl_3$	Deuterated chloroform
MeOH	Methanol
$CHCl_3$	Chloroform

CH_2Cl_2	Dichloromethane
EtOAc	Ethyl acetate
DMSO	Dimethylsulfoxide
KBr	Potassium bromide
SiO_2	Silicon dioxide
g	Gram (s)
mg	Milligram (s)
mL	Milliliter (s)
μg	Microgram (s)
μL	Microliter (s)
μM	Micromolar
mM	Millimolar
L	Liter (s)
M	Molar
min	Minute
h	Hour
rpm	Round per minute
m	Meter (s)
mm	Millimeter (s)
cm	Centimeter (s)
nm	Nanometer
Hz	Hertz
MHz	Megahertz
cm^{-1}	Reciprocal centimeter (unit of wave number)
ppm	part per million
NMR	Nuclear magnetic resonance
MS	Mass spectrometry
IR	Infared
UV	Ultraviolet
m.p.	Melting point
α	Alpha

β	Beta
m/z	Mass to charge ratio
$[M+H]^+$	Protonated molecule
$[M+Na]^+$	Pseudomolecular ion
$[\alpha]_D^{20}$	Specific rotation at 20 ^oC and sodium D line (589 nm)
λ_{max}	Wavelength of maximum absorption
c	Concentration
ε	Molar extinction coefficient
Å	Angstrom
°C	Degree celcius
deg.	Degree
sp.	Species
No.	Number

CHAPTER I

INTRODUCTION

1.1 Thai natural products as leads for drug candidates

Natural products still play a crucial role for drug discovery and development. They often provide lead compounds or structures which can further be developed to be a real drug [1, 2]. In some Asian countries, particularly India, China and Thailand, up to 50% of the population still relies on traditional medicines for their primary health care needs. Medicinal herbs used as folk remedies have attracted considerable attention from natural product and medicinal scientists as sources of targeted active substances, since they have been exploited for the treatment of human diseases such a long time ago. In addition, understanding of therapeutic benefits deepens and demands for natural products increase, previously accidental discoveries thus evolve into active searches for new medicines.

To look for drug candidates, it is important to realize the methods and rationale utilized to provide the best opportunities to obtain the natural sources that can produce the interesting metabolites. One is the screening of extracts of those sources for the presence of new compounds and an investigation of their targeted activity. Interestingly, selection of plants or natural sources is also a principle role, and one of them is plants growing in areas of great biodiversity, for example, in tropical area. Therefore Thai medicinal plants should be a great home of drug leads, since Thailand is located near the equator and the climate is generally hot and humid. Experiences and successes of Thai scientists in this specialized area have resulted in a number of widely commercial drugs, although not in single-drug form; however, their active principles have been identified. The most popular ones are *Andrographis paniculata* and *Curcuma longa* capsules (Figure 1.1) for curing fever and indigestion, respectively.

(a) (b)

Figure 1.1 Thai medicinal plant drugs: (a) *Andrographis paniculata* capsules (b) *Curcuma longa* capsules (Image from: http://www.gpoproduct.com/tabid/39/language/th-TH/Default.aspx) (Site on November 25, 2012)

1.2 Plants in the genus *Harrisonia*

Among the medicinal plants available in Thailand, plant in the genus *Harrisonia* (family Simaroubaceae) is one of the most widely used herbs in traditional Thai medicines. The genus *Harrisonia* comprises three species including *H. perforata*, *H. brownii* and *H. abyssinica* (Oliv.). However, *H. perforata* (Blanco) Merr. or Khonthaa in Thai is the only species of this genus growing in Thailand, and is applied in Thai folklore medicine. Its dried root is considered antipyretic and anti-inflammatory, and it is utilized as a remedy for the treatment of wound healing and diarrhea [3].

1.2.1 Botanical characteristics of *Harrisonia perforata*

H. perforata belongs to the family Simaroubaceae. The taxonomic classification of this plant is shown in Table 1.1.

Table 1.1 Taxonomy of *Harrisonia perforata*

Kingdom	Plantae
Class	Rosopsida
Order	Sapindales
Family	Simaroubaceae
Genus	Harrisonia
Species	H. perforata

H. perforata is a shrub or small tree native to Southeast Asia including Thailand. Its habitat is usually in dry, open localities such as light secondary forest, thickets and forest edges, often on limestone rocks, less common in monsoon forest. It prefers distinctly seasonal conditionals from sea-level up to 700-900 m altitude. *H. perforata* is a scandent to erect prickly shrub up to 4-6 m tall. The leaves pinnate with unpaired terminal leaflet up to 20 cm long, with 1-15 pairs of leaflets supported by a 5-30 mm long stalk. The stipulate thorns are slightly curved backward or downward, increasing in size to 7 mm. Its leaflets are rhomboid to ovate-lance-shaped, 10-20 mm × 5-15 mm, nearly entire to lobed with narrowly winged rachis. Flowers are with a pedicel, small sepal, triangular lobes, petals are lance-shaped, 6-9 mm × 2-4 mm which are red outside and pale red to white inside. The stamens are (8-)10 with anthers 1.5-4.5 mm long, filaments are 7-10 mm long, at the base with an elongated flattened strap-shaped structure which is densely woolly at the margin, disk is cup-shaped, ovary is slightly lobed, styles 5-8 mm long and pubescent. The fruit is a berry, 4-9 mm × 11-15 mm, exocarp of leathery texture, at least 1 mm thick, endocarp hard, without suture. The picture of the parts of *H. perforata* is depicted in Figure 1.2.

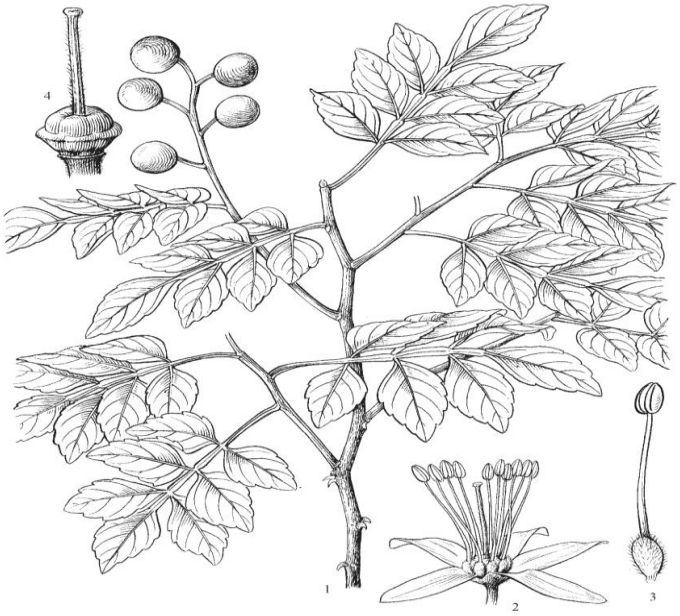

Figure 1.2 Parts of *Harrisonia perforata*: 1) fruiting branch, 2) flower, 3) stamen with scales at base of filament, 4) pistil
(Image from: http://www.efloras.org/object_page.aspx?object_id=109692&flora_id=2) (Site on January 5,2013)

1.2.2 Secondary metabolites of the genus *Harrisonia*

Chemical constituents mainly found in plants in the genus *Harrisonia* were chromones and highly rearranged limonoids. A number of examples are presented here.

In 1994 Ohmoto and co-workers reported the isolation and characterization of two new rearranged limonoids, namely brownins C (**1**) and G (**2**) from the bark and the wood of *H. brownii*, respectively [4].

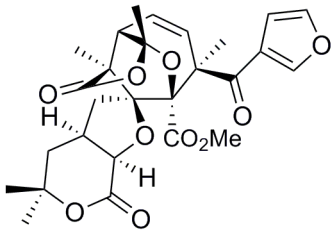

1

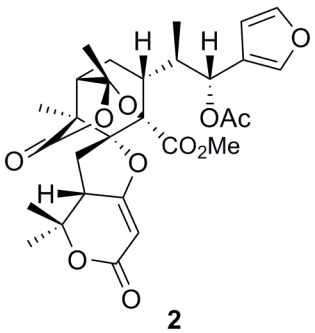

2

In 1995 Koike and co-workers described the isolation and structural elucidation of five new chromones, perforatins C-G (**3**-**7**), along with six known derivatives (**8**-**13**), from the wood of *H. perforata* collected in Hainan, China [5].

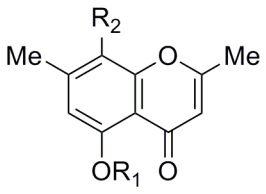

	R_1	R_2
3	H	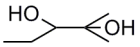
4	Me	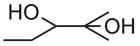
5	Me	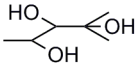
6	Me	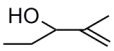
8	H	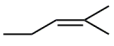
9	Me	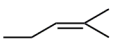

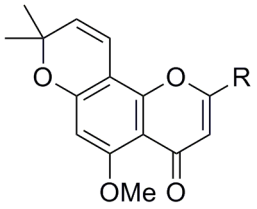

	R
7	CH_2O-β-D-glc
10	CH_2OH
11	Me
12	COOH
13	COOMe

In addition, a number of chromones from the branches of *H. perforata* collected in Thailand were reported in the next year by Tuntiwachwuttikul and co-workers [6]. Four new chromones namely perforamones A-D (**14**-**17**), together with six known analogs (**18**-**23**), were isolated and identified. All isolated compounds were tested for their antiplasmodial and antimycobacterial activities. Only compound **21** showed good activity on antiplasmodial assay with an EC_{50} value of 10.5 μg/mL, while most of them exhibited antimycobacterial activity with MIC values ranging from 25-200 μg/mL.

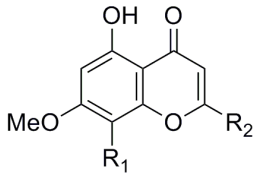

	R_1	R_2
14		Me
15		Me
16		Me
18	H	Me
19	H	CH_2OH

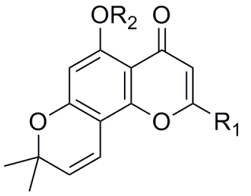

	R_1	R_2
17	H	CH_2OH
20	COOH	Me
21	Me	Me

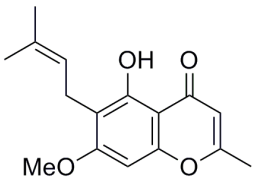

22

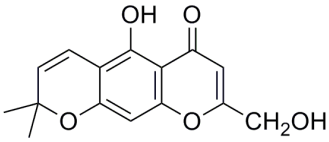

23

In 1997 Fischer and co-workers have revised the structures of two known limonoids, harrisonin (**24b**) and 12β-acetoxyharrisonin (**25b**), from the root of *H. abyssinica*, which have been previously reported as **24a** and **24b**, respectively [7]. Structure revision of these limonoids was peformed by reanalysis with modern 1D- and 2D-NMR spectroscopic methods and, in addition, by single crystal X-ray diffraction for the latter one [8].

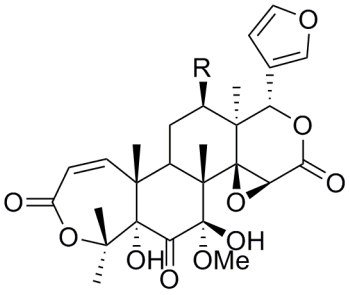

R

24a H

25a OAc

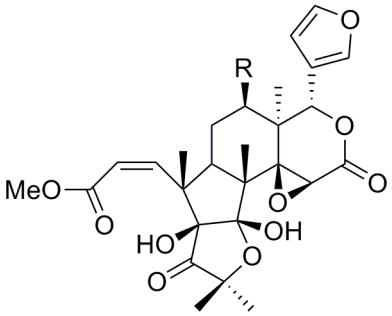

R

24b H

25b OAc

In 2001 Khuong-Huu and co-workers described the isolation and identification of three new rearranged limonoids, haperforins C2 (**26**), F (**27**) and G (**28**), from *H. perforata* leaves collected in Central Vietnam. Their structures were mainly determined by analysis of single-crystal X-ray diffraction data [9].

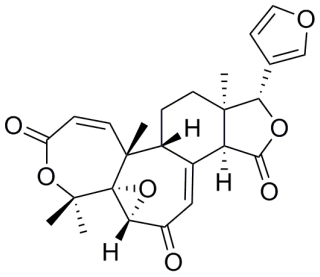

26

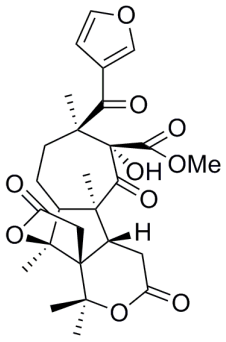

27

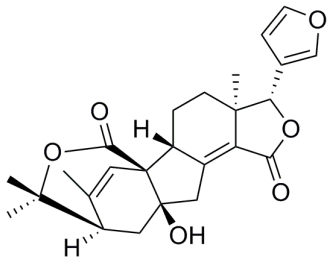

28

In 2011 chemical constituents of fruits of *H. perforata* was first studied by Hao and co-workers. Plant samples were collected from Hainan, China. This study has led to the isolation and characterization of three new limonoids with highly rearranged A, B and D-*seco*-16-nor skeletons (**29**-**31**). Isolated limonoids were tested for their cytotoxicity toward human leukaemia (HL-60) and lung adenocarcinoma (A-549) cell lines. Only limonoid **30** exhibited weak activity with inhibition rates of 63.6 and 64.9%, respectively, whereas the other compounds were shown to be inactive [10].

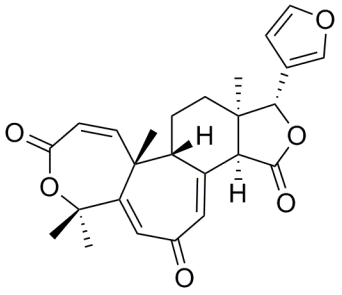

29

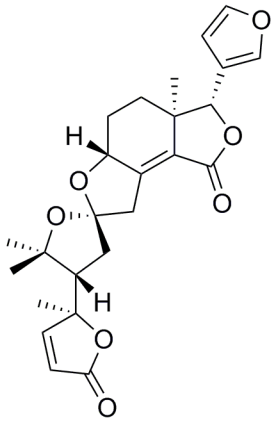

30

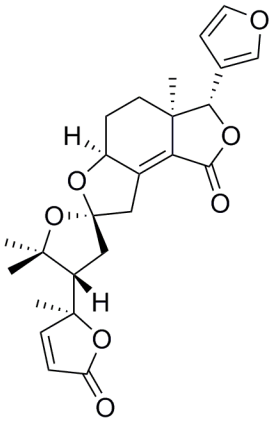

31

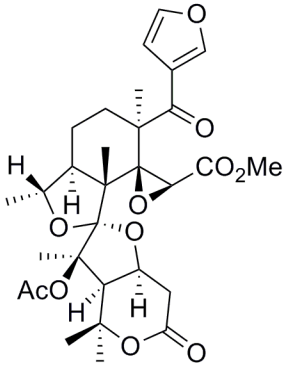

32

In the year 2000, Païs and co-worker have also reported the isolation and identification of a new rearranged limoniod with D-ring cleavage, foritin (**32**), from *H. perforata* bark, collected in Hanoi, Vietnam [11].

1.3 Aim and scope of the present study

As presented above, secondary metabolites isolated from various parts of *H. perforata*, mostly collected in China and Southeast Asia, have considerably attracted attention from natural product researchers, including our group. This is because of the unique structures of rearranged limonoids found in this plant. Study of *H. perforata* chemical constituents collected in Thailand, was performed only by one research group, Tuntiwachwuttikul and co-workers, and only one report has been internationally published; however, only chromone derivatives, no any limonoids, have been isolated [6]. Most importantly, the anti-inflammatory activity of its

metabolites has not been studied yet, although *H. perforata* is utilized in traditional medicine for wound healing treatment and considered anti-inflammatory. In the present study, based on its application in folklore medicine, the isolation and characterization of the constituents of *H. perforata* found in Thailand would thus be performed, and anti-inflammatory agents would further be identified.

The objectives of this research could be divided into the following three parts as follows:

1. To extract, isolate and purify the chemical constituents of *H. perforata* fruits and roots collected in Sukhothai and Nakornsawan province, respectively.

2. To elucidate the structures of the isolated compounds from *H. perforata* fruits and roots by spectroscopic techniques.

3. To evaluate the anti-inflammatory activity of the isolated metabolites using nitric oxide inhibitory assay.

CHAPTER II

EXPERIMENTAL

2.1 Plant materials

Fruits of *H. perforata* were collected from Si Satchanalai, Sukhothai Province, Thailand in April 2010, while its roots were obtained from Takhli, Nakhonsawan Province, Thailand in August 2010 and March 2012, respectively. Plant materials were identified by Royal Forest Department, Bangkok, Thailand.

2.2 General experimental Procedures

2.2.1 Fourier transform infrared spectrophotometer (FT-IR)

The FT-IR spectra were measured with a Perkin-Elmer Model 1760X Fourier Transform Infrared Spectrophotometer. Solid samples were formally examined by incorporating the sample with potassium bromide (KBr) to form a pellet.

2.2.2 Mass spectrometer (MS)

HRESIMS spectra were obtained with a Bruker micrOTOF.

2.2.3 Melting point

Melting points were recorded on a Fisher-Johns melting point apparatus.

2.2.4 Nuclear magnetic resonance spectrometer (NMR)

The NMR spectra were recorded in chloroform-*d* ($CDCl_3$) and acetone-d_6 ($(CD_3)_2CO$) on a Bruker AV400 and Varain Mecury 400 plus spectrometer at 400 MHz for ^{1}H NMR and at 100 MHz for ^{13}C NMR using TMS (tetramethylsilane) as internal standard.

2.2.5 Optical rotation

Optical rotations were acquired on a Perkin-Elmer 341 polarimeter at 589 nm.

2.2.6 Ultraviolet-visible spectrophotometer (UV-vis)

UV data were recorded in MeOH on a CARY 50 Probe UV-visible spectrophotometer**.**

2.2.7 X-ray diffraction spectrometer

The crystal structure was solved by direct methods and using the SHELXS97 program. Crystallographic data, excluding structure factors, have been deposited at the Cambridge Crystallographic Data Centre.

2.2.8 Microplate spectrophotometer

The absorbance for biological assays was measured with a Biotek PowerWave XS2 microplate spectrophotometer.

2.2.9 CO_2 cell culture incubator

Cells using in present study were cultured in a Panasonic MCO-5AC CO_2 cell culture incubator.

2.2.10 Biosafety cabinet

All biological procedurs including cell passage, biological assays were worked in a biosafety cabinet BIOHAZARD Class II MICROTECH Model V6-T.

2.3 Chemicals

2.3.1 Solvents

All commercial grade solvents, used in this research such as hexane, dichloromethane (CH_2Cl_2), ethyl acetate (EtOAc), acetone and methanol (MeOH), were purified by distillation prior to use.

The deuterated solvents for NMR experiments are chloroform-*d* and acetone-d_6.

2.3.2 Other chemicals

Silica gel 60 No. 7734 and No. 9385 (Merck), and Sephadex LH-20 (Pharmacia) were used for open column chromatography (CC). Silica gel 60 F_{254} (Merck) plates were used for thin layer chromatography (TLC). Spots were detected by ultraviolet light at wavelengths of 254 nm and dipped with $(NH_4)_6Mo_7O_{24}$ and 1% $CeSO_4$ solution in 10% aqueous H_2SO_4 following by heating.

2.4 Extraction and isolation

Dried roots of *H. perforata* were chopped into small pieces and soaked in MeOH for 3 days, three times (4L per each). After filtration, MeOH was evaporated and the residue was subsequently partitioned between H_2O and EtOAc (1:1). The organic layer was concentrated to dryness on a rotary evaporator under reduced pressure to yield EtOAc crude extract. The extraction procedure is shown in Scheme 2.1.

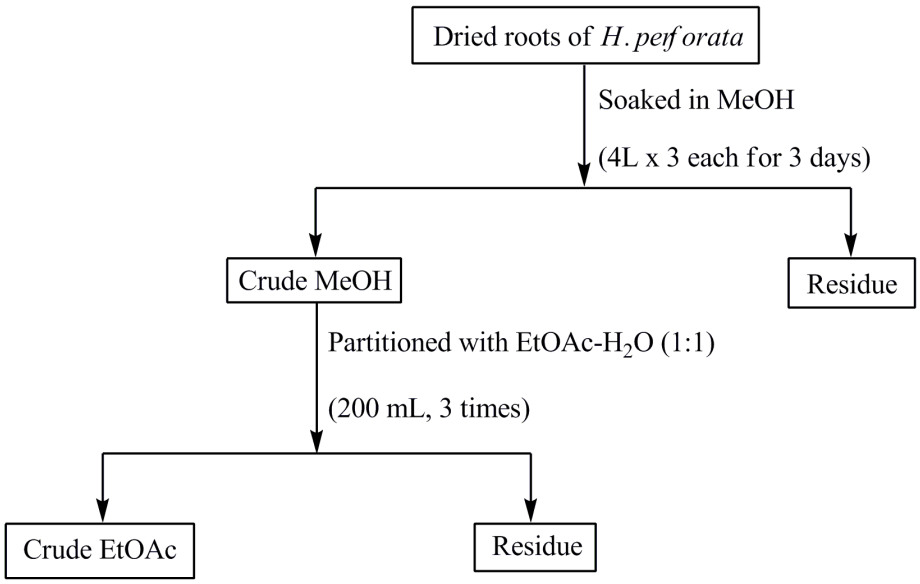

Scheme 2.1 The extraction procedure of *H. perforata* roots. (April 2010)

The EtOAc crude extract (52 g) of roots (2 kg, collected in April 2010) was fractionated by quick column chromatography on a siliga gel column eluted with EtOAc-hexane gradient (10-100%) to yield eight fractions (A-H). Fraction B (4.5 g) was subjected to siliga gel column using acetone-CH_2Cl_2 (5-10%) as eluent to give 10 fractions (B1-10). The fraction B6 (0.15 g) was separated on a siliga gel column eluted with acetone-CH_2Cl_2 (5-10%) to afford seven fractions (B6.1-B6.7), then faction B6.4 (41 mg) was repeatedly chromatographed on a siliga gel column (acetone-hexane, 20%) to give compound **9** (9 mg). The fraction B9 was purified by a column of siliga gel using acetone-hexane (20%) to obtain two limonoids, which were eluted in the order compounds **1** (0.58 g) and **2** (18 mg). The isolation of fraction B is described in Scheme 2.2.

Isolation of the extract of *H. perforata* roots (2 kg) collected in March 2012 is shown in Schemes 2.3 and 2.4. The EtOAc crude extract (100 g) was quickly chromatographed on a column of siliga gel eluted with EtOAc-hexane gradient (10-100%) to yield eight fractions (A-I). Fraction C (1 g) was chromatographed on a siliga gel column eluted with acetone-hexane (30%) and repeatedly purified by the same condition to obtain compound **5** (9.5 mg). Fraction E (3.5 g) was subjected to Sephadex LH-20 column chromatography using MeOH as eluent to give seven fractions (E1-E7). The fraction E5 (0.91 g) was rechromatographed on a Sephadex LH-20 column to afford 10 fractions (E5.1-E5.10). Compound **6** (9.1 mg) was purified by a siliga gel column (MeOH-CH_2Cl_2, 1%) from fraction E5.7 (75 mg). The fraction E5.8 (0.2 g) was subjected to a siliga gel column eluted with acetone-CH_2Cl_2 (5%) to give eight fractions (E5.8.1-E5.8.8). Fraction E5.8.1 (20 mg) provided compound **8** (12 mg) by separating on a siliga gel column using acetone-CH_2Cl_2 (1%). Fraction F was rechromatographed on a Sephadex LH-20 column to give six fractions (F1-F6). Fraction F6.4 (0.38 g) was further subjected to column chromatography on siliga gel (5-7% acetone-CH_2Cl_2) to afford compounds **7** (7.1 mg) and **3** (7 mg) which were recrystallized by MeOH.

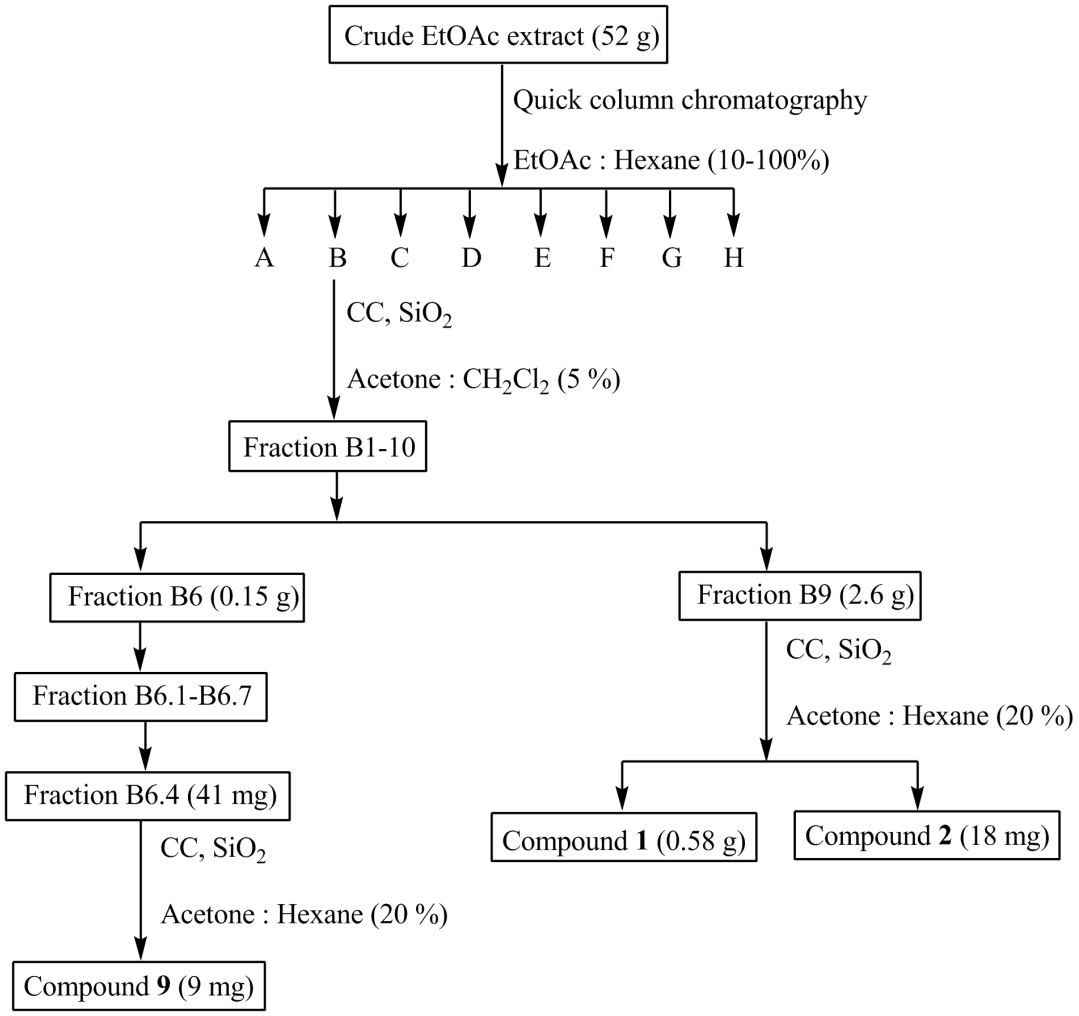

Scheme 2.2 The isolation from fraction B of EtOAc extract of *H. perforata* roots. (collected in April 2010)

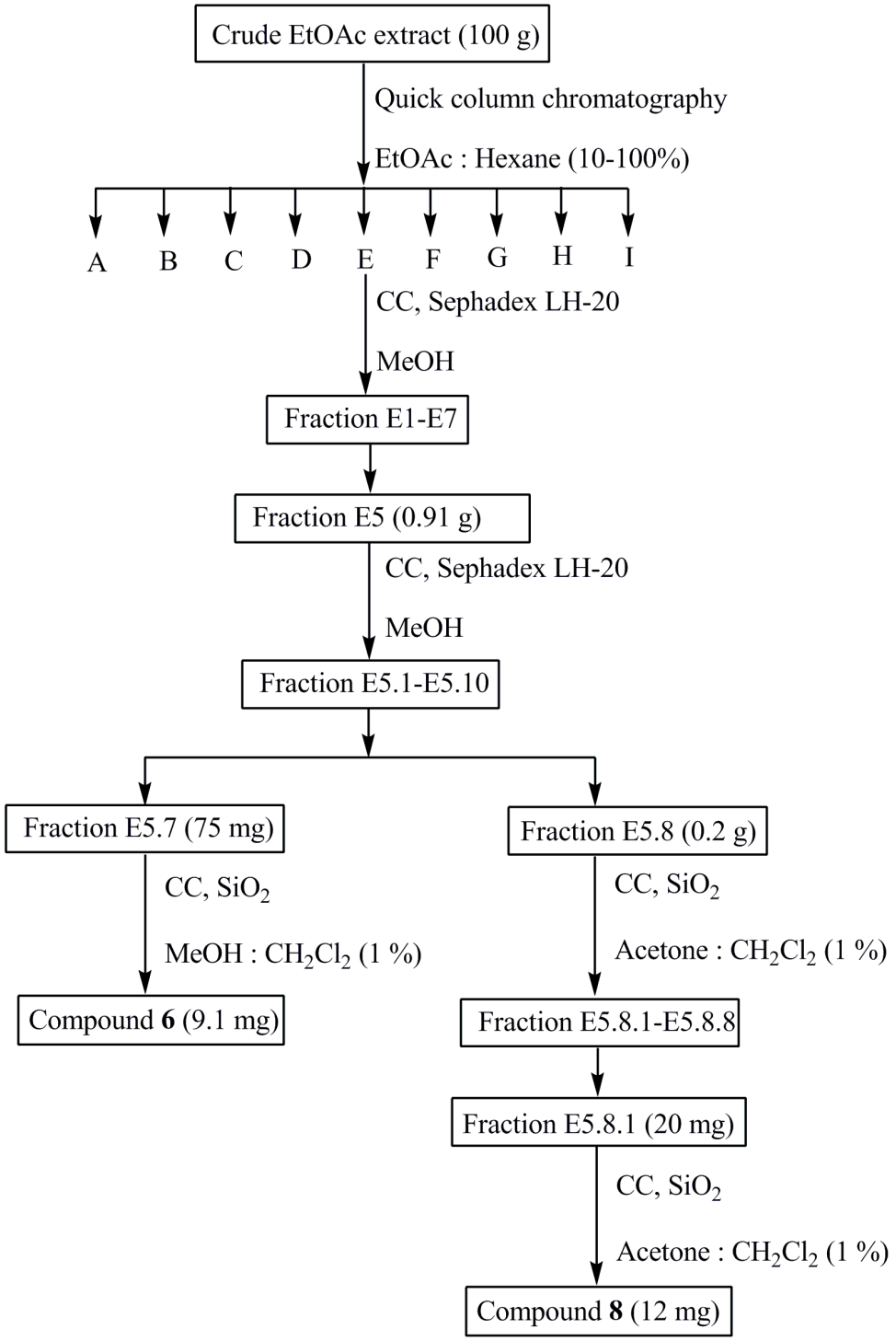

Scheme 2.3 The isolation of EtOAc extract of *H. perforata* roots from fraction E (collected in March 2012).

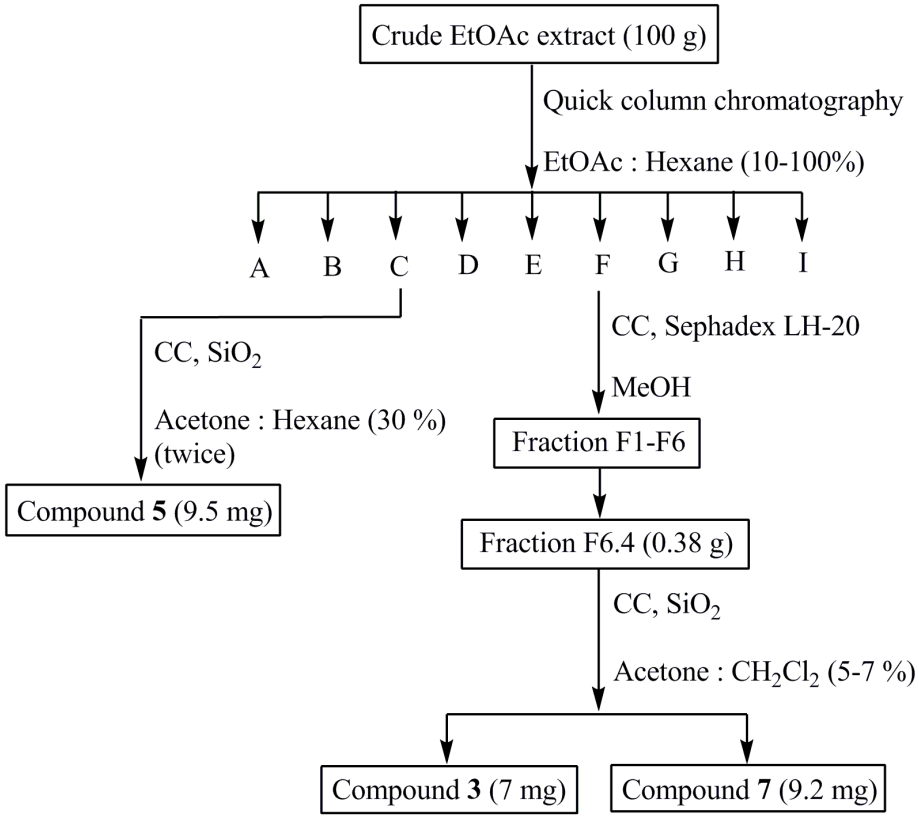

Scheme 2.4 The isolation of EtOAc extract of *H. perforata* roots from fractions C and F (collected in March 2012).

The MeOH residue of dried fruits (2 kg) of the same plant was deffated with hexane before partitioned in H_2O-EtOAc as shown in Scheme 2.5. EtOAc crude extract (177 g) was done with quick chromatography on a siliga gel column eluting with EtOAc-hexane gradient (10-100%) to afford 17 fractions (A-Q). The fraction N (20 g) was separated on a column of siliga gel (10% MeOH-CH_2Cl_2) to give eight fractions (N1-N8), then fraction N1 (0.15 g) was rechromatographed by elution with acetone-CH_2Cl_2 (5%) on siliga gel column and further recrystallized from MeOH to obtain compound **4** (5 mg). The extraction and isolation procedure of *H. perforata* fruits is presented in Scheme 2.5.

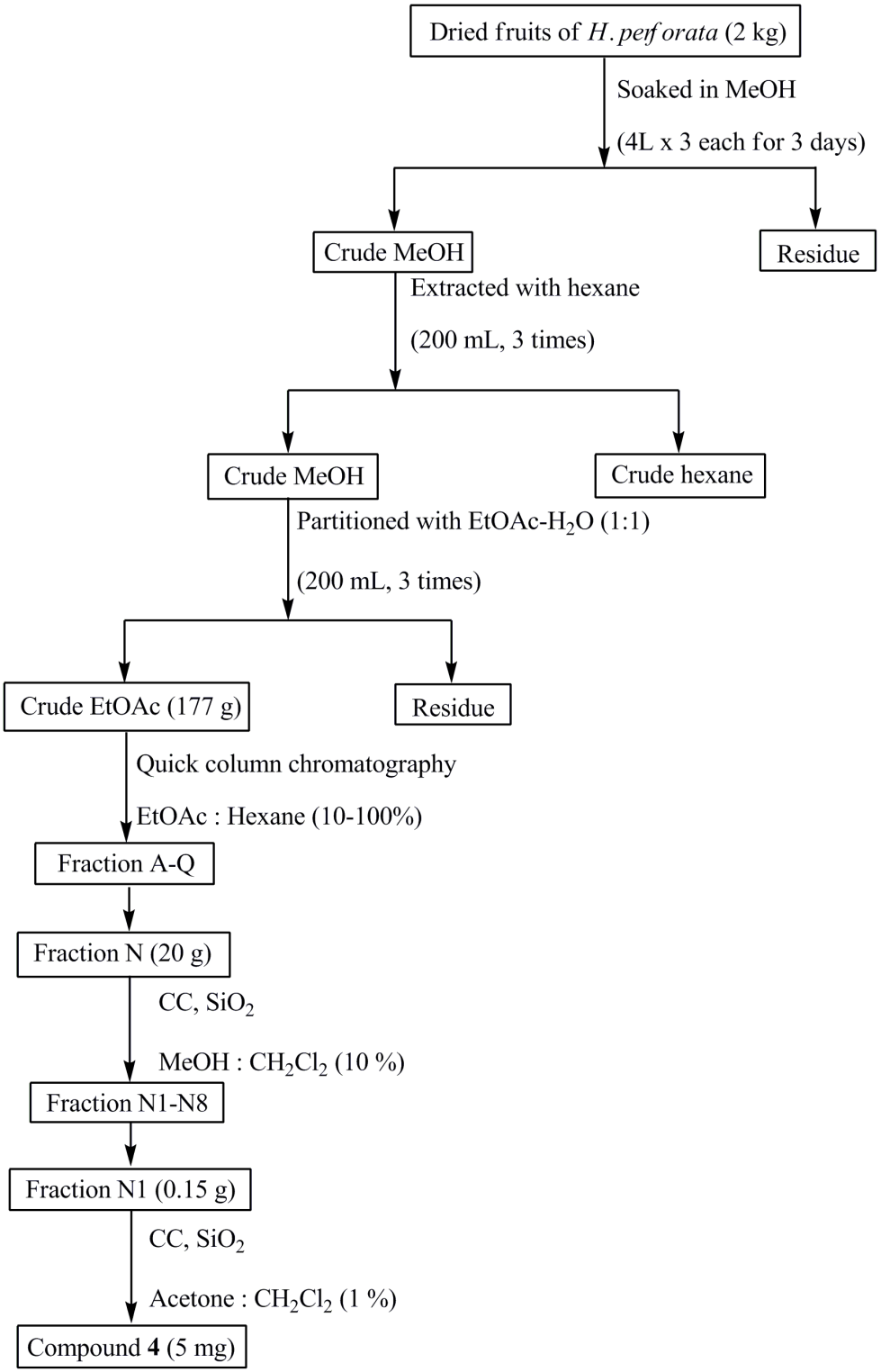

Scheme 2.5 The extraction and isolation procedure of *H. perforata* fruits.

2.5 Biological activity

2.5.1 Nitric oxide inhibitory assay

Murine macrophage J774.A1 cell lines were purchased from Cell Line Service (CLS) and were cultured in Dulbecco's modified Eagle's medium (DMEM) containing 10% heat-inactivated fetal bovine serum (FBS), penicillin G (100 units/mL) and streptomycin (1 μg/mL). The cell lines were seeded in 24-well plates with 1×10^5 cells/well and allow to adhere for 24 h at 37 ^{o}C in a humidified atmosphere with 5% CO_2. The cells were pretreated with various concentrations of test compounds or vehicle (DMSO) for 2 h, and then activated with 1 μg/mL of lipopolysaccharide (LPS) from *Escherichia coli* for 20 h. The culture supernatant (50 μL) of each well was collected and the concentration of nitric oxide (NO) was further measured by using Griess reagent. Those collected supernatants were added 50 μL of 1% sulfanilamide, per well, incubated under the dark condition at room temperature for 10 min. After that 50 μL of 0.1% *N*-1-napthylethylenediamine dihydrochloride (NED) were added incubated under the dark condition for further 10 min. The absorbance was measured at 540 nm with a microplate reader. Nitrite level in the samples was calculated from the standard curve created from known concentrations of sodium nitrite [12].

2.5.2 Cytotoxicity assay

To determine the cell viability of the active compounds, the 3-(4,5-dimethyl-2-thiazolyl)-2,5-diphenyl-*2H*-tetrazolium bromide (MTT) colorimetric method was performed [12]. The cells were seeded in 96-well plate with 1×10^4 cells/well and incubated for 24 h at 37 ^{o}C in a humidified atmosphere containing 5% CO_2. After treatment with samples or vehicle (DMSO) for 24 h, MTT solution (10 μL, 5 mg/mL in phosphate buffer saline (PBS)) was then added to each well and incubated further for 4 h. The medium was removed and DMSO (100 μL/well) was added to dissolve the produced formazan crystals and the absorbance was measured at 540 nm using a microplate reader. Cells treated with only DMSO were used as a positive control.

2.5.3 Western Blot Analysis

After treatment of the cells with the indicated concentrations of harperfolide (**2**) and stimulation with LPS (1 μg/mL) in the same manner as 2.5.1, cells were washed with cold PBS and lysed with M-PER mammalian protein extraction reagent (Pierce, Rockford, IL, USA). Lysates were centrifuged at 5000 rpm for 5 min, and supernatants were collected. Protein concentration was determined using the microBCA protein assay kit (Pierce, Rockford, IL, USA) with bovine serum albumin (BSA) as standard. Thirty micrograms (μg) of protein were separated on sodiumd sulfate-polyacrylamide gel electrophoresis (SDS-PAGE) and transferred to polyvinylidenefluoride (PVDF) membrane. After blocking with 3% skim milk in PBS containing 0.05% Tween 20, the membrane was successively probed with primary antibody (Cell Signaling Technology), with iNOS at 4 ^{o}C overnight and with β-actin for 1 h at room temperature. The signals were detected using the chemiluminescent method [13].

CHAPTER III

RESULTS AND DISCUSSION

3.1 Isolated compounds from the roots and fruits of *H. perforata*

In the present study, the EtOAc crude extracts of the roots and fruits of *H. perforata* were subjected to column chromatography on siliga gel and Sephadex LH-20 leading to the isolation of a new chromone, harperamone (**8**), and two new rearranged limonoids, harperfolide (**2**) and harperforatin (**4**), along with six known compounds classified as limonoid, chromone, coumarin, diterpene and polyketide. These includes harrisonin (**1**), obacunone (**3**), (+)-vouacapenic acid (**5**), harrisonal A (**6**), peucenin-7-methyl ether (**7**) and braylin I (**9**). A coumarin braylin I (**9**) and a diterpene (+)-vouacapenic acid (**5**) were found to be first isolated from the genus *Harrisonia*. Structures of the isolated compounds are presented in Figure 3.1

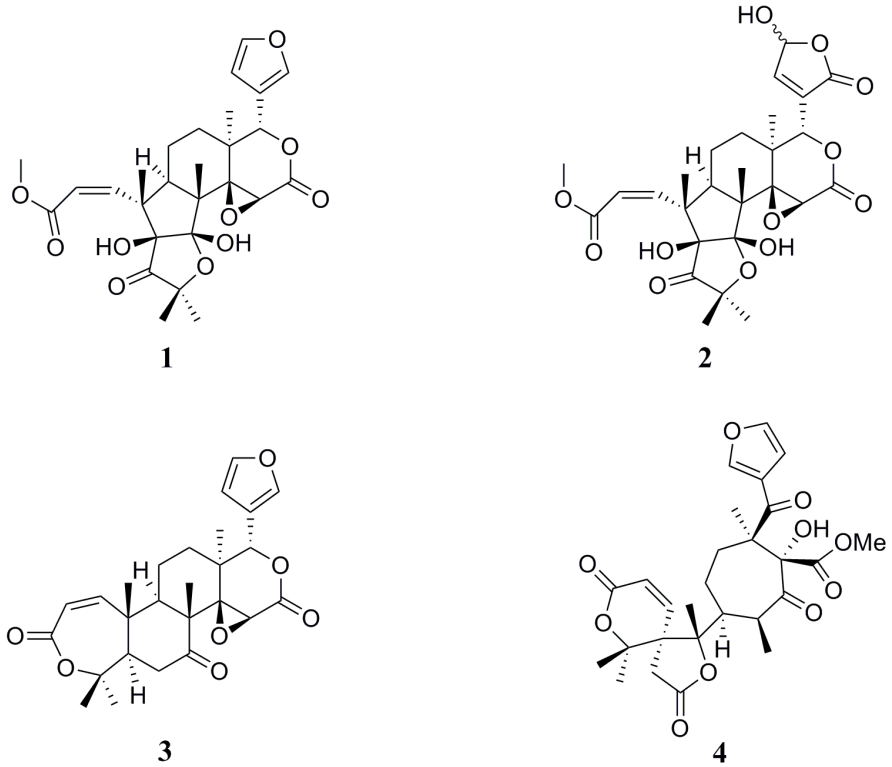

Figure 3.1 The chemical structures of isolated compounds from *H. perforata*

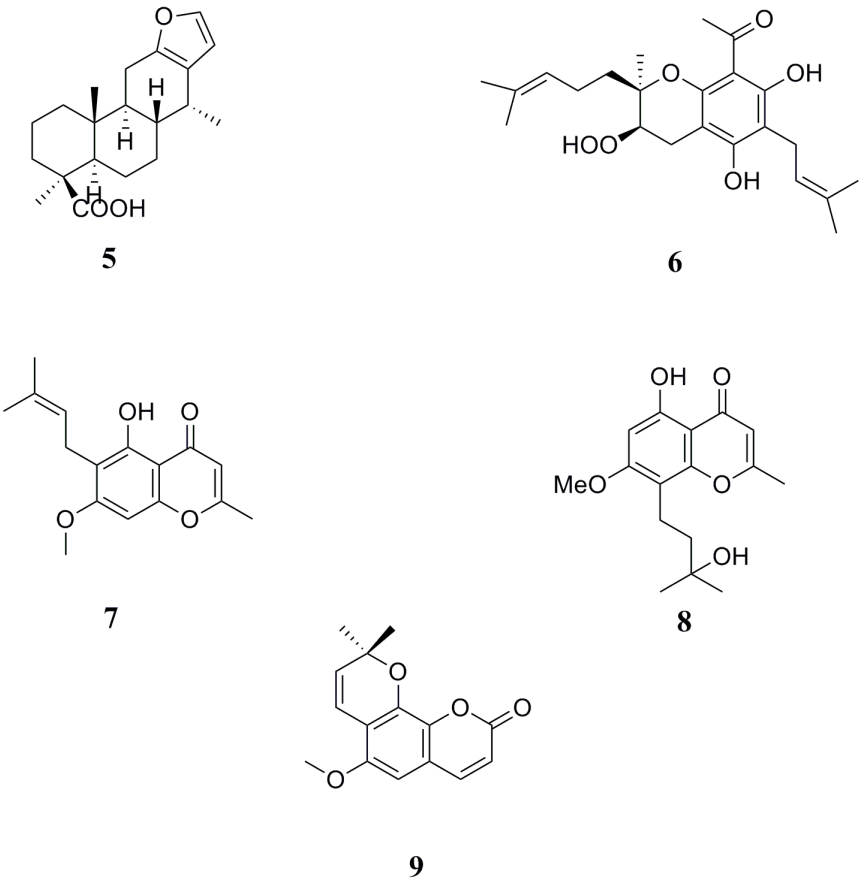

Figure 3.1 The chemical structures of isolated compounds from *H. perforata* (continued)

3.2 Structure elucidation of isolated compounds

3.2.1 Structure elucidation of compound 1

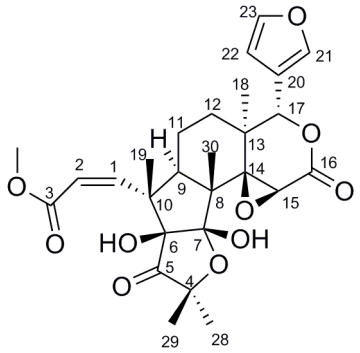

Figure 3.2 Compound **1**

Molecular formula	$C_{27}H_{32}O_{10}$
Appearance	Colorless needles
Melting point	158-160 °C
$[\alpha]_D^{20}$ (c 0.1 , MeOH)	+ 40
UV (MeOH) λ_{max} (log ε)	209 nm (3.76)
IR (KBr)	3443, 2979, 2947, 1739, 1715, 1637, 1435, 1385, 1268, 1208, 1180, 1017 and 875 cm^{-1}
^1H and ^{13}C NMR ($CDCl_3$)	See Table 3.1

Compound **1** was obtained as colorless needles and had the molecular formula $C_{27}H_{32}O_{10}$ based on the NMR data analysis. IR spectrum of **1** showed the typical bands at ν_{max} 3443 cm^{-1} of hydroxyl and a series of carbonyl bands at ν_{max} 1739, 1715 and 1637 cm^{-1}. The ^1H NMR spectrum of **1** displayed signals of five tertiary methyls (δ_H 1.14, 1.17, 1.26, 1.35 and 1.49), a furan ring (δ_H 6.32, 7.39 and 7.41), α,β unsaturated ketone/ester (δ_H 5.76 and 6.00), and a methoxy group (δ_H 3.78). In the ^{13}C NMR spectrum, signals for six olefinic carbons (δ_C 109.8, 120.9, 123.1, 141.1, 142.9 and 153.8), a hemiketal (δ_C 108.2) and epoxide carbons (δ_C 57.3 and 68.5) were observed. Based on the above data, it was suggested that the structure

of **1** was based on a rearranged limonoid, harrisonin, which had a five-membered ring B, Table 3.1 [8]. The structure was further confirmed by 2D NMR data. ^{1}H-^{1}H COSY correlations indicated the presence of –C(9)H–C(11)H_2–C(12)H_2– and –C(1)H=C(2)H– fragments. Observed HMBC correlations including between epoxide ring proton (δ_H 4.27) and quaternary carbons (δ_C 68.5, C-14) and carbonyl ester (δ_C 167.8, C-16), between two methyls (δ_C 1.17, 1.35) and oxygen-bearing carbon (δ_C 88.6, C-4) and ketone (δ_C 216.8, C-5) helped to establish the structure of **1** and to identify as harrisonin as shown in Figure 3.3. On the basis of the literature study, harrisonin has been reported from all three species belonging to the genus *Harrisonia*.

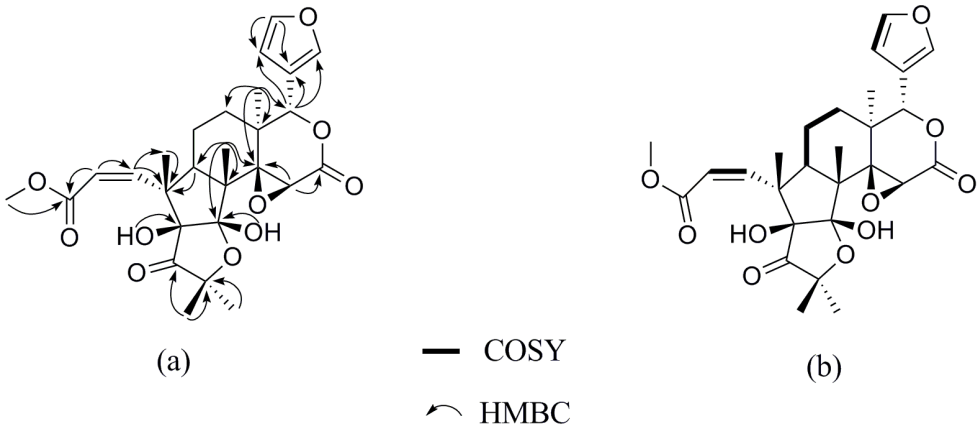

Figure 3.3 HMBC (a) and ^{1}H-^{1}H COSY (b) correlations of compound **1**

Table 3.1 The NMR data of compound **1** and harrisonin ($CDCl_3$)[a]

Position	Harrisonin[b]	Compound **1**[c]	
	δ_C	δ_H (mult, *J* in Hz)	δ_C
1	153.9	6.00 (d, *J* = 12 Hz, 1H)	153.8
2	123.1	5.76 (d, J = 12 Hz, 1H)	123.1
3	166.7		166.6
4	80.9		80.9
5	216.9		216.8
6	88.6		88.6
7	108.2		108.2
8	49.9		49.6
9	46.8	2.99/2.96 (m, 1H)	46.7
10	49.7		49.9
11	15.2	1.80 (m, 2H)	15.1
12	26.3	1.65 (m, 2H)	26.2
13	39.5		39.5
14	68.5		68.5
15	57.3	4.27 (s, 1H)	57.3
16	167.8		167.8
17	78.4	5.66 (s, 1H)	78.4
18	18.3	1.26 (s, 3H)	18.3
19	17.3	1.49 (s, 3H)	17.2
20	121.0		120.9
21	141.1	7.41 (brs, 1H)	141.1
22	109.9	6.32 (brs, 1H)	109.8
23	143.0	7.39 (brs, 1H)	142.9
28	24.1	1.17 (s, 3H)	24.0
29	27.4	1.35 (s, 3H)	27.3
30	14.7	1.14 (s, 3H)	14.6
3-OMe	52.0	3.78 (s, 3H)	52.0
6-OH		5.07 (brs, 1H)	
7-OH		3.68 (brs, 1H)	

[a] Spectra were recorded in $CDCl_3$, [b] 300 MHz, [c] 400 MHz

3.2.2 Structure elucidation of compound 2

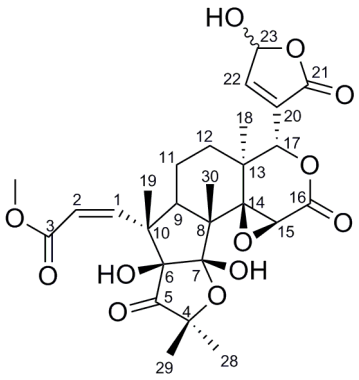

Figure 3.4 Compound **2**

Molecular formula	$C_{27}H_{32}O_{12}$
Appearance	Colorless crystals
Melting point	178-180 °C
$[\alpha]_D^{20}$ (c 0.1 , MeOH)	+ 11
UV (MeOH) λ_{max} (logε)	206 nm (4.21)
IR (KBr)	3454, 2976, 2947, 1764, 1725, 1630, 1438, 1382, 1268, 1208, 1020 and 935 cm^{-1}
^1H and ^{13}C NMR ($CDCl_3$)	See Table 3.2

Compound **2** was isolated as colorless crystals and had the molecular formula as $C_{27}H_{32}O_{12}$ by HR-ESI-MS (*m/z* 547.1886 $[M - H]^-$, Calcd 547.1810). The IR spectrum showed absorption bands at ν_{max} 3454 cm^{-1} for hydroxyl group, and at ν_{max} 1764, 1725 and 1630 cm^{-1} for a series of carbonyl groups. The ^1H NMR and ^{13}C NMR spectra displayed signals of an α,β-unsaturated methyl ester (δ_H 5.77, 6.00/6.01, 3.78 and δ_C 52.1 CH_3, 123.2/123.3 CH, 153.6/153.7 CH, 166.8), a γ-hydroxybutenolide ring (δ_H 6.18/6.22, 7.32/7.34 and δ_C 96.6/97.4, 134.3/134.6, 149.5/150.3, 169.3), and five tertiary methyls (δ_H 1.24/1.25, 1.15, 1.19, 1.24/1.25, 1.37 and δ_C 14.6, 17.3, 17.9, 24.1, 27.4). The existence of an α,β-epoxy-δ-lactone ring was confirmed by HMBC cross peaks from H-17 to both bridgehead carbons

(C-13 and C-14) and the C-16 ester carbonyl, from Me-18 to C-13, C-14 and C-17, and from H-15 to C-14 and C-15 (Figure 3.5). The NMR data of **2** were similar to those of harrisonin (**1**), a known rearranged limonoid isolated from this plant. This indicated they must share the same basic skeleton, except for the presence of a γ-hydroxybutenolide moiety instead of a furanyl ring in **1**. Moreover, observed HMBC correlations from H-17 to C-20, C-21 and C-22 of a butenolide group clarified the location of a γ-hydroxybutenolide at C-17 as shown in Figure 3.5. In addition, the appearance of pairs of most proton and carbon resonances in the NMR spectra of **2** (Table 3.2) suggested the presence of C-23 epimers, the same as those in moluccensin N [14]. Thus the compound **2** was found to be new, named as harperfolide.

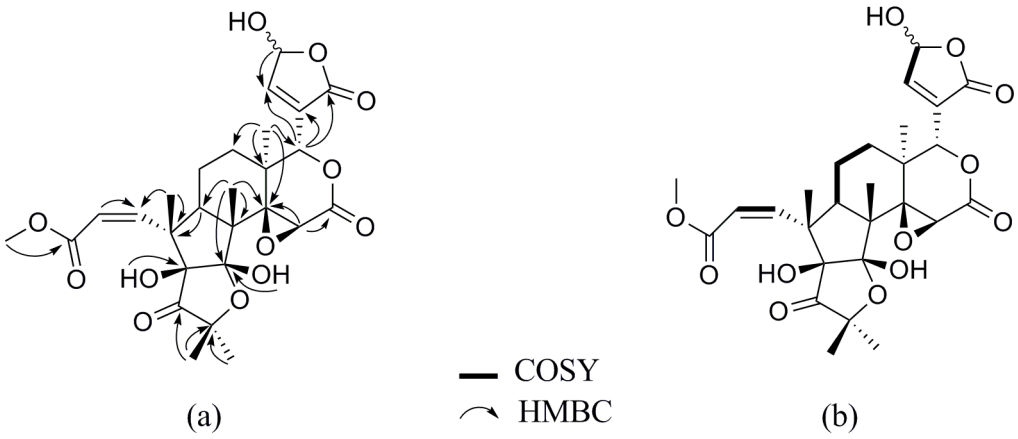

Figure 3.5 HMBC (a) and ^{1}H-^{1}H COSY (b) correlations of compound **2**

Table 3.2 The NMR data of compound **2** ($CDCl_3$, 400 MHz)

postition	δ_H (mult, *J* in Hz)	δ_C
1	6.00 (d, *J* = 12.4 Hz, 1H)	153.6
	6.01 (d, *J* = 12.4 Hz, 1H)	153.7
2	5.77 (d, *J* = 12.4 Hz, 1H)	123.2/123.3
3		166.8
4		81.0
5		216.6
6		88.5
7		108.3
8		49.6
9	2.97 (m, 1H)	46.7
10		50.0
11	1.75 (m, 2H)	15.1
12	1.80 (m, 2H)	25.8/25.9
13		40.1/40.2
14		68.4/68.6
15	4.28 (s, 1H)	57.0
16		167.1/167.6
17	5.59 br s/5.60 br s	76.2/76.6
18	1.24 (s, 3H)/1.25 (s, 3H)	17.9
19	1.50 (s, 3H)/1.51 (s, 3H)	17.3
20		134.6/134.6
21		169.3
22	7.32 (br s, 1H)/7.34 (br s, 1H)	149.5/150.3
23	6.18 (d, *J* = 4.0 Hz, 1H)	96.6
	6.22 (d, *J* = 12.0 Hz, 1H)	97.4
28	1.37 (s, 3H)	27.4
29	1.19 (s, 3H)	24.1
30	1.15 (s, 3H)	14.6
3-OMe	3.78 (s, 3H)	52.1
6-OH	5.10 (s, 1H)	
7-OH	3.64 (s, 1H)	
23-OH	3.66 (s, 1H)	

3.2.3 Structure elucidation of compound 3

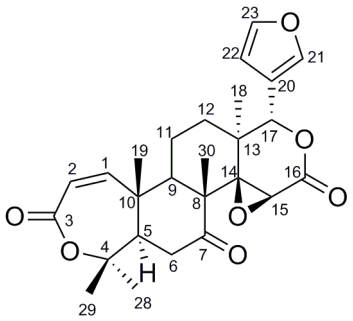

Figure 3.6 Compound **3**

Molecular formula	$C_{26}H_{30}O_7$
Appearance	Colorless crystals
Melting point	226-229 °C
UV (MeOH) λ_{max} (logε)	211 nm (4.11)
IR (KBr)	3447, 2969, 2944, 1739, 1704, 1622, 1452, 1392, 1282, 1165, 1027 and 804 cm^{-1}
^1H and ^{13}C NMR ($CDCl_3$)	See Table 3.3

Compound **3** was obtained as colorless crystals and its molecular formula $C_{26}H_{30}O_7$ was suggested by NMR data. IR and UV spectra showed absorption bands of carbonyls (ν_{max} 1739, 1704 and 1622 cm^{-1}) and β-substituted furan ring (λ_{max} 211 nm). The ^1H NMR spectrum presented typical signals of α,β unsaturated furan ring at δ_H 6.36, 7.39 and 7.41, α,β unsaturated 7-membered ring lactone at δ_H 5.95 and 6.51. These data and ^{13}C NMR spectrum indicated that **3** was a limonoid with five tertiary methyls (δ_C 16.4, 17.0, 21.1, 26.8 and 32.0), and three carbonyl carbons (δ_C 166.6 and 166.9 (lactones), and 207.4 (ketone)). Analysis of ^1H-^1H COSY correlations led to the establishment of four discrete spin systems, –C(9)H–C(11)H_2–C(12)H_2–, –C(5)H–C(6)H_2–, –C(1)H–C(2)H–, and –C(21)H–C(22)H– as shown in Figure 3.7(b). HMBC correlations from an epoxy ring (δ_H 3.65, H–15) to

C-14 and C-16 established the connectivity between an epoxide and a lactone carbonyl. In addition, correlations from H-5 (δ_H 2.59) to C-4 and from H_2-6 (δ_H 2.28 and 2.97) to C-10 resulted in the attachment of ring A to ring B at C-4, and the presence of a ketone at C-10, respectively. Further comparison of its NMR data with those in literature suggested compound **3** was obacunone, a limonoid previously isolated from plants in the genus *Harrisonia* and *Xylocarpus* as shown in Table 3.3 [15]. Moreover, the structure and relative configuration of **3** was subsequently confirmed by single crystal X-ray diffraction analysis as shown in Figure 3.8. In this study, the monoclinic form was obtained and its crystal data are presented in Table 3.4. An orthorhombic form of this compound was also previously reported [16].

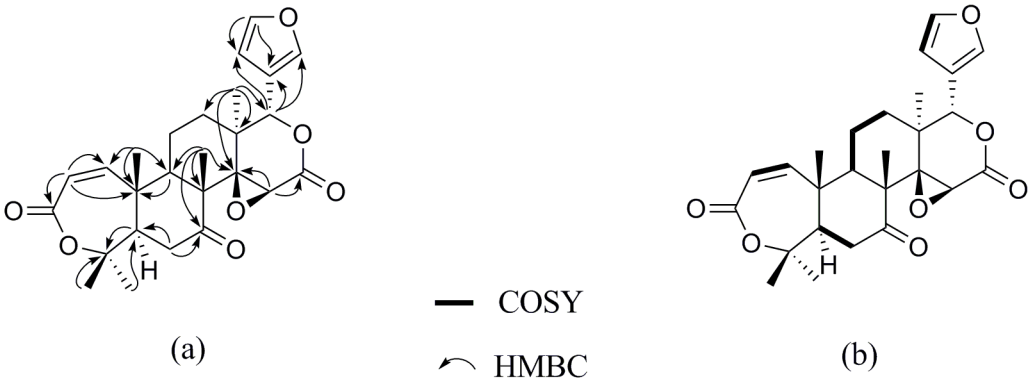

Figure 3.7 HMBC (a) and COSY (b) correlations of compound **3**

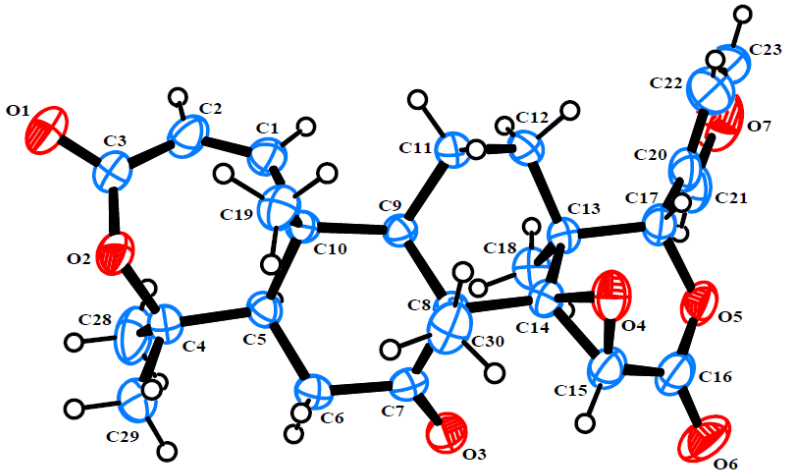

Figure 3.8 ORTEP diagram of compound **3**

Table 3.3 The NMR data of compound **3** ($CDCl_3$, 400 MHz)

Position	Obacunone	Compound **3**	
	δ_C	δ_H (mult, *J* in Hz)	δ_C
1	156.5	6.51 (d, *J* = 11.6 Hz, 1H)	156.7
2	122.4	5.95 (d, J = 11.6 Hz, 1H)	123.0
3	166.3		166.9
4	84.0		80.0
5	57.0	2.59 (m, 1H)	57.4
6	39.7	2.28 (d, *J* = 4.8 Hz, 1H)	39.9
		2.97 (d, *J* = 4.8 Hz, 1H)	
7	207.2		207.4
8	53.1		53.0
9	49.1	2.14 (m, 1H)	49.2
10	43.1		43.1
11	17.1	1.87 (m, 2H)	19.4
12	32.5	1.47 (m, 1H)	32.8
		1.89 (m, 1H)	
13	37.5		37.4
14	65.2		65.0
15	53.3	3.65 (s, 1H)	53.3
16	167.1		166.6
17	78.1	5.45 (s, 1H)	78.0
18	19.2	1.12 (s, 3H)	21.1
19	17.1	1.50 (s, 3H)	16.4
20	120.1		120.1
21	143.2	7.41 (brs, 1H)	141.0
22	109.5	6.36 (brs, 1H)	109.7
23	141.1	7.39 (brs, 1H)	143.2
28	21.1	1.50 (s, 3H)	26.8
29	32.1	1.45 (s, 3H)	32.0
30	26.1	1.24 (s, 3H)	17.0

Table 3.4 Crystal data and structure refinement for compound **3**

Formula	$C_{26}H_{30}O_7$
Molecular weight	454.50
Crystal size (mm)	0.7 × 0.26 × 0.24
Crystal system	monoclinic
Space group	$P2_12_12_1$
***a* (Å)**	7.8244(5)
***b* (Å)**	11.9408(10)
***c* (Å)**	12.5882(11)
***V* (Å^3)**	1172.38(16)
Z	2
D_{calc} **(g/cm^{-3})**	1.287
μ (mm^{-1})	0.093
***F*(000)**	484
Independent reflections/ Observed reflections [I > 4σ(I)], R_{int}	4129/3536, 0.0197
R_1	0.0557
wR_2 **[I > 2σ(I)]**	0.1614

3.2.4 Structure elucidation of compound 4

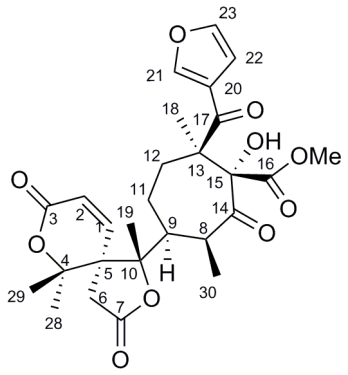

Figure 3.9 Compound **4**

Molecular formula	$C_{27}H_{32}O_{10}$
Appearance	Colorless crystals
Melting point	229-231 °C
$[\alpha]_D^{20}$ (c 0.1 , MeOH)	- 45
UV (MeOH) λ_{max} (logε)	203 nm (4.03)
IR (KBr)	3436, 2944, 2923, 1793, 1746, 1690, 1654, 1392, 1307, 1247, 1105, 1024 and 825 cm^{-1}
^1H and ^{13}C NMR ($CDCl_3$)	See Table 3.4

Compound **4** was obtained as colorless crystals and assigned the molecular formula $C_{27}H_{32}O_{10}$ from its HRESIMS (*m/z* 517.1947 $[M+H]^+$, cald 517.2068). The ^1H NMR spectrum of **4** (Table 3.5) displayed signals attributable to four tertiary methyls (δ_H 1.35, 1.51, 1.57, 1.59), one secondary methyl (δ_H 1.40, d, J = 8.0 Hz), one methoxy (δ_H 3.74), two olefinic protons (δ_H 6.30, 6.63, each d, J = 10.0 Hz), and a β-furanyl ring (δ_H 6.77, 7.40, 8.04, each br s). The ^{13}C NMR (Table 3.5) and HSQC data revealed the presence of five methyls (four tertiary, one secondary), three methylenes, eight methines (six olefinic), five quaternary carbons (three oxygenated), one methoxy, three ester and two ketone carbonyls. On the basis of the above NMR data, compound **4** had a tetracyclic skeleton due to eight units of the 12 unsaturations coming from five carbonyl groups and three carbon-carbon double

bonds. One ketone (δ_C 196.2) was connected to the C-20 of a β-furanyl ring because of the downfield shift of H-22 (δ_H 8.04), and its HMBC correlation with Me-18 (Figure 3.10). The other ketone moiety (δ_C 208.4) was assigned to C-14 by HMBC correlation between Me-30/C-14 and H-8/C-14. Observed HMBC correlations of Me-18/C-12, Me-18/C-13, Me-18/C-15, H-12/C-15 and Me-30/C-14, coupled with the connectivity of the partial structure –CH_2(12)-CH_2(11)-CH(9)-CH(8)Me– by ^{1}H-^{1}H COSY correlations, suggested the existence o of seven-membered ring in **4** (Figure 3.10). In addition, the presence of two lactone rings connecting together through the C-5 spiro carbon were corroborated by HMBC cross peaks between H-1/C-5, Me-28/C-5, Me-29/C-9, H_2-6/C-7, H_2-6/C-10 and Me-19/C-10. This unit was further connected to a seven-membered ring at C-9 by a strong HMBC correlation from Me-19 to C-9. The complete structure and relative configuration of **4** was finally established by single-crystal X-ray diffraction analysis using Mo Kα radiation as shown in Figure 3.11 and its crystal data are presented in Table 3.6. To the best of our knowledge, the structure of **4** possesses a very unique two lactones connecting together through a spiro carbon. The biosynthetic pathway of **4** can plausibly be traced back to harperforin F, a highly rearranged limonoid also previously isolated from *H. perforata* [9]. Compound **4** might be a parent compound of harperforin F *via* Michael addition of C8 enolate to α,β-unsaturated ketone at C1 position as shown in Fig. 3.12.

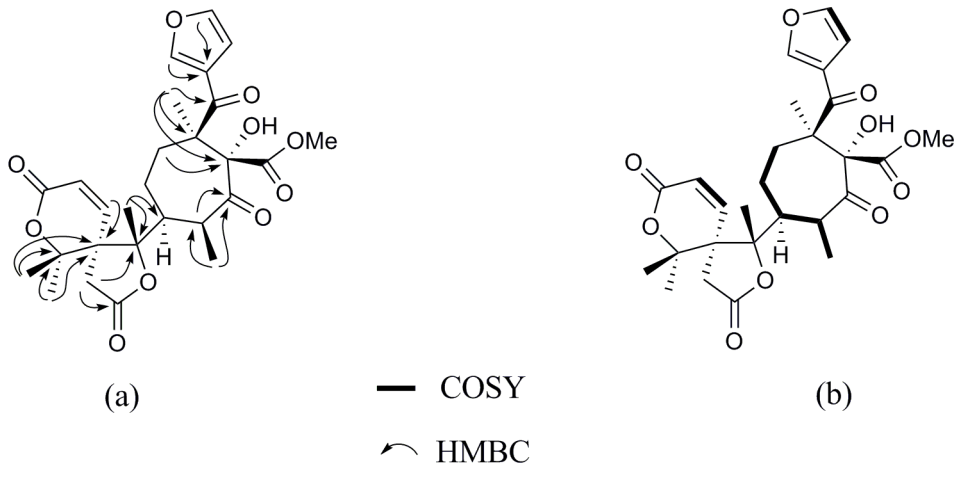

Figure 3.10 HMBC (a) and COSY (b) correlations of compound **4**

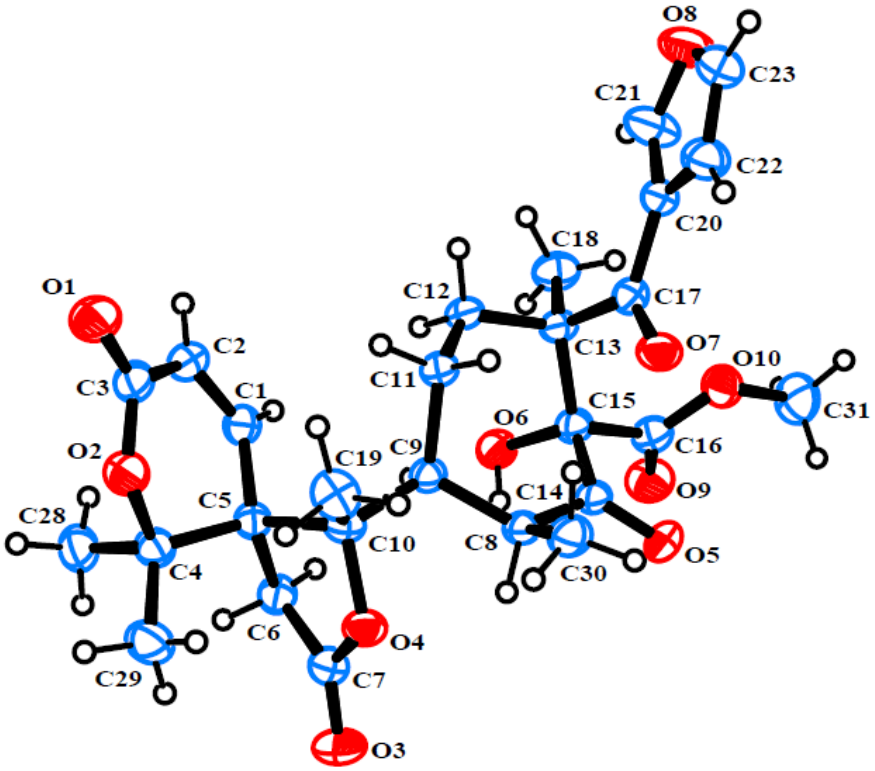

Figure 3.11 ORTEP diagram of compound **4**

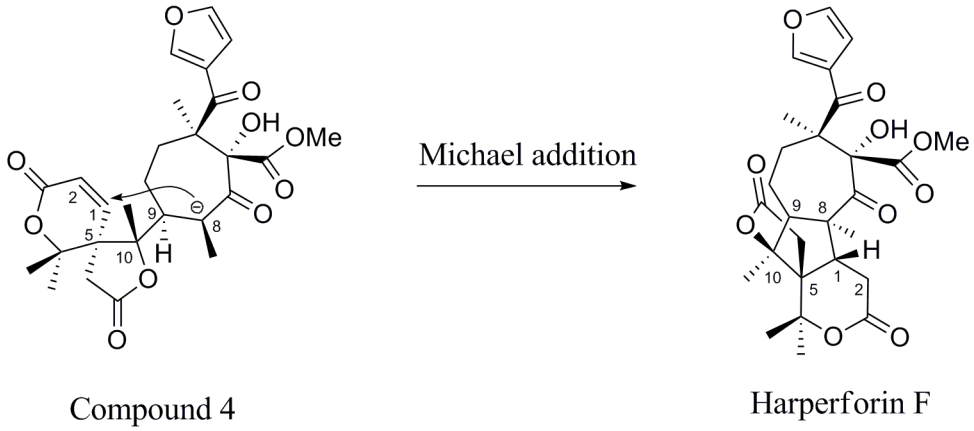

Figure 3.12 Proposed biosynthetic pathway between compound **4** and harperforin F

Table 3.5 The NMR data of compound **4** ($CDCl_3$, 400 MHz)

position	δ_H (mult, *J* in Hz)	δ_C
1	6.63 (d, *J* = 10.0 Hz, 1H)	146.9
2	6.30 (d, *J* = 10.0 Hz, 1H)	123.1
3		162.3
4		83.7
5		54.6
6	2.78 (d, *J* = 16.0 Hz, 1H)	38.4
	2.60 (d, *J* = 16.0 Hz, 1H)	
7		171.7
8	3.12 (m, 1H)	47.7
9	2.35 (m, 1H)	45.5
10		95.4
11	1.80 (m, 1H)	24.3
	1.62 (m, 1H)	
12	1.96 (m, 1H)	34.3
	2.02 (m, 1H)	
13		55.5
14		208.4
15		87.6
16		171.6
17		196.2
18	1.35 (s, 3H)	20.5
19	1.57 (s, 3H)	19.0
20		125.2
21	7.40 (br s, 1H)	143.1
22	8.04 (br s, 1H)	146.4
23	6.77 (br s, 1H)	110.6
28	1.59 (s, 3H)	25.6
29	1.51 (s, 3H)	28.8
30	1.40 (d, *J* = 8.0 Hz, 3H)	22.0
16-OMe	3.74 (s, 3H)	53.4

Table 3.6 Crystal data and structure refinement for compound **4**

Formula	$C_{27}H_{32}O_{10}$
Molecular weight	516.53
Crystal size (mm)	0.45 × 0.24 × 0.12
Crystal system	prism
Space group	$P2_12_12_1$
***a* (Å)**	8.3954(9)
***b* (Å)**	10.9498(11)
***c* (Å)**	14.3710(12)
***V* (Å^3)**	1266.8(2)
Z	2
D_{calc} **(g/cm^{-3})**	1.354
μ (mm^{-1})	0.103
***F*(000)**	548
Independent reflections/ Observed reflections [I > 4σ(I)], R_{int}	4185/3768, 0.0194
R_1	0.0319
wR_2 **[I > 2σ(I)]**	0.0793

3.2.5 Structure elucidation of compound 5

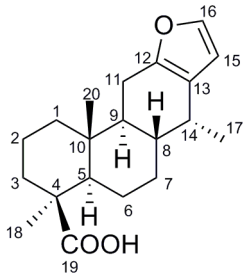

Figure 3.13 Compound **5**

Molecular formula	$C_{20}H_{28}O_3$
Appearance	pale yellow solid
Melting point	227-230 °C
UV (MeOH) λ_{max} (logε)	203 (3.68), 250 (3.27) and 355 nm (2.63)
IR (KBr)	3433, 2926, 2862, 1690, 1455, 1442, 1385, 1275 and 1013 cm^{-1}
^1H and ^{13}C NMR ($CDCl_3$)	See Table 3.7

Compound **5** was obtained as a pale yellow solid and established the molecular formula $C_{20}H_{28}O_3$ from NMR data analysis, suggesting seven degrees of unsaturation. Broad IR absorption at ν_{max} 3428 cm^{-1}, combined with absorption band at 1694 cm^{-1}, indicated the existence of a carboxylic acid group in the molecule. The ^1H and ^{13}C NMR spectra showed signals for a pair of aromatic protons (δ_H 6.18 and 7.22) and four carbon-carbon double bonds (δ_C 109.5, 122.5, 140.4 and 149.4), indicating the presence of a 2,3-disubstituted furan ring. Thus three remaining DBEs indicated that compound **5** had a tricarbocyclic skeleton. These features suggested that **5** was a cassane furanoditerpenoid. Doublet protons of a secondary methyl (δ_H 0.98, δ_C 17.6), showing HMBC correlations to C-8, C-13 and C-14, were assigned to Me-17. Singlet protons of a tertiary methyl (δ_H 1.24, δ_C 16.8), exhibiting HMBC correlations to C-3, C-4 and C-5, were identified as Me-18, while those of another tertiary methyl (δ_H 0.94, δ_C 14.6), showing HMBC correlations to C-1, C-5,

C-9 and C-10, were assigned to Me-20. The location of the carboxylic acid at C-19 was deduced from HMBC cross peak from Me-18 to a carboxyl carbon at δ_C 184.8. Based on the above data and 2D information (^{1}H-^{1}H COSY, HSQC and HMBC) studies could be concluded that compound **5** was (+)-vouacapenic acid. Comparison of its NMR data with those previously reported was also presented in Table 3.7, [17]. This is the first report for the isolation of (+)-vouacapenic acid from *Harrisonia* plant.

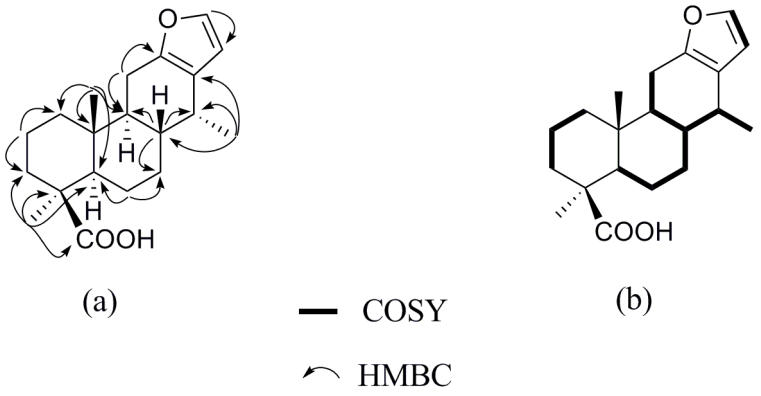

Figure 3.14 HMBC (a) and COSY (b) correlations of compound **5**

Table 3.7 The NMR data of compound **5** and (+)-vouacapenic acid

Position	(+)-vouacapenic acid[a]	Compound **5**[b]	
	δ_C	δ_H (mult, *J* in Hz)	δ_C
1	40.2	1.13 (m, 1H)	38.6
		1.74 (m, 1H)	
2	19.8	1.61 (m, 2H)	17.8
3	38.1	1.66 (m, 1H)	36.9
		1.78 (m, 1H)	
4	44.4		47.2
5	56.8	1.80 (m, 1H)	49.3
6	23.5	1.34 (m, 1H)	24.1
		1.51 (m, 1H)	
7	32.3	1.48 (m, 1H)	30.8
		1.66 (m, 1H)	
8	36.2	1.78 (m, 1H)	35.7
9	45.5	1.58 (m, 1H)	45.8
10	38.5		36.8
11	22.9	2.38 (m, 1H)	22.0
		2.57 (m, 1H)	
12	150.1		149.4
13	122.7		122.5
14	32.0	2.60 (m, 1H)	31.5
15	110.0	6.18 (d, *J* = 4.0 Hz, 1H)	109.5
16	140.8	7.22 (br s, 1H)	140.4
17	18.0	0.98 (d, *J* = 7.2 Hz, 3H)	17.6
18	29.6	1.24 (s, 3H)	16.8
19	185.0		184.8
20	13.9	0.94 (s, 3H)	14.6

[a] Spectra were recorded in $CDCl_3$, 500 MHz, [b] 400 MHz

3.2.6 Structure elucidation of compound 6

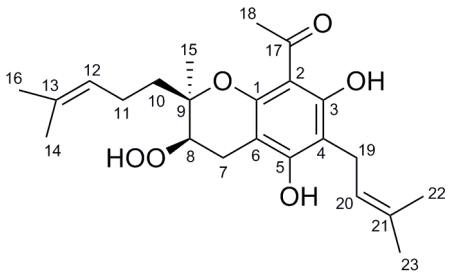

Figure 3.15 Compound **6**

Molecular formula	$C_{23}H_{32}O_6$
Appearance	yellow amorphous solid
Melting point	199-200 °C
UV (MeOH) λ_{max} (logε)	203 (3.95), 296 (3.72) and 334 nm (3.12)
IR (KBr)	3429, 2969, 2926, 1622, 1435, 1375, 1318, 1240 and 1077 cm^{-1}
^1H and ^{13}C NMR ($CDCl_3$)	See Table 3.8

Compound **6** was isolated as yellow amorphous solid, and its molecular formula was determined as $C_{23}H_{32}O_6$ (eight units of unsaturation) on the basis of NMR data analysis. UV absorption bands at 203, 296 and 334 nm and IR absorption bands at 1629 and 3429 cm^{-1} presented the presence of carbonyl and hydroxyl groups. The ^1H NMR data (Table 3.8) showed signals attributable to two olefinic protons at δ_H 5.12 and 5.24, and six tertiary methyl groups displaying as singlet at δ_H 1.28, 1.62, 1.69, 1.76, 1.81 and 2.63 (the last signal being due to methyl carbonyl group). The ^{13}C NMR spectrum displayed signals of a quaternary carbon bearing oxygen (δ_C 90.5), a chelating ketone carbonyl (δ_C 203.3), four unsaturated carbons (δ_C 121.3, 124.0, 132.3 and 135.5) and six aromatic carbons (Table 3.8). Thus the two remaining DBEs indicated the molecule of **6** was bicyclic. Studies on ^1H-^1H COSY correlations resulted in the construction of three subfragments, including –C(7)H_2–C(8)H–, –C(20)H=C(21)–, and –C(10)H_2–C(11)H_2–C(12)H= as shown in

Figure 3.16. Two tertiary methyls (δ_H 1.62 and 1.69) were assigned to Me-14 and Me-16 by the HMBC correlations of H_2-12/C-13, H_2-12/C-16 and Me-16/C-14, while the other two tertiary methyls (δ_H 1.77 and 1.82) were identified as Me-22 and Me-23 by those of Me-22/C-21 and Me-23/C-21. Singlet protons of a remaining tertiary methyl (δ_H 1.28), showing HMBC correlations to C-8, C-9 and C-10, were assigned to Me-15. A methyl carbonyl was located at C-2 of the aromatic ring due to its HMBC correlation to C-2. These data showed that compound **6** was a polyketide (Figure 3.16). Finally, Comparison of its NMR data with those in the literature (Table 3.8) helped to confirm that **6** was harrisonol A, which has been isolated from *H. perforata* in 2009 [18].

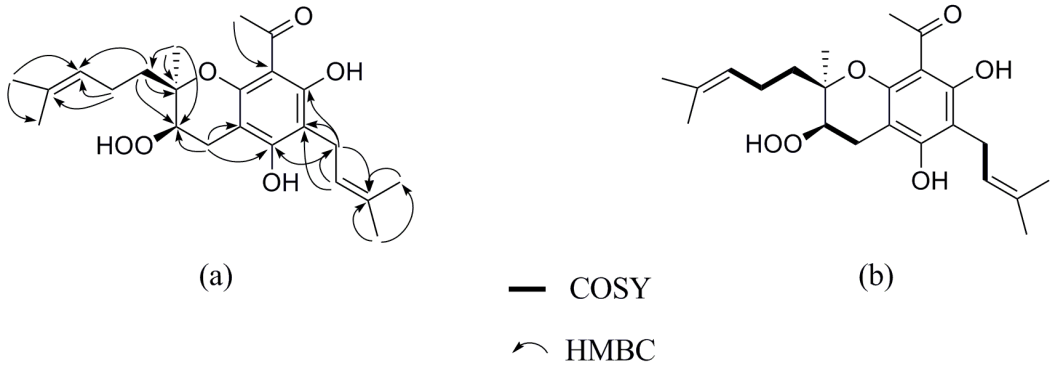

Figure 3.16 HMBC (a) and COSY (b) correlations of compound **6**

Table 3.8 The NMR data of compound **6** and harrisonol A ($CDCl_3$, 400 MHz)

	Harrisonol A		Compound **6**	
Position	δ_H (mult, *J* in Hz)	δ_C	δ_H (mult, *J* in Hz)	δ_C
1		157.2		157.0
2		105.7		105.7
3		161.2		161.0
4		101.2		101.0
5		164.2		164.2
6		104.0		104.0
7	3.06 (dd, *J* = 8.3, 2.8 Hz , 2H)	26.9	3.06 (d, *J* = 8.0 Hz, 2H)	26.8
8	4.73 (t, *J* = 9.8 Hz, 1H)	90.5	4.73 (t, *J* = 8.0 Hz, 1H)	90.5
9		73.8		73.7
10	1.56 (m, 2H)	37.1	1.54 (m, 2H)	37.0
11	2.12 (m, 2H)	22.0	2.08 (m, 2H)	22.0
12	5.12 (br t, *J* = 5.6 Hz, 1H)	124.0	5.11 (br t, *J* = 8.0 Hz, 1H)	124.0
13		132.3		132.2
14	1.69 (s, 3H)	25.7	1.69 (s, 3H)	25.7
15	1.28 (s, 3H)	22.6	1.28 (s, 3H)	22.6
16	1.62 (s, 3H)	17.7	1.62 (s, 3H)	17.7
17		203.3		203.3
18	2.63 (s, 3H)	32.8	2.63 (s, 3H)	32.8
19	3.27 (d, *J* = 7.3 Hz, 2H)	22.4	3.27 (d, *J* = 8.0 Hz, 2H)	22.4
20	5.24 (br t, *J* = 6.0 Hz, 1H)	121.3	5.24 (br t, *J* = 8.0 Hz, 1H)	121.3
21		135.5		136.0
22	1.76 (s, 3H)	25.8	1.77 (s, 3H)	25.8
23	1.81 (s, 3H)	17.9	1.82 (s, 3H)	17.9

3.2.7 Structure elucidation of compound 7

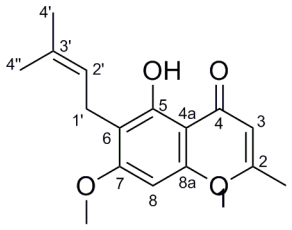

Figure 3.17 Compound **7**

Molecular formula	$C_{16}H_{18}O_4$
Appearance	pale yellow needles
Melting point	105-106 °C
UV (MeOH) λ_{max} (logε)	235 (3.93), 259 (4.13), 298 (3.46) and 329 nm (3.40)
IR (KBr)	3436, 2993, 2912, 1665, 1615, 1591, 1417, 1378, 1328, 1275, 1212, 1080 and 861 cm^{-1}
^1H and ^{13}C NMR ($CDCl_3$)	See Table 3.9

Compound **7** was obtained as pale yellow needles, with a molecular formula $C_{16}H_{18}O_4$ (eight degrees of unsaturation). The UV absorption at 204, 230, 259 and 329 nm and the IR spectrum observed at ν_{max} 3436 and 1665 cm^{-1} suggested the presence of hydroxyl, carbonyl and aromatic groups. In addition, these data indicated that compound **7** was a chromone derivative. The ^1H NMR spectrum exhivited typical signals of phenolic proton chelated to carbonyl carbon (δ_H 12.77), three olefinic protons (δ_H 5.14, 5.99 and 6.35), three tertiary methyls bonded to double bonds (δ_H 1.67, 1.79 and 2.35) and one methoxy (δ_H 3.67). The ^{13}C NMR spectrum showed 10 unsaturated carbons (six for an aromatic) and an aryl ketone (δ_C 182.3). This compound was isolated as a major product from *H. perforata* roots, and its structure was confirmed by comparing its 1D NMR data to those previously

reported as shown in Table 3.9 [19]. Therefore compound **9** was identified as peucenin-7-methyl ether.

Table 3.9 The NMR data of compound **7** and peucenin-7-methyl ether ($CDCl_3$, 400 MHz)

Position	peucenin-7-methyl ether	Compound **7**	
	δ_C	δ_H (mult, *J* in Hz)	δ_C
2	105.3		104.6
3	112.7	5.99 (s, 1H)	107.6
4	182.3		182.9
4a	156.4		154.6
5	166.2		166.7
6	108.7		108.2
7	162.7		162.6
8	89.3	6.35 (s, 1H)	94.9
8a	158.3		160.4
1′	25.7	3.37 (d, *J* = 4.0 Hz, 2H)	25.7
2′	122.0	5.14 (t, *J* = 8.0 Hz, 1H)	122.0
3′	131.6		131.5
4′	20.2	1.79 (s, 3H)	21.5
4″	17.6	1.67 (s, 3H)	17.7
2-Me	21.4	2.35 (s, 3H)	20.5
7-OMe	55.7	3.67 (s, 3H)	56.0
5-OH		12.77 (s, 1H)	

3.2.8 Structure elucidation of compound 8

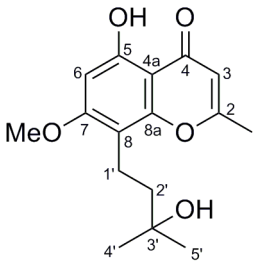

Figure 3.18 Compound **8**

Molecular formula	$C_{16}H_{20}O_5$
Appearance	light yellow solid
Melting point	108-110 °C
UV (MeOH) λ_{max} (logε)	232 (3.52), 258 (3.69), 292 (3.18) and 326 nm (3.04)
IR (KBr)	3449, 2969, 2930, 1654, 1619, 1591, 1424 1385, 1204, 1151 and 833 cm^{-1}
^1H and ^{13}C NMR ($CDCl_3$)	See Table 3.10

Compound **8** was obtained as a light yellow solid and the molecular formula $C_{16}H_{20}O_5$ was determined by HR-ESI-MS (*m/z* 293.1383 $[M + H]^+$, Calcd 293.1316). The UV absorption maxima showed at 232, 258, 292 and 326 nm and the IR spectrum observed at ν_{max} 3449, 1654, 1619 and 1591 cm^{-1} suggested the presence of hydroxyl, carbonyl and aromatic groups. The ^1H NMR spectrum displayed characteristic signals for three tertiary methyls (δ_H 1.30 (Me× 2), 2.36), one methoxy (δ_H 3.88), two olefinic protons (δ_H 6.02, 6.37), and one phenolic proton bonded to a carbonyl group (δ_H 12.75). Analysis of ^{13}C NMR and HSQC data further revealed the presence of three tertiary methyls, two methylenes, two olefinic methines, six olefinic quaternary carbons (three oxygenated), one oxygenated methine, and one ketone. These data indicated that **8** should be a chromone derivative. In addition, its 2D NMR spectra revealed the existence of a 3-hydroxy-4-methylbutyl

moiety due to the ^{1}H-^{1}H COSY correlation of –CH_2(1')–CH_2(2')–, combined with the HMBC correlations of Me-4'/C-2', Me-4'/C-3', Me-5'/C-2', and Me-5'/C-3' (Figure. 3.19). The attachment of this unit at C-8 of the chromone nucleus was confirmed by HMBC correlations from H_2-1' to C-7, C-8 and C-8a. The NMR data of **8** were similar to those of perforamone A [6], except for the presence of an additional methylene instead of an oxygenated methine. The position of the methoxy at C-7 and another tertiary methyl at C-2 was supported by HMBC correlations between methoxy methyl at δ_H 3.88 and C-7, and between the olefinic methyl at δ_H 2.36 and C-2, respectively. Thus, compound **8** was determined to be new and was named as harperamone.

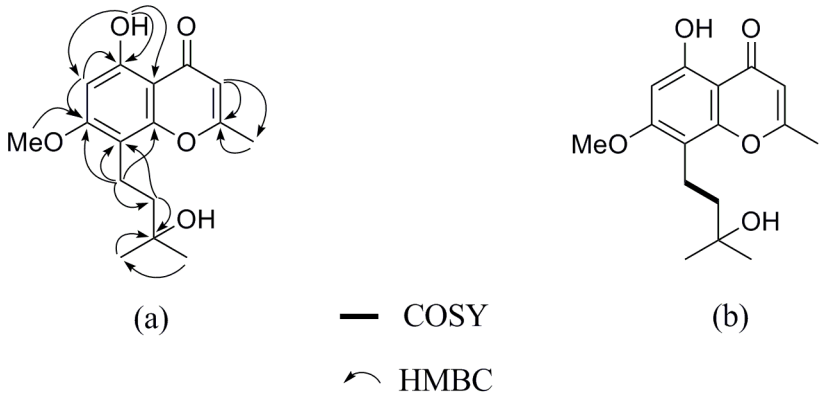

Figure 3.19 HMBC (a) and COSY (b) correlations of compound **8**

Table 3.10 The NMR data of compound **8** ($CDCl_3$, 400 MHz)

postition	δ_H (mult, *J* in HZ)	δ_C
2		166.7
3	6.02 s	108.3
4		183.0
4a		104.7
5		160.5
6	6.37 s	95.0
7		164.7
8		108.3
8a		154.7
1'	2.77 m	17.4
2'	1.64 m	42.9
3'		71.1
4'	1.30 s	29.0
5'	1.30 s	29.0
2-Me	2.36 s	20.5
7-OMe	3.88 s	56.0
5-OH	12.75 s	

3.2.9 Structure elucidation of compound 9

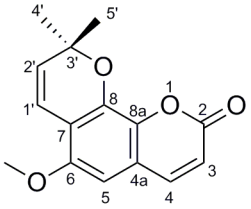

Figure 3.20 Compound **9**

Molecular formula	$C_{15}H_{14}O_4$
Appearance	light amorphous solid
Melting point	149-150 °C
UV (MeOH) λ_{max} (logε)	203 (3.38), 227 (3.62), 258 (3.23) and 349 nm (3.18)
IR (KBr)	2912, 1729, 1630, 1559 1467, 1297, and 1127 cm^{-1}
^1H and ^{13}C NMR ($CDCl_3$)	See Table 3.11

Compound **9** was isolated as a light amorphous solid and had the molecular formula as $C_{15}H_{14}O_4$ determined by HR-ESI-MS (*m/z* 259.0889 $[M + H]^+$, Calcd 259.0965). The IR and UV spectra showed absorptions for carbonyl at ν_{max} 1729 cm^{-1} and maxima absorptions at 203, 227, 258 and 349 nm, which was a characteristic of a coumarin. The ^1H and ^{13}C NMR spectra suggested the presence of one methoxy group (δ_H 3.88, δ_C 56.6) and a cyclic isopentenyl moiety. The attachment of the methoxy at C-6 was assigned by its HMBC correlation to C-6. An α,β-unsaturated lactone ring was corroborated by ^1H-^1H COSY correlation of -C(3)H=C(4)H- and their HMBC correlations of H-3/C-2, H-3/C-4a, H-4/C-2 and H-4/C-8a. The absence of any oxygenation at C-5 was confirmed by HMBC correlations of H-4 to its carbon (δ_C 108.8). Based on the above data, compound **9** was determined to be braylin I, and it was further confirmed by comparison of its NMR data with those in the literature as presented in Table 3.11. In addition, it was found that this is the first report of braylin I from *H. perforata*.

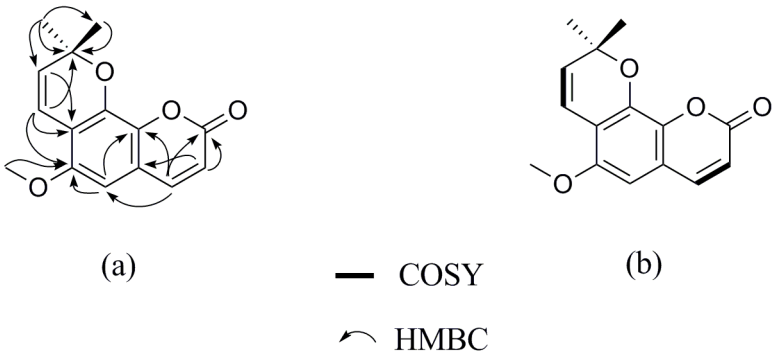

Figure 3.21 HMBC (a) and COSY (b) correlations of compound **9**

Table 3.11 The NMR data of compound **9** and braylin I ($CDCl_3$, 400 MHz)

position	δ_H (mult, *J* in HZ)	δ_C
2		161.2
3	6.25 (d, *J* = 8 Hz,1H)	113.2
4	7.57 (d, *J* = 8 Hz,1H)	143.7
4a		111.4
5	6.76 (s, 1H)	108.8
6		146.0
7		110.3
8		145.7
8a		145.0
1'	6.87 (d, J = 8 Hz, 1H)	115.2
2'	5.74 (d, J = 8 Hz, 1H)	130.8
3'		78.0
4'	1.52 (s, 3H)	28.0
5'	1.52 (s, 3H)	28.0
6-OMe	3.88 (s, 3H)	56.6

3.3 Anti-inflammatory activity of isolated compounds

Nitric oxide (NO) is one of the most important mediators in inflammatory processes. Upon inflammatory stimulation, macrophages are activated and produce nitric oxide and pro-inflammatory cytokines such as tumor necrosis factor (TNF)-alpha and interleukin (IL)-6. Overproduction of these mediators in macrophages causes many inflammatory diseases, including rheumatoid arthritis, atherosclerosis, and hepatitis [21-23]. Additionally, NO is mainly produced by inducible nitric oxide synthase (iNOS) [24], the inhibition of NO production by suppressing iNOS expression is thus an important target in the treatment of inflammatory diseases.

H. perforata root is considered to have antipyretic and anti-inflammatory effects, and it is utilized as a remedy for treatment of wound healing and diarrhea [3]. In the present study, the anti-inflammatory activity of isolated compounds from *H. perforata* fruits and roots was thus evaluated by monitoring the inhibition of nitric oxide (NO) production in LPS-activated murine macrophage J774.A1 cells, and the results expressed as IC_{50} ± SD are shown in Table 3.12. Among the tested compounds, the most potent activity was demonstrated by harperfolide (**2**), a new rearranged limonoid, with IC_{50} value of 6.51 ± 2.10 μM. Its activity was 20-fold greater than its analog harrisonin **3** (IC_{50} = 134.54 ± 5.66 μM), indicating that the presence of a γ-hydroxybutenolide group may significantly enhance the NO production inhibitory activity of this type limonoid. Acute toxicity of compound **2** on unstimulated cell lines was further investigated. Cell viability, as measured by the MTT colorimetric method, displayed harperfolide (**2**) did not significant toxicity on macrophage J774.A1 cells at tested concentrations as shown in Figure 3.22. This result implied that harperfolide inhibited nitrite release without causing cell death.

Table 3.12 Inhibitory effect of isolated compounds on NO production in LPS-induced macrophages

Compound	IC_{50} (μM)
Harrisonin (**1**)	134.54 ± 12.66
Harperfolide (**2**)	6.51 ± 2.10
Obacunone (**3**)	83.61 ± 3.52
(+)-Vouacapenic acid (**5**)	131.81 ± 2.47
Harrisolanol A (**6**)	31.04 ± 0.72
Peucenin-7-methyl ether (**7**)	56.36 ± 1.45
Harperamone (**8**)	49.59 ± 2.58
Indomethacin	28.42 ± 3.51

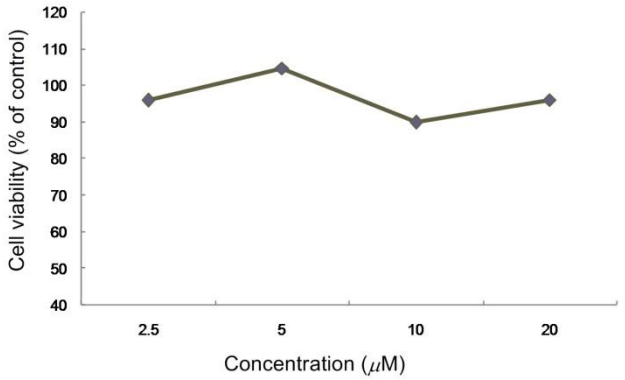

Figure 3.22 Effect of harperfolide (**2**) on cell viability

To investigate whether the inhibitory effect of harperfolide (**2**) on NO production was via the inhibition of the corresponding gene expression, the protein iNOS was evaluated by Western blot analysis. In unstimulated J774.A1 cells, the iNOS protein expression level was almost undetectable, while, after treatment with LPS, the protein expression level of iNOS was augmented markedly. Pretreatment of the cells with various concentrations of **2** attenuated LPS-induced iNOS protein expression in a concentration-dependent manner as shown in Figure 3.23. These data suggested harperfolide (**2**) can down regulate LPS-induced iNOS expression at the transcriptional level.

(a)

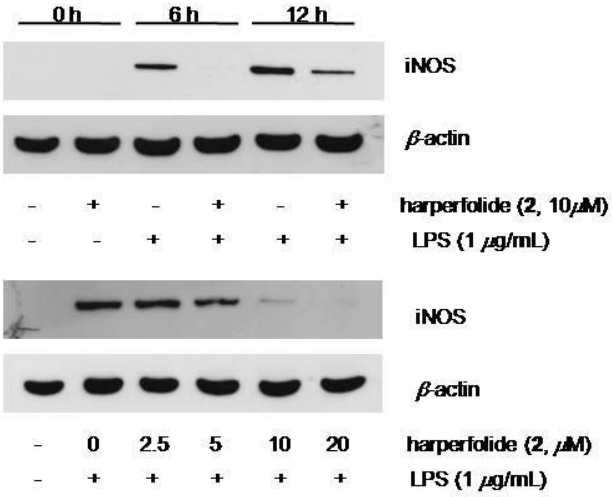

(b)

Figure 3.23 Effect of harperfolide (**2**) on the expression of iNOS protein in LPS-induced macrophages (a) at the indicated time (b) at various doses

CHAPTER IV

CONCLUSION

The EtOAc extracts of fruits and roots of *H. perforata* (Blanco) Merr. were repeatedly isolated by chromatography techniques. Isolation of the EtOAc crude extract of the fruits provided a new highly rearranged limonoid, namely harperforatin (**4**), while that of the root extract yielded a new chromone, harperamone (**8**) and a new rearranged limonoid, harperfolide (**2**), along with six known compounds including harrisonin (**1**), obacunone (**3**), (+)-vouacapenic acid (**5**), harrisonol A (**6**), peucenin-7-methyl ether (**7**) and braylin I (**9**) as shown below. The structures of isolated compounds were elucidated by analysis of spectroscopic data, particulary 1D and 2D NMR, as well as single-crystal X-ray diffraction analysis, and by comparing with those previously reported in literature.

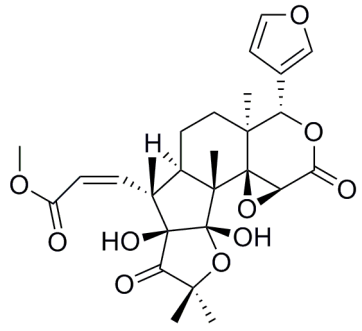

1

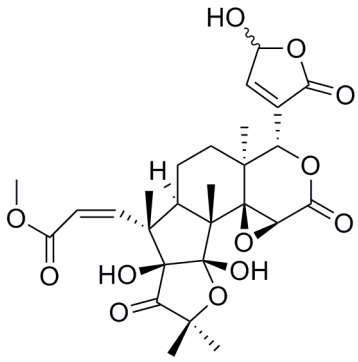

2

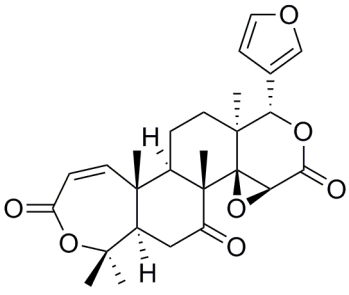

3

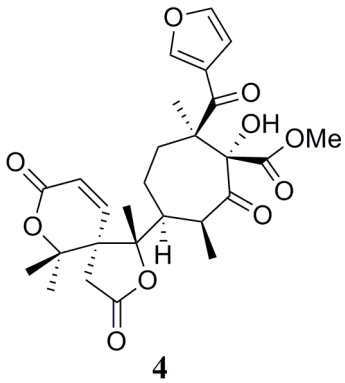

4

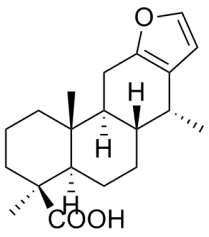

5

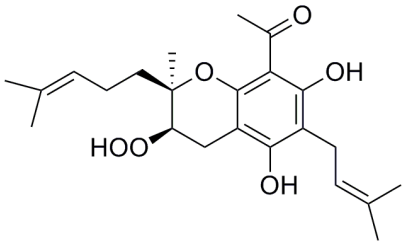

6

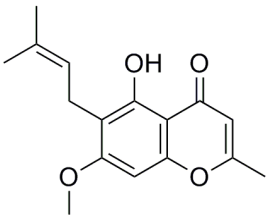

7

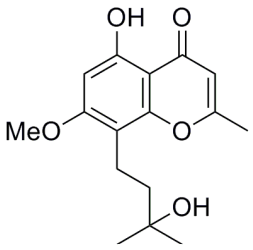

8

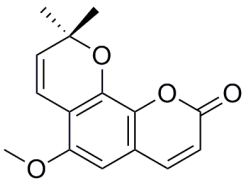

9

Further, compounds **1**-**8**, except for **4**, were tested for their anti-inflammatory activity using monitoring the inhibition of nitric oxide (NO) production in LPS-activated murine macrophage J774.A1 cells. Harperfolide (**2**) exhibited the most potent activity with IC_{50} value of 6.51 ± 2.10 μM. Its activity was around 20-fold greater than its analog harrisonin (**3**) (IC_{50} = 134.54 ± 5.66 μM), indicating that the presence of a γ-hydroxybutenolide group may significantly enhance the NO production inhibitory activity of this type limonoid. Furthermore, it was found that harperfolide (**2**) did not showed significant toxicity on macrophage J774.A1 cells, determined by the MTT colorimetric method. This result implied that **2** inhibited nitrite release without causing cell death. In addition, its anti-inflammatory effect was found to be mediated by the reduction of the iNOS protein expression as assessed by immunoblotting using a specific anti-iNOS antibody.

REFERENCES

[1] Newman, D. J., Cragg, G. M. and Snader, K. M. 2000. The influence of natural products upon drug discovery. Nat. Prod. Res. 17: 215-234.

[2] Newman, D. J., Cragg, G. M. and Snader, K. M. 2003. Natural products as source of new drugs over the period 1981-2002. J. Nat. Prod. 66: 1022-1037.

[3] Perry, L. M. 1980. Medicinal plants of East and Southeast Asia, pp. 389-390, MIT press, Boston, MA.

[4] Mitsunaga, K., Koike, K., Ishii, K. and Ohmoto, T. 1994. Rearranged limonoids from *Harrisonia brownii*. Phytochemistry 35: 451-454.

[5] Tanaka, T., Koike, K., Mitsunaga, K., Narita, K., Takano, S., Kamioka, A., Sase, E., Ouyang, Y. and Ohmoto, T. 1995. Chromones from *Harrisonia perforata*. Phytochemistry 40: 1787-1790.

[6] Tuntiwachwuttikul, P., Phanasa, P., Pootaeng-on, Y. and Taylor, W. C. 2006. Chromones from the branches of *Harrisonia perforata*. Chem. Pharm. Bull. 54: 44-47.

[7] Kubo, I., Tanis, S. P., Lee, Y. W., Miura, I., Nakanishi, K. and Chaya, A. 1976. The structure of harrisonin. Heterocycles 5: 485-498.

[8] Rajab, M. S., Rugutt, J. K., Fronczek, F. R. and Fischer, N. H. 1997. Structural revision of harrisonin and 12β-acetoxyharrisonin, two limonoids from *Harrisonia abyssinica*. J. Nat. Prod. 60: 822-825.

[9] Khuong-Huu, Q., Chiaroni, A., Riche, C., Nguyen-Ngoc, H., Nguyen-Viet, K. and Khuong-Huu, F. 2001. New rearranged limonoids from *Harrisonia perforata*. III. J. Nat. Prod. 64: 634-637.

[10] Yan, X.-H., Di, Y.-T., Fang, X., Yang, S.-Y., He, H.-P., Li, S.-L., Lu, Y. and Hao, X.-J. 2011. Chemical constituents from fruits of *Harrisonia perforata*. Phytochemistry 72: 508-513.

[11] Thi-Thu, H. D., Tri, M. V., Ngoc, N. B., Sèvenet, T., Païs, M. and Martin, M.-T. 2011. Foritin, a new limonoid from *Harrisonia perforata*. Nat. Prod. Lett. 14: 191-195.

[12] Khan, S., Shin, E. M., Choi, R. J., Jung, Y. H., Kim, J., Tosun, A. and Kim, Y. S. 2011. Suppression of LPS-induced inflammatory and NF-κB responses by anomalin in RAW 264.7 macrophages. J. Cell. Biochem. 112: 2179-2188.

[13] Hsu, F. J., Chen, B. W., Wen, Z H., Huang, C. H., Dai, C. F., Du, J. H., Wu, F. J. and Sheu, J. H. 2011. Klywollins A-H, bioactive eunicellin-based diterpenoids from the Formosan soft coral *Klysum molle*. J. Nat. Prod. 74: 2467-2471.

[14] Wu, J., Yang, S.-X., Li, M.-Y., Feng, G., Pan, J.-Y., Xiao, Q., Sinkkonen, J, and Satyanandamurty, T., 2010. Limonoids and tirucallane derivatives from the seeds of a Krishna mangrove, *Xylocarpus moluccensis*. J. Nat. Prod. 73: 644-649.

[15] Chidambara Murthy, K. N., Jayaprakasha, G. K. and Patil, B. S. 2011. Obacunone and obacunone glucoside inhibit human colon cancer (SW480) cells by the induction of apoptosis. Food Chem. Toxicol. 49: 1616-1625.

[16] Zhou, X., Ji, C., Fu, J., Li, Y.-G. and Chen, J. 2006. Obacunone. Acta Cryst. E62: o5544-o5546.

[17] Kido, T., Taniguchi, M. and Baba, K. 2003. Diterpenoids from Amazonian crude drug of Fabaceae. Chem. Pharm. Bull. 51: 207-208.

[18] Yin, S., Chen, X., Su, Z.-S., Yang, S.-P., Fan, C.-Q., Ding, J. and Yue, J.-M. 2009. Harrisotones A-E, five novel prenylated polyketides with a rare spirocyclic skeleton from *Harrisonia perforata*. Tetrahedron 65: 1147-1152.

[19] Thadaniti, S., Archakunakorn W., Tuntiwachwuttikul, P. and Bremner, J. B. 1994. Chromones from *Harrisonia perforata* (Blanco.) Merr. J. Sci. Soc. Thailand 20: 183-187.

[20] Anet, F. A. L., Hughes, G. K. and Ritchie, E. 1949. The chemical constituents of Australian Flindersia species. II. Braylin and brayleyanin. Aust. J. Sci. Res., Ser B, Biological Sciences 2A: 608-615.

[21] Isomäki, P. and Punnonen, J. 1997. Pro- and anti-inflammatory cytokines in rheumatoid arthritis. Ann. Med. 29: 499-507.

[22] Libby, P., Ridker, P. M., and Maseri, R. 2002. Inflammation and atherosclerosis. Circulation 105: 1135-1143.

[23] Tilg, H., Wilmer, A., Vogel, W., Herold, M., Nolchen, B., Judmaier, G. and Huber, C. 1992. Serum levels of cytokines in chronic liver diseases. Gastroenterology 103: 264-274.

[24] Pokharel, Y, R., Liu, Q. H., Oh, J. W., Woo, R. and Kang, K. W. 2007. 4-Hydroxykobusin inhibits the induction of nitric oxide synthase by inhibiting NF-κB and AP-1 activation. Biol. Pharm. Bull. 30: 1097-1101.

Appendix

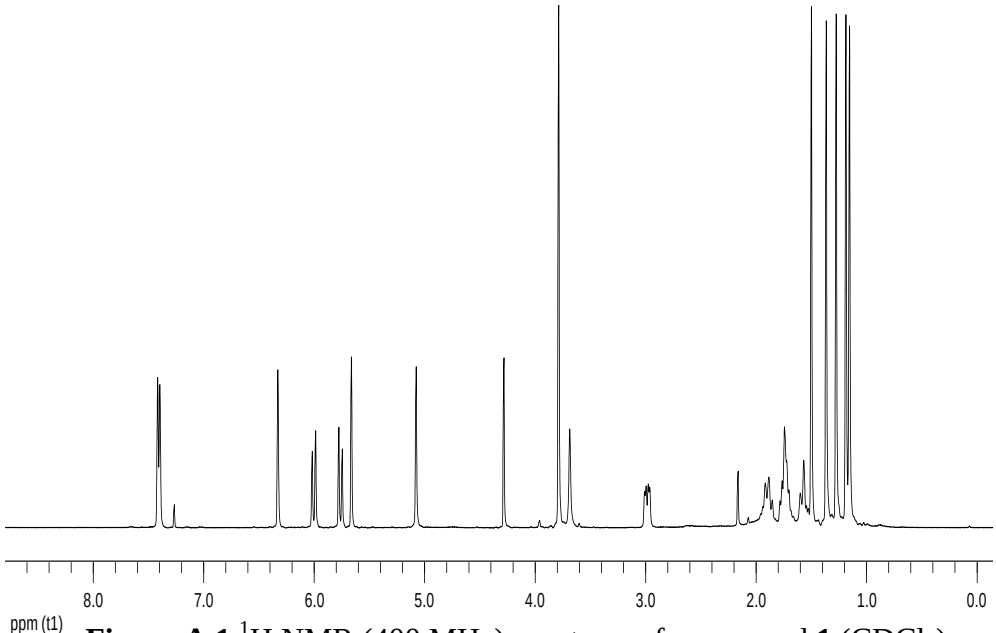

Figure A.1 ^{1}H NMR (400 MHz) spectrum of compound **1** ($CDCl_3$)

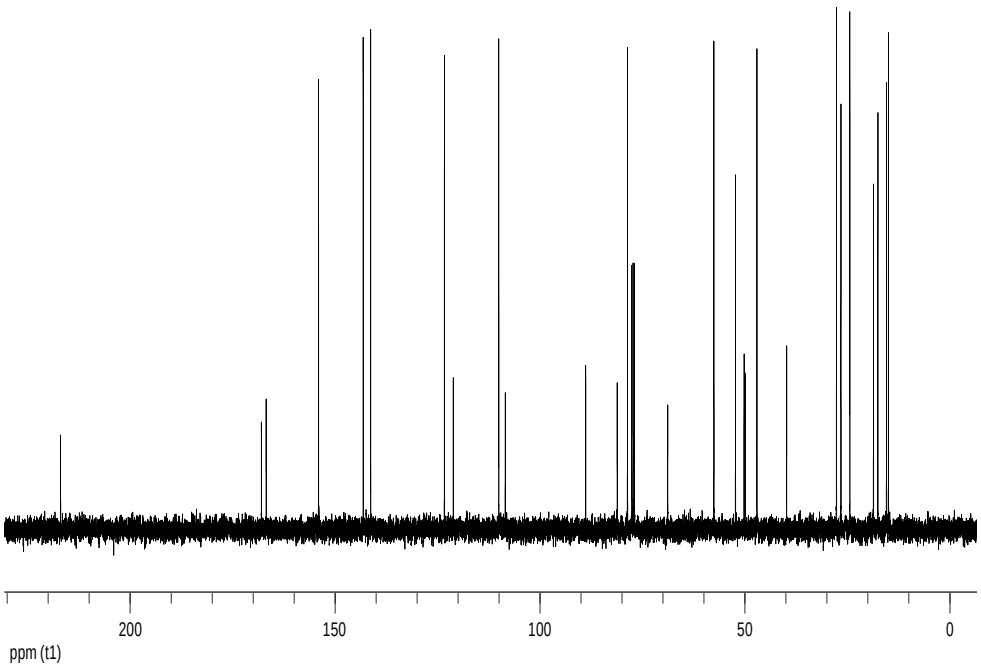

Figure A.2 ^{13}C NMR (400 MHz) spectrum of compound **1** ($CDCl_3$)

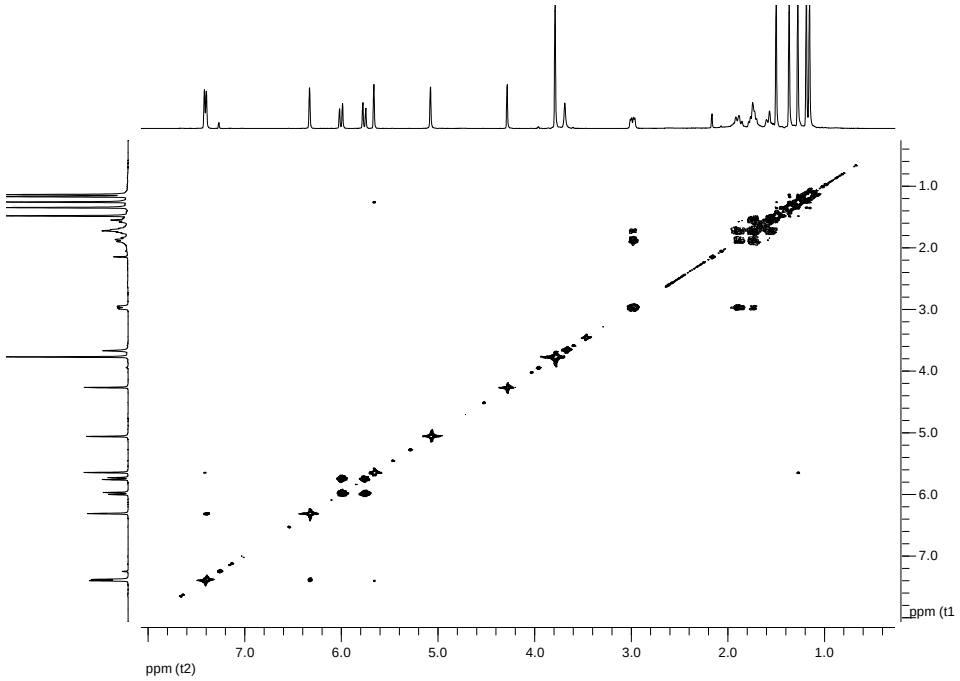

Figure A.3 COSY (400 MHz) spectrum of compound **1** ($CDCl_3$)

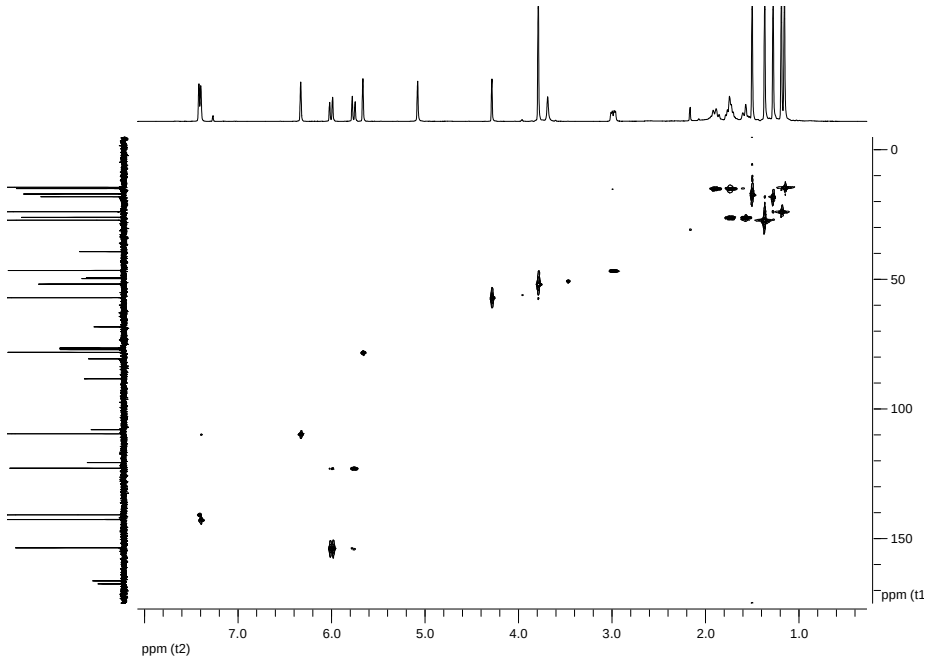

Figure A.4 HSQC (400 MHz) spectrum of compound **1** ($CDCl_3$)

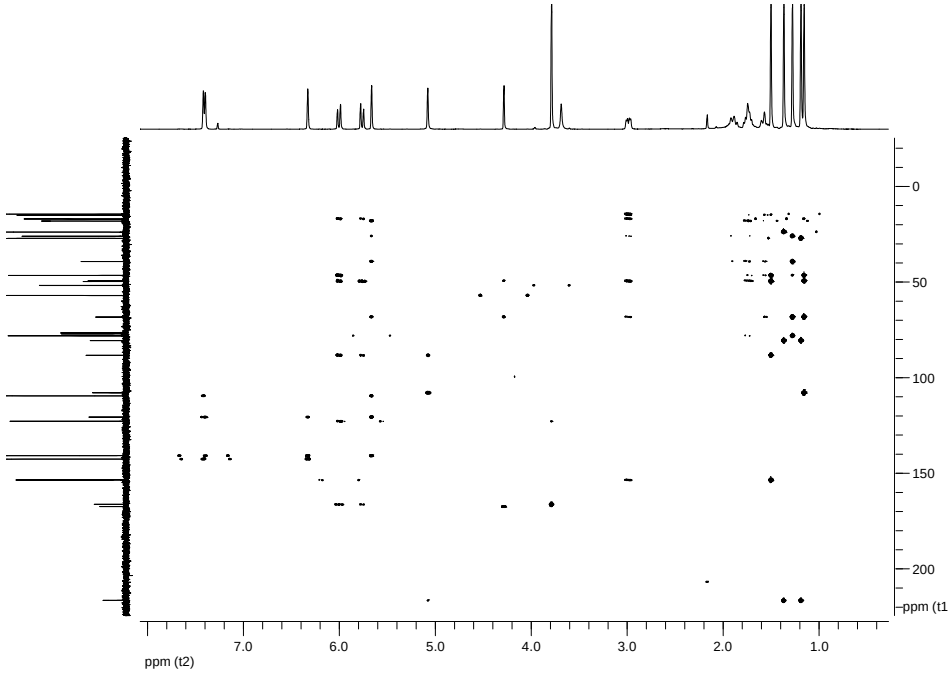

Figure A.5 HMBC (400 MHz) spectrum of compound **1** ($CDCl_3$)

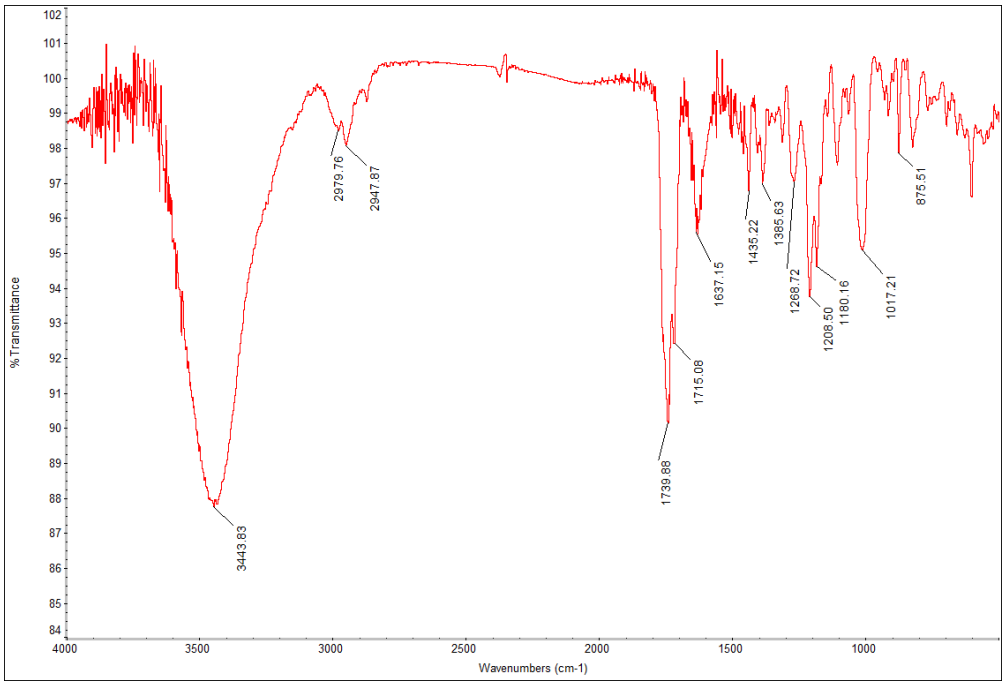

Figure A.6 IR spectrum of compound **1** (KBr)

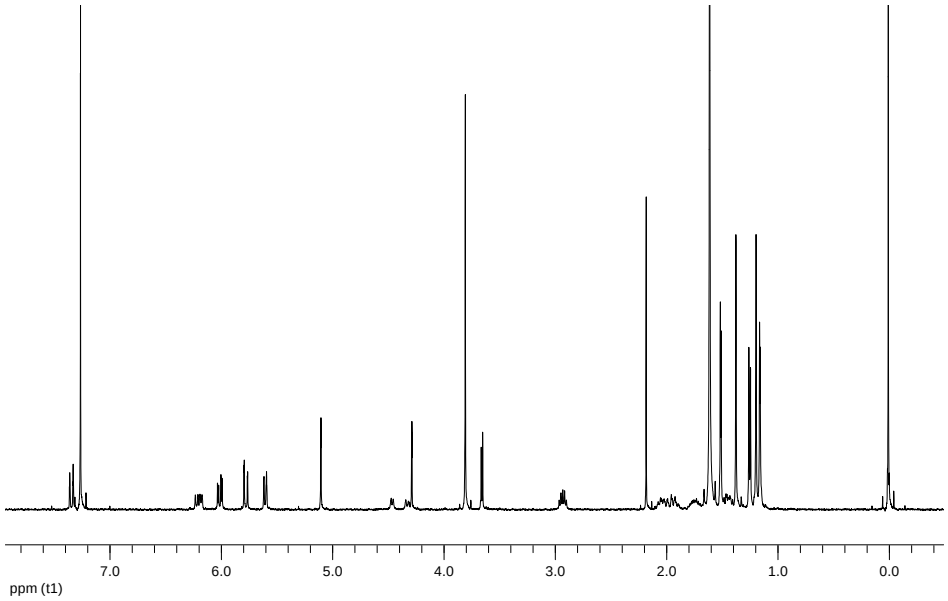

Figure A.7 ^{1}H NMR (400 MHz) spectrum of compound **2** ($CDCl_3$)

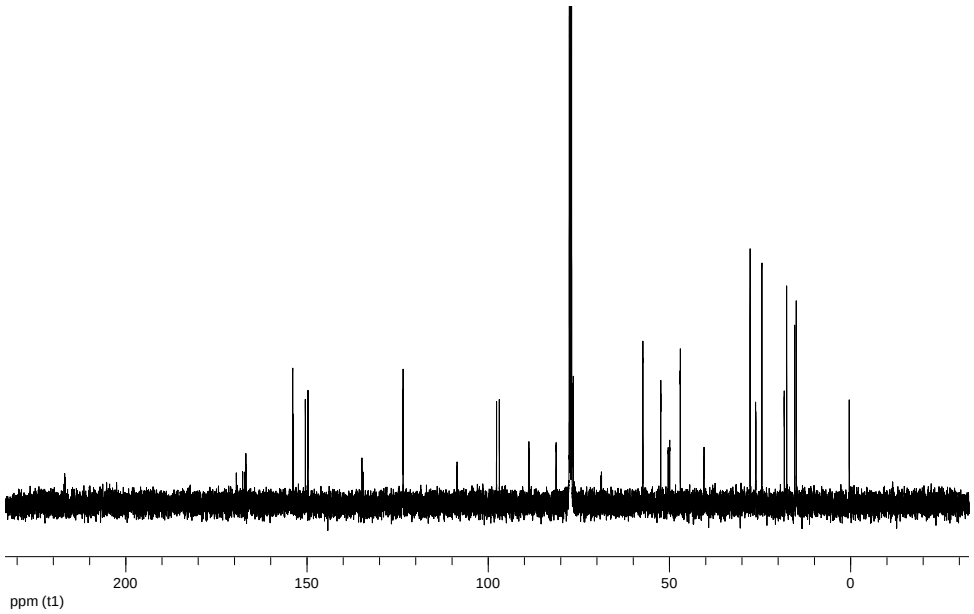

Figure A.8 ^{13}C NMR (400 MHz) spectrum of compound **2** ($CDCl_3$)

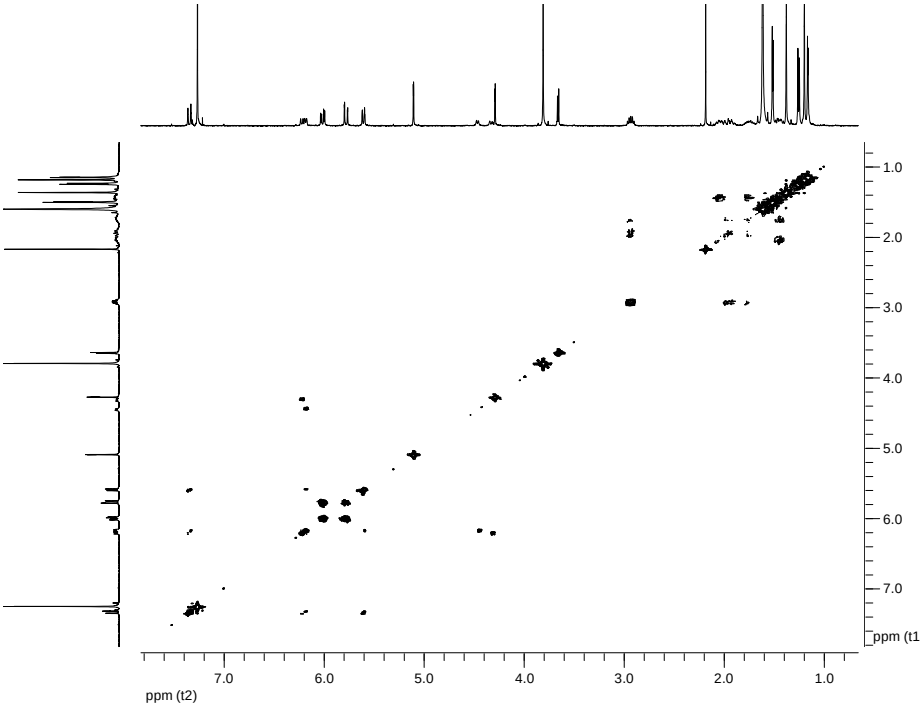

Figure A.9 COSY (400 MHz) spectrum of compound **2** ($CDCl_3$)

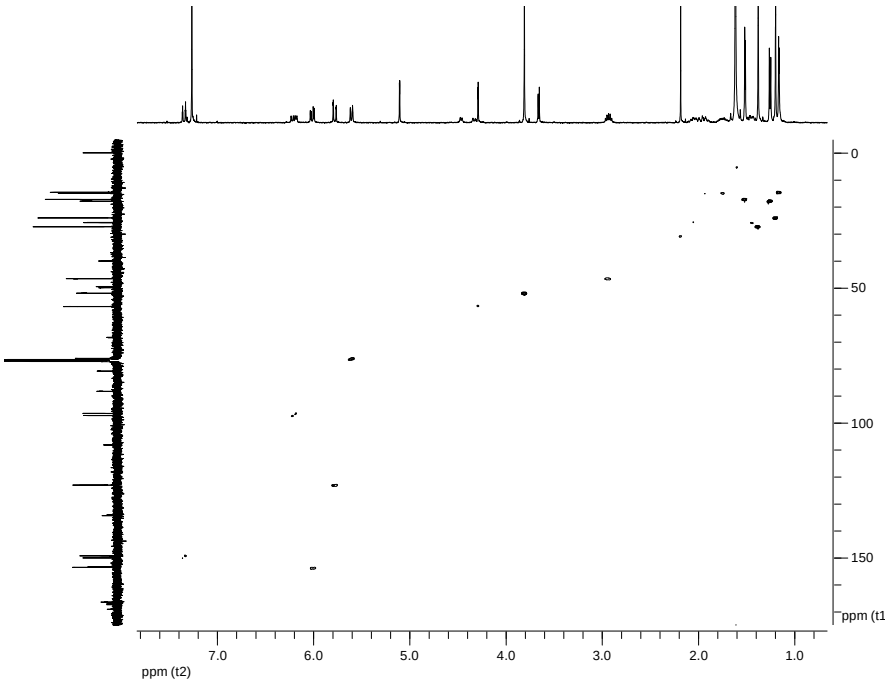

Figure A.10 HSQC (400 MHz) spectrum of compound **2** ($CDCl_3$)

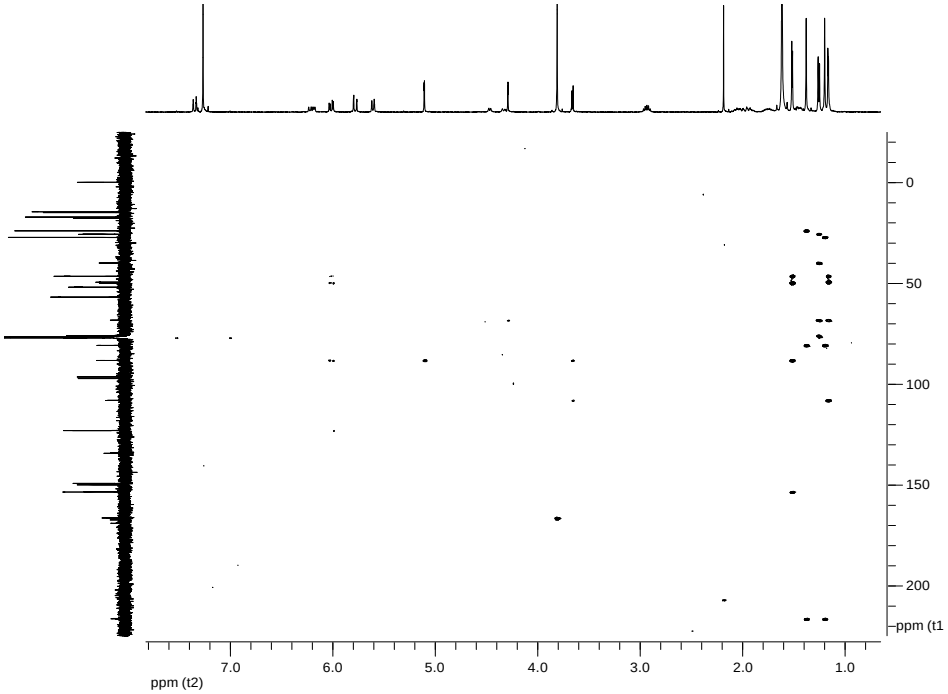

Figure A.11 HMBC (400 MHz) spectrum of compound **2** ($CDCl_3$)

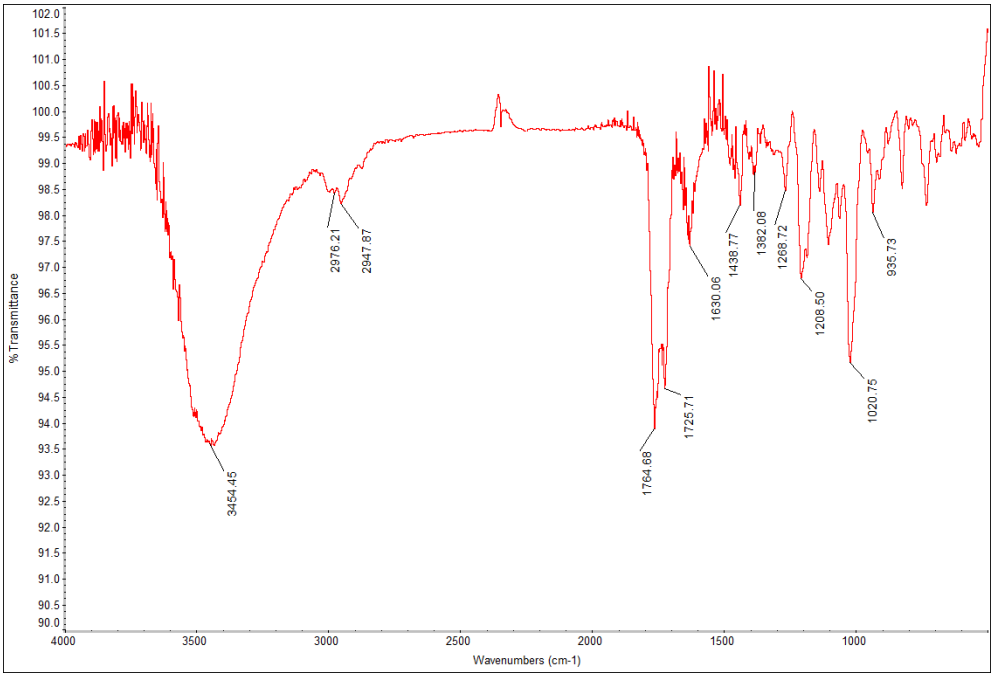

Figure A.12 IR spectrum of compound **2** (KBr)

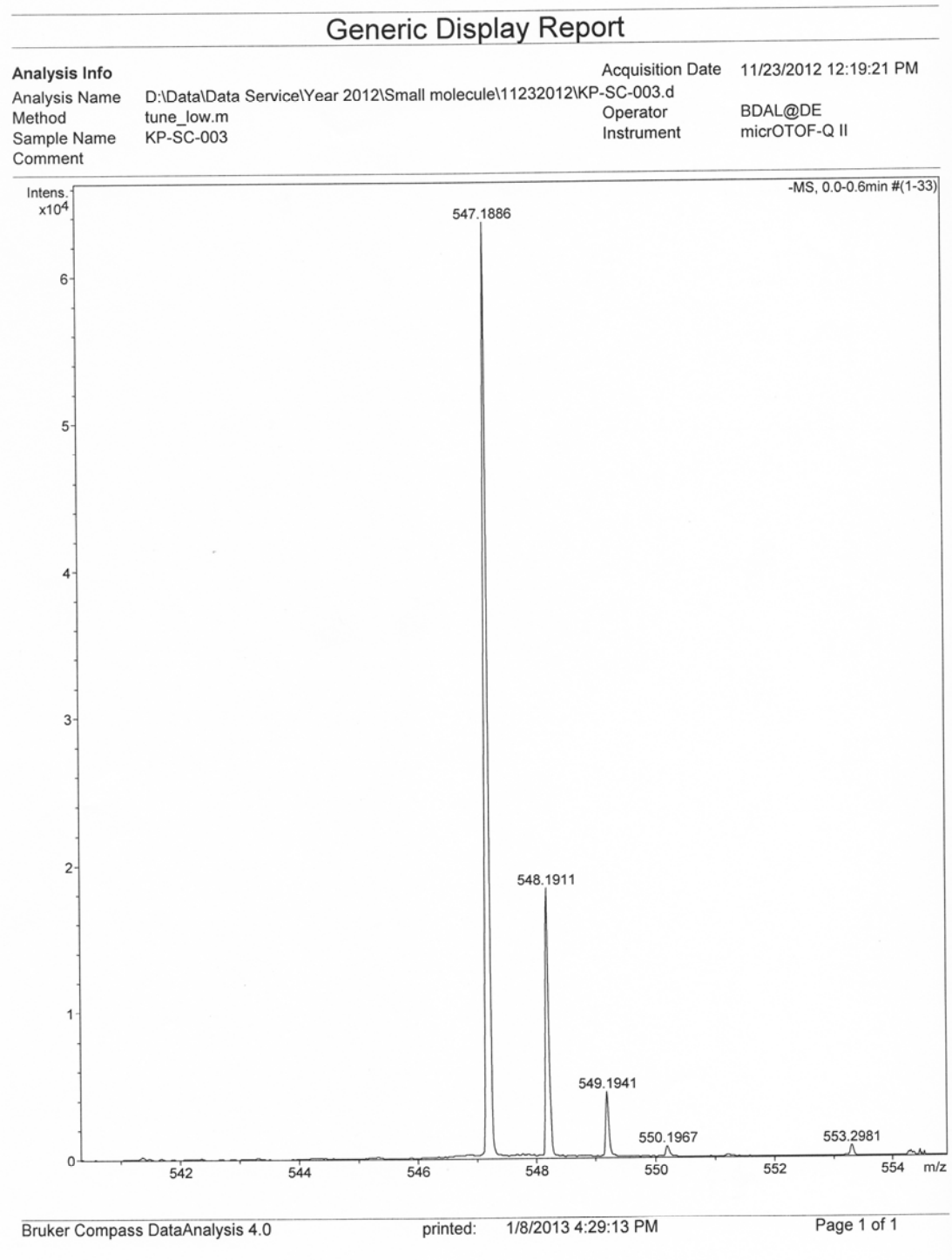

Figure A.13 HRESIMS Mass spectrum of compound **2**

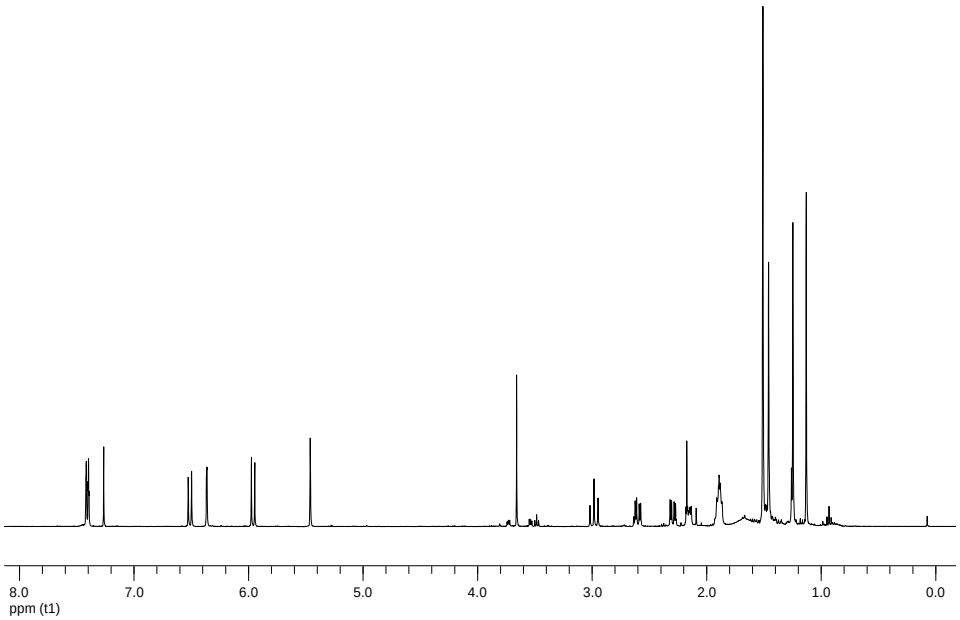

Figure A.14 ^{1}H NMR (400 MHz) spectrum of compound **3** ($CDCl_3$)

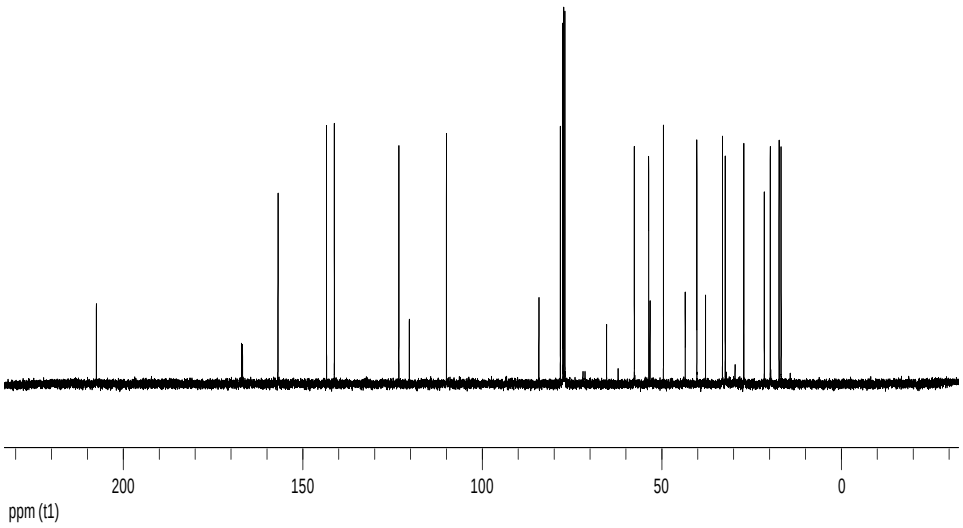

Figure A.15 ^{13}C NMR (400 MHz) spectrum of compound **3** ($CDCl_3$)

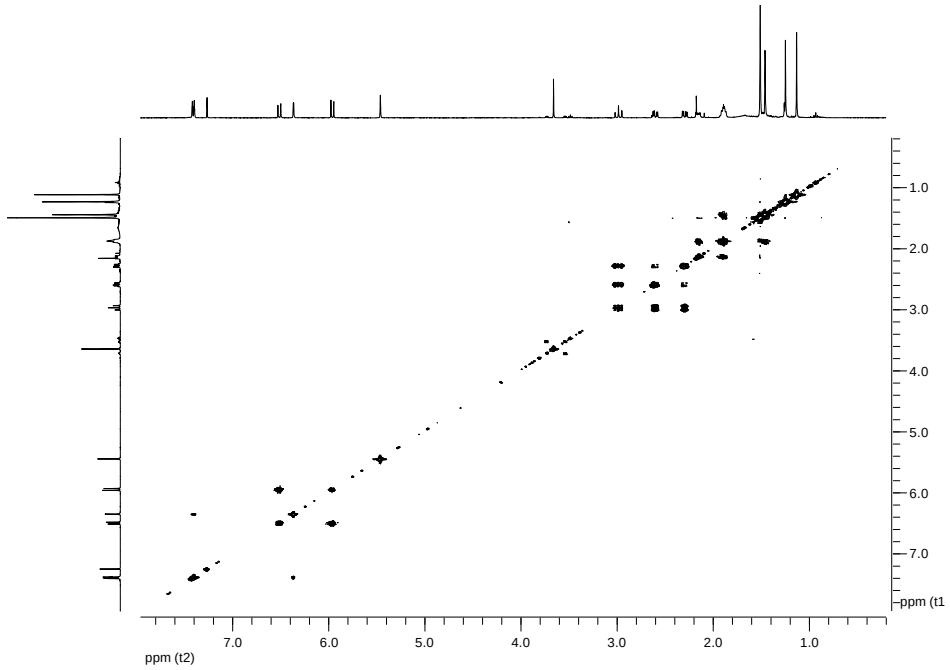

Figure A.16 COSY (400 MHz) spectrum of compound **3** ($CDCl_3$)

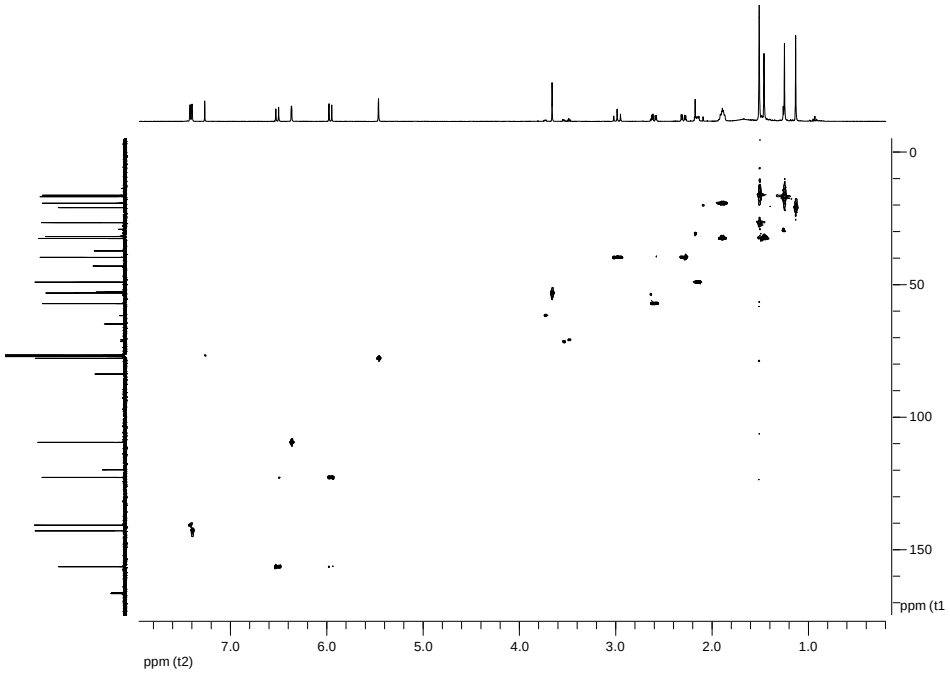

Figure A.17 HSQC (400 MHz) spectrum of compound **3** ($CDCl_3$)

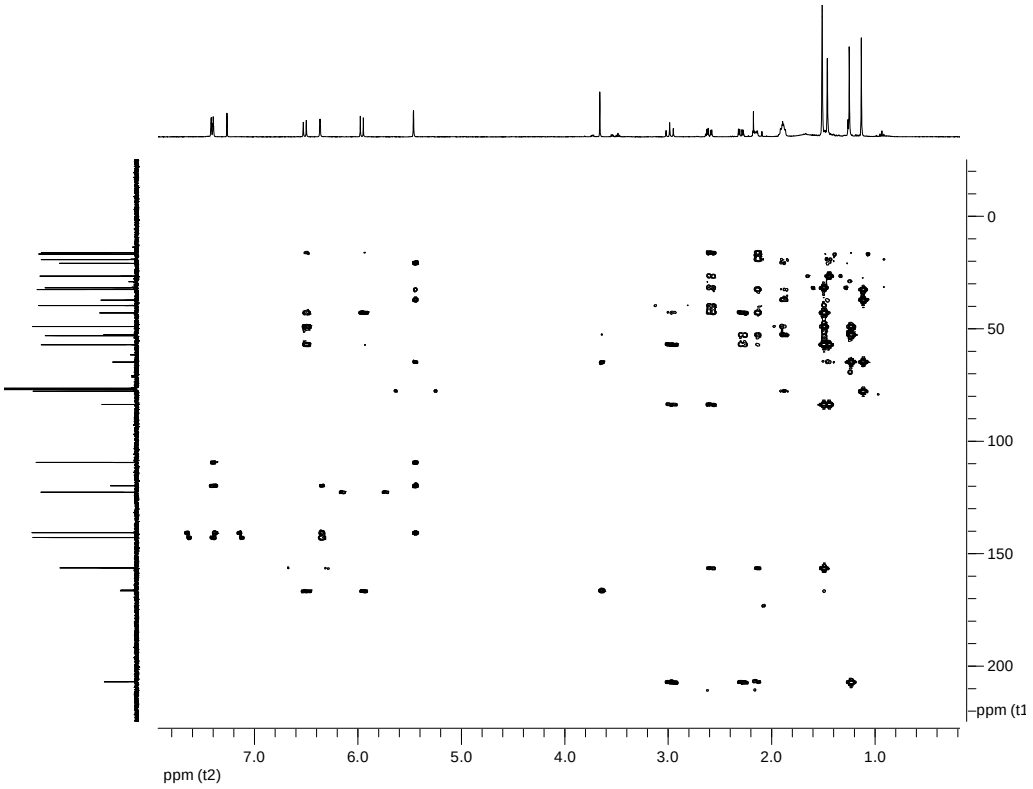

Figure A.18 HMBC (400 MHz) spectrum of compound **3** ($CDCl_3$)

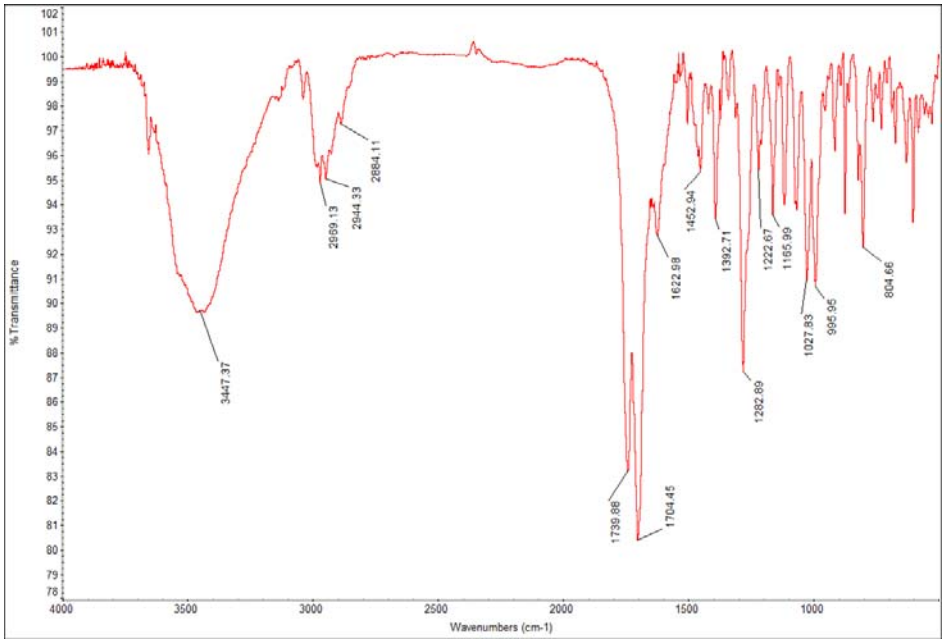

Figure A.19 IR spectrum of compound **3** (KBr)

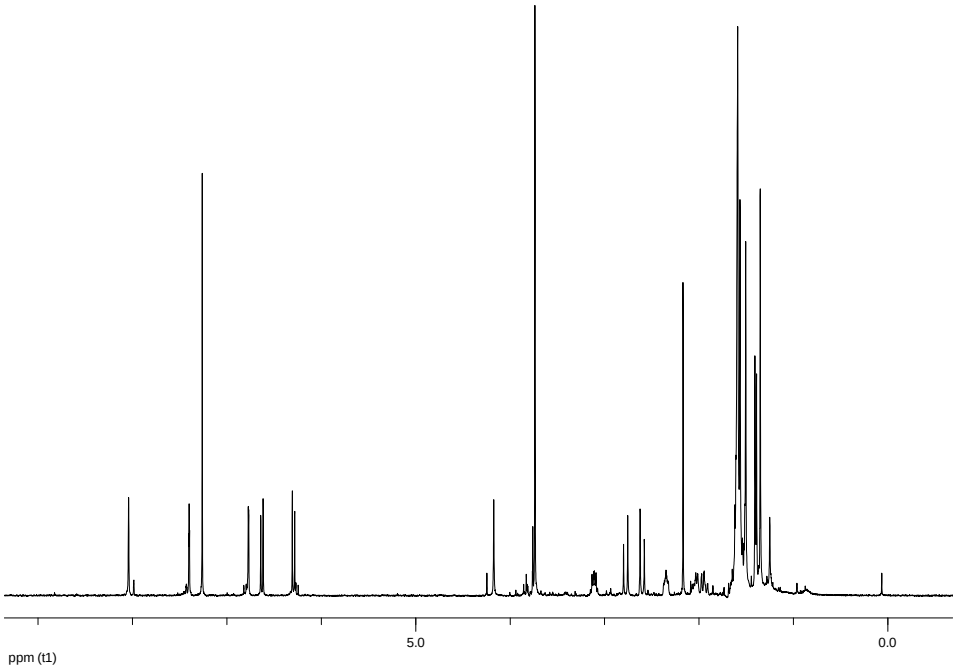

Figure A.20 ^{1}H NMR (400 MHz) spectrum of compound **4** ($CDCl_3$)

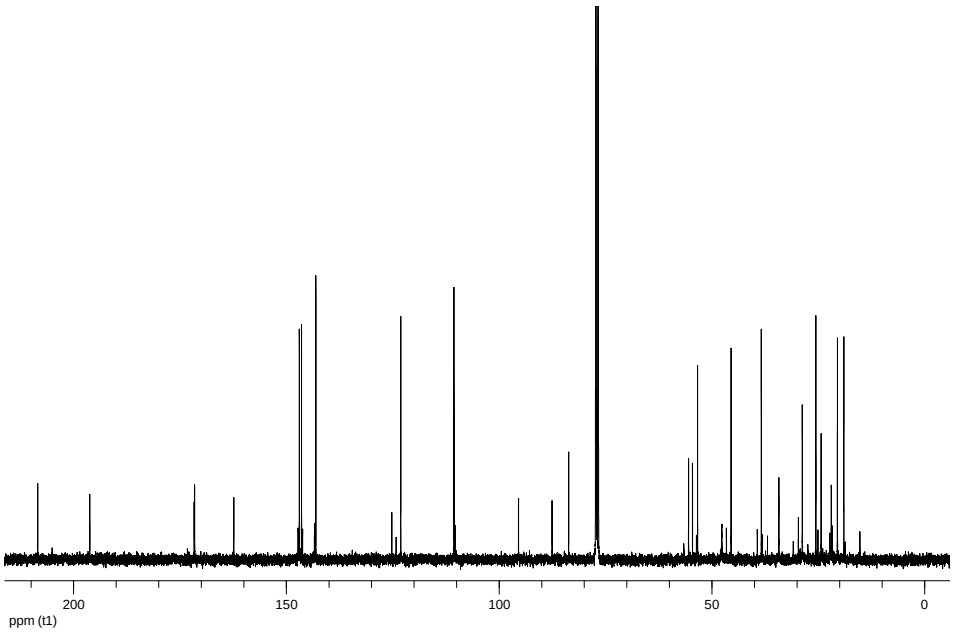

Figure A.21 ^{13}C NMR (400 MHz) spectrum of compound **4** ($CDCl_3$)

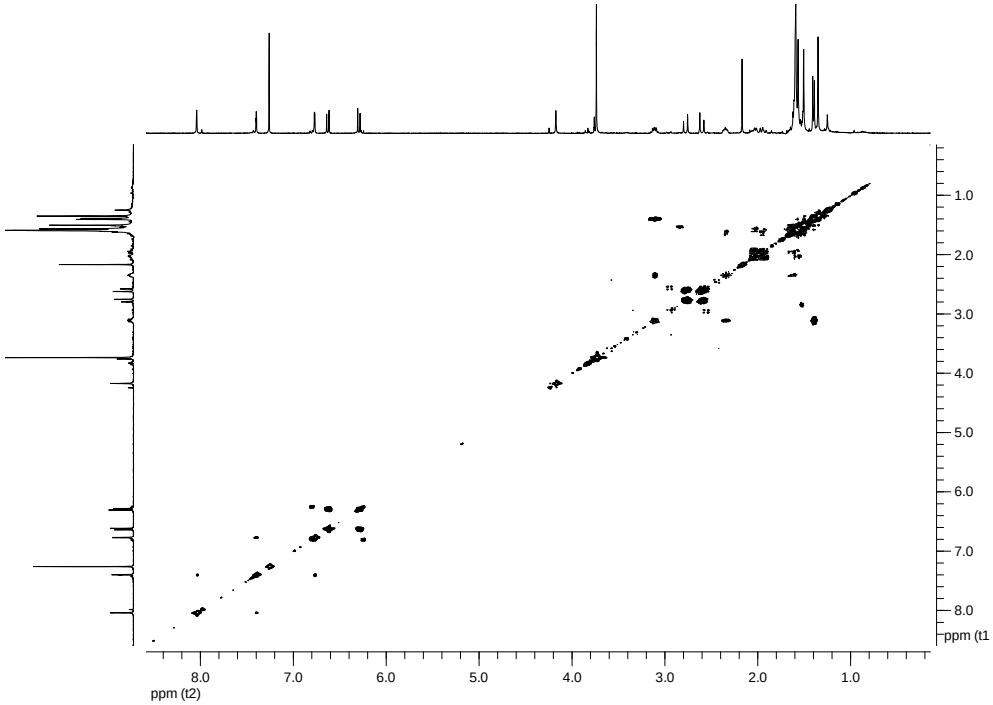

Figure A.22 COSY (400 MHz) spectrum of compound **4** ($CDCl_3$)

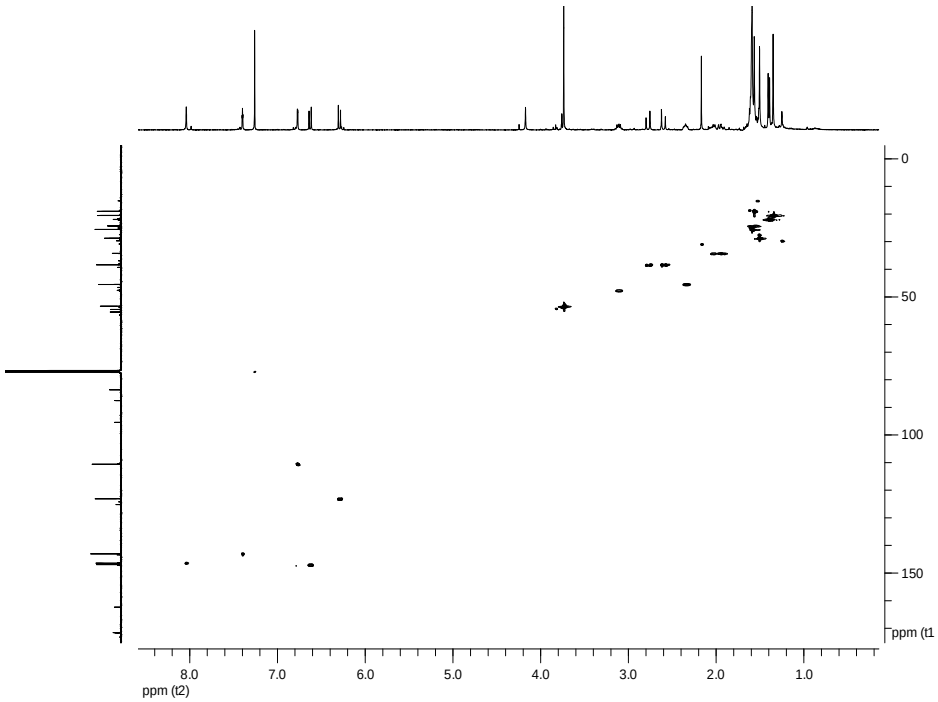

Figure A.23 HSQC (400 MHz) spectrum of compound **4** ($CDCl_3$)

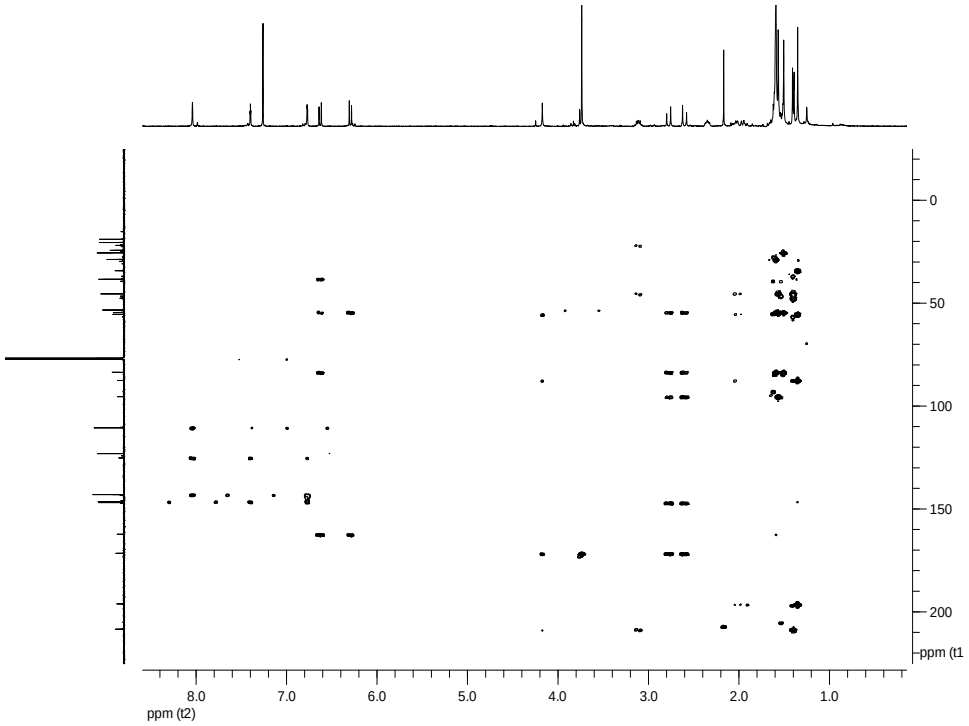

Figure A.24 HMBC (400 MHz) spectrum of compound **4** ($CDCl_3$)

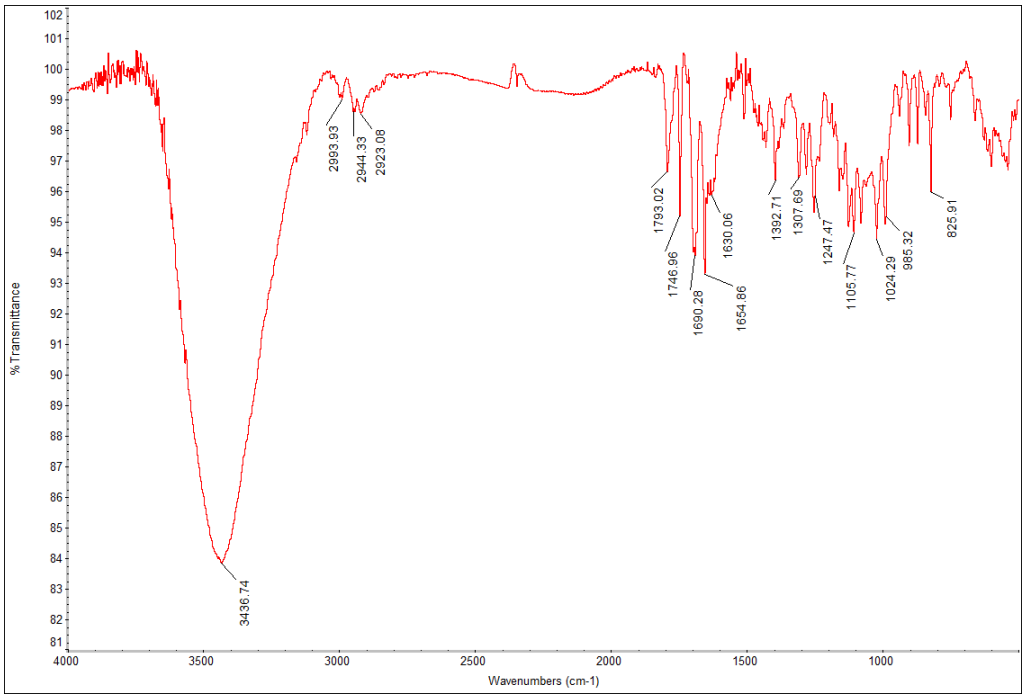

Figure A.25 IR spectrum of compound **4** (KBr)

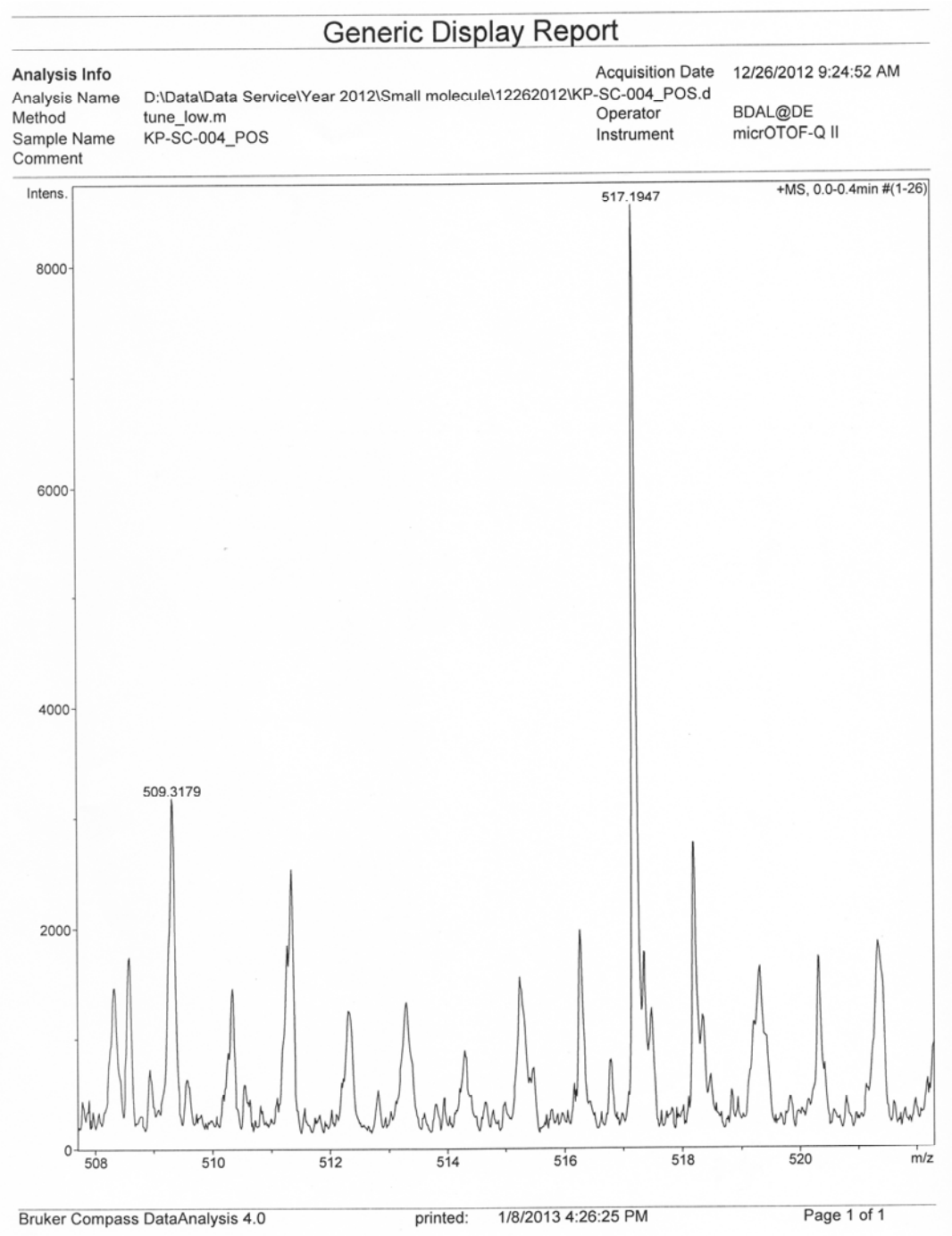

Figure A.26 HRESIMS Mass spectrum of compound **4**

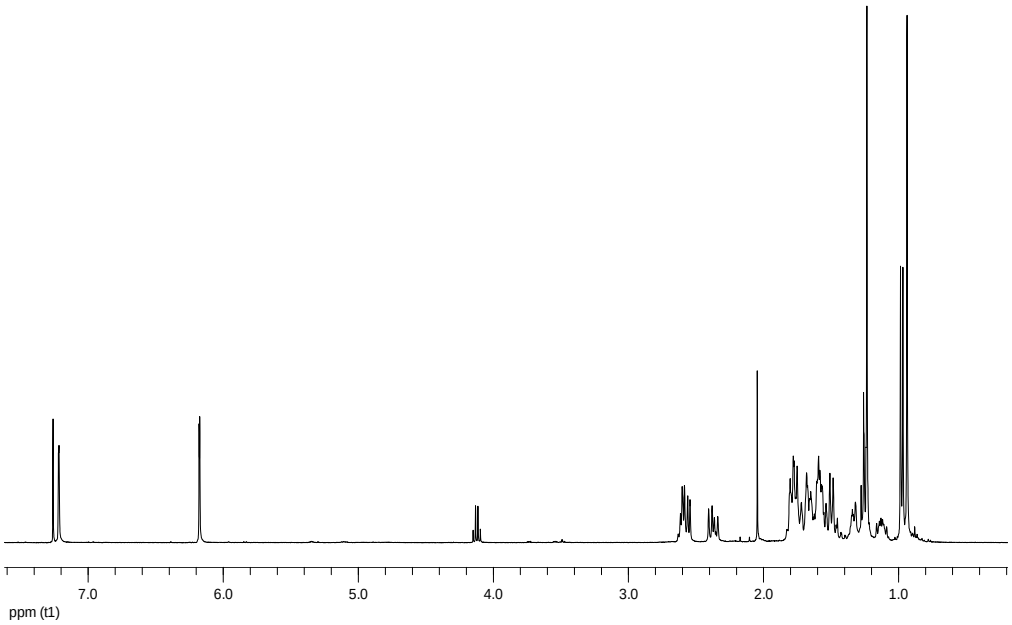

Figure A.27 ^{1}H NMR (400 MHz) spectrum of compound **5** ($CDCl_3$)

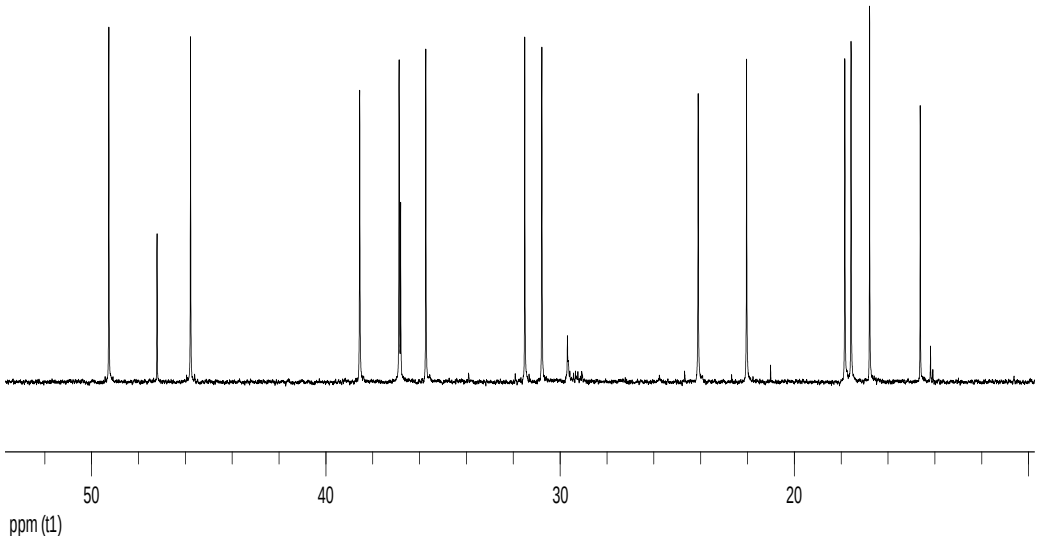

Figure A.28 ^{13}C NMR (400 MHz) spectrum of compound **5** ($CDCl_3$)

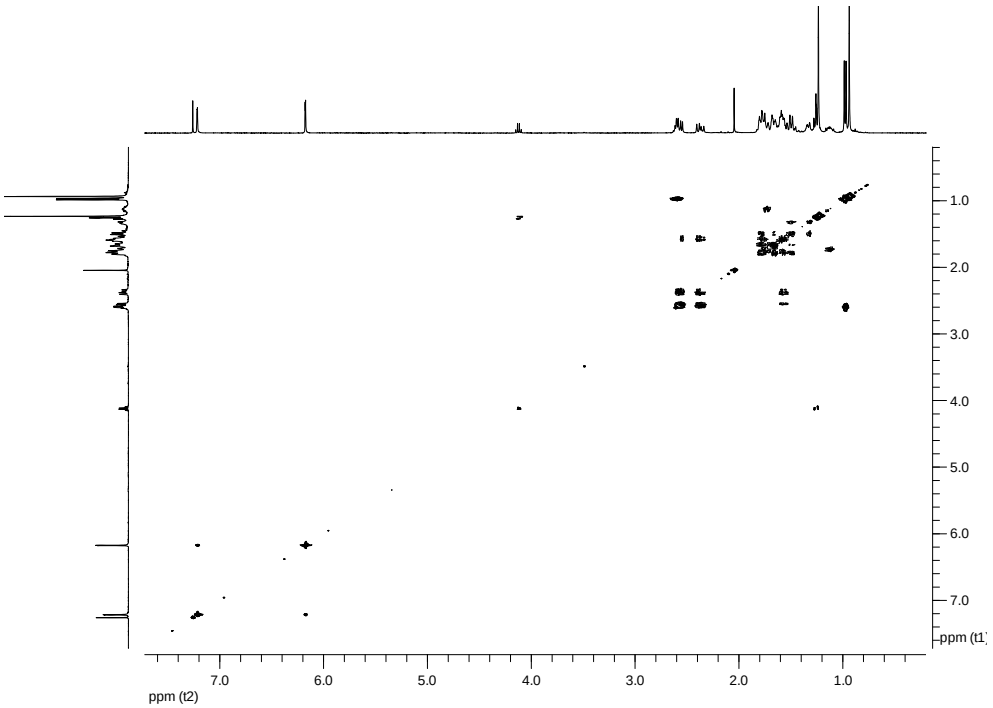

Figure A.29 COSY (400 MHz) spectrum of compound **5** ($CDCl_3$)

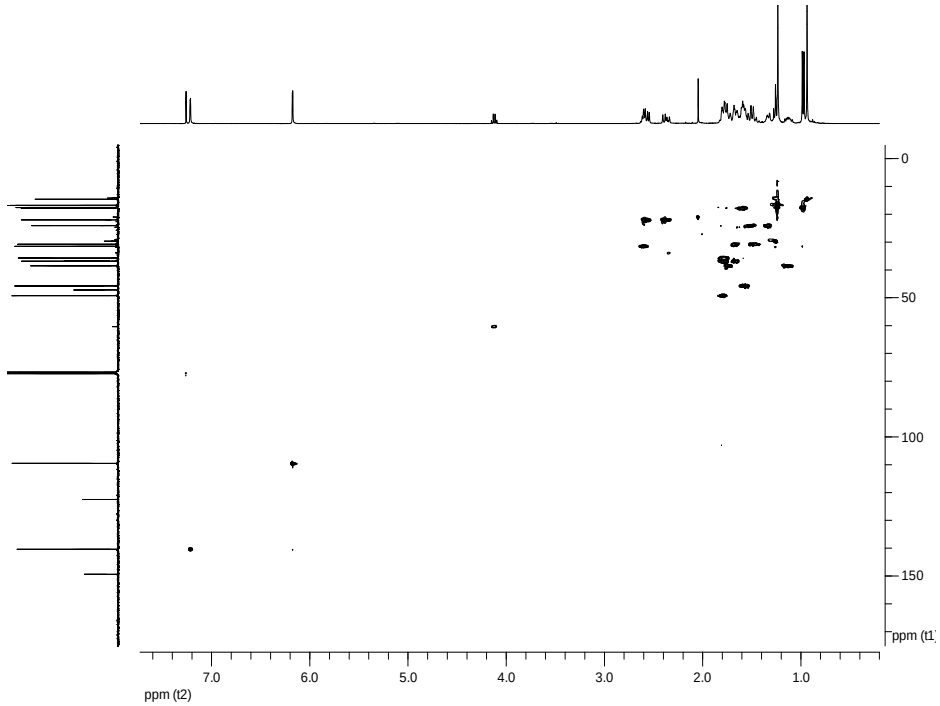

Figure A.30 HSQC (400 MHz) spectrum of compound **5** ($CDCl_3$)

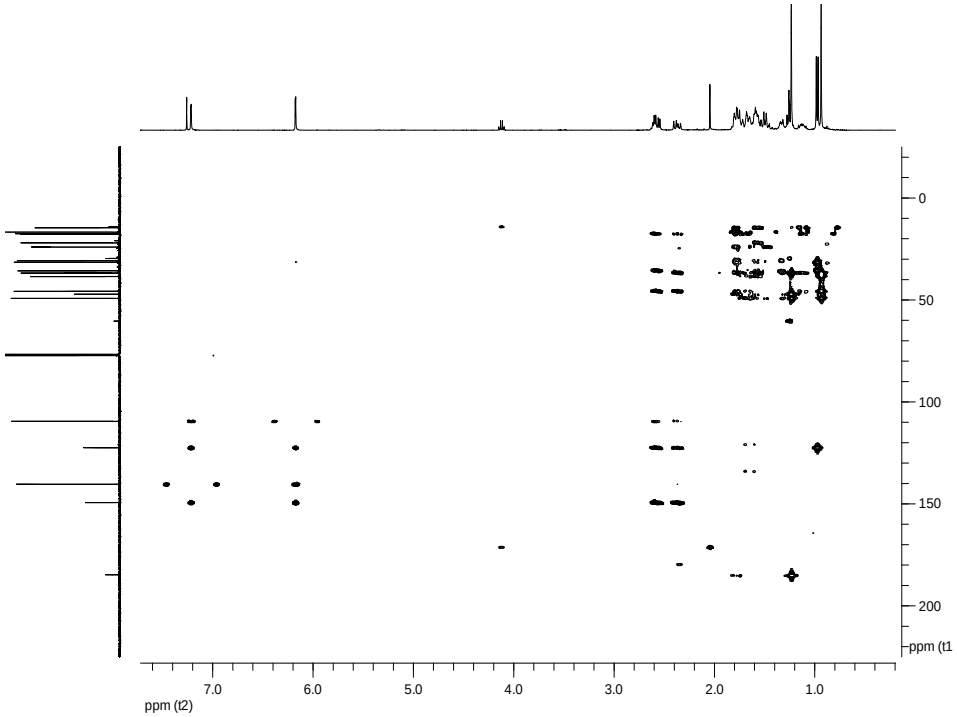

Figure A.31 HMBC (400 MHz) spectrum of compound **5** ($CDCl_3$)

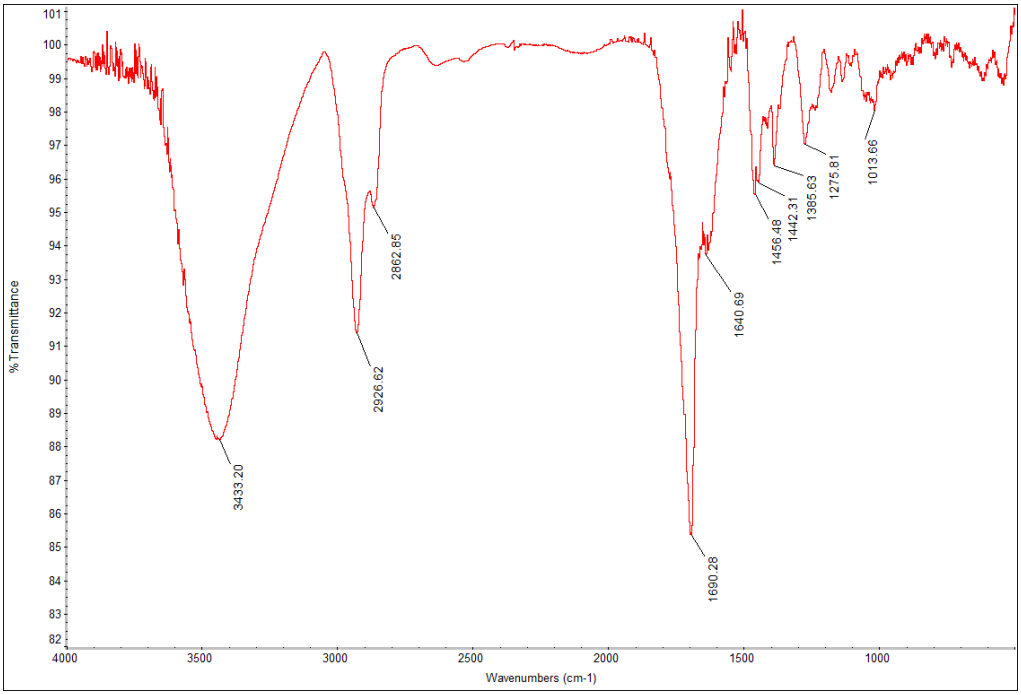

Figure A.32 IR spectrum of compound **5** (KBr)

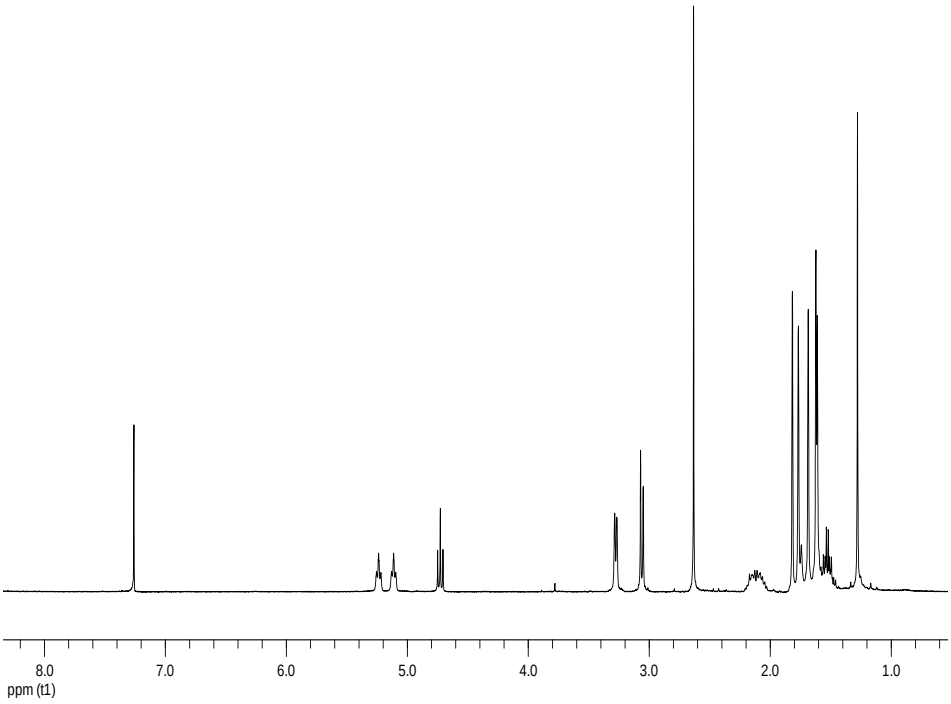

Figure A.33 ^{1}H NMR (400 MHz) spectrum of compound **6** ($CDCl_3$)

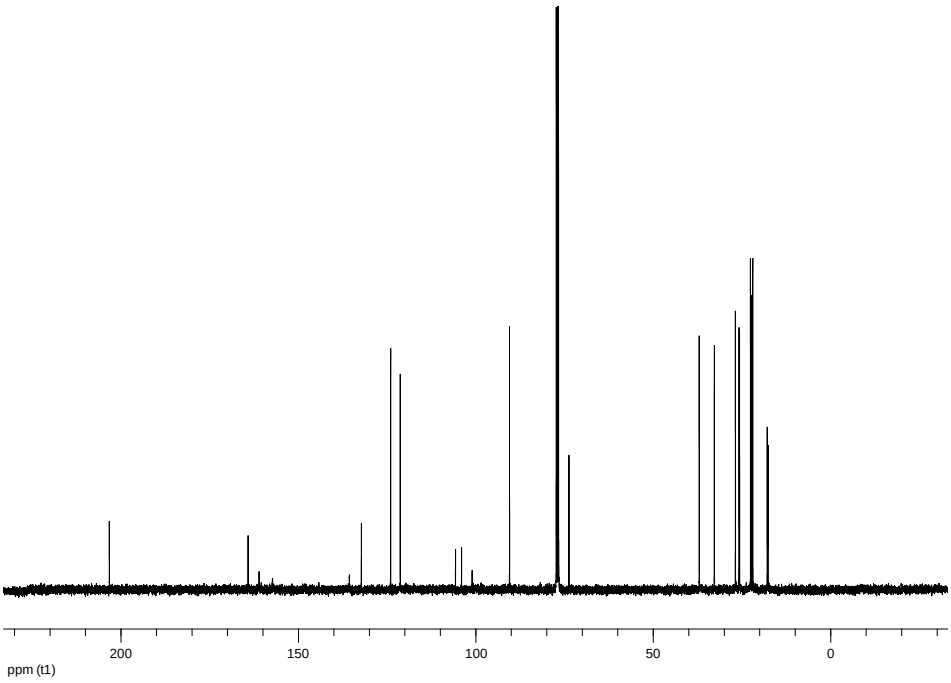

Figure A.34 ^{13}C NMR (400 MHz) spectrum of compound **6** ($CDCl_3$)

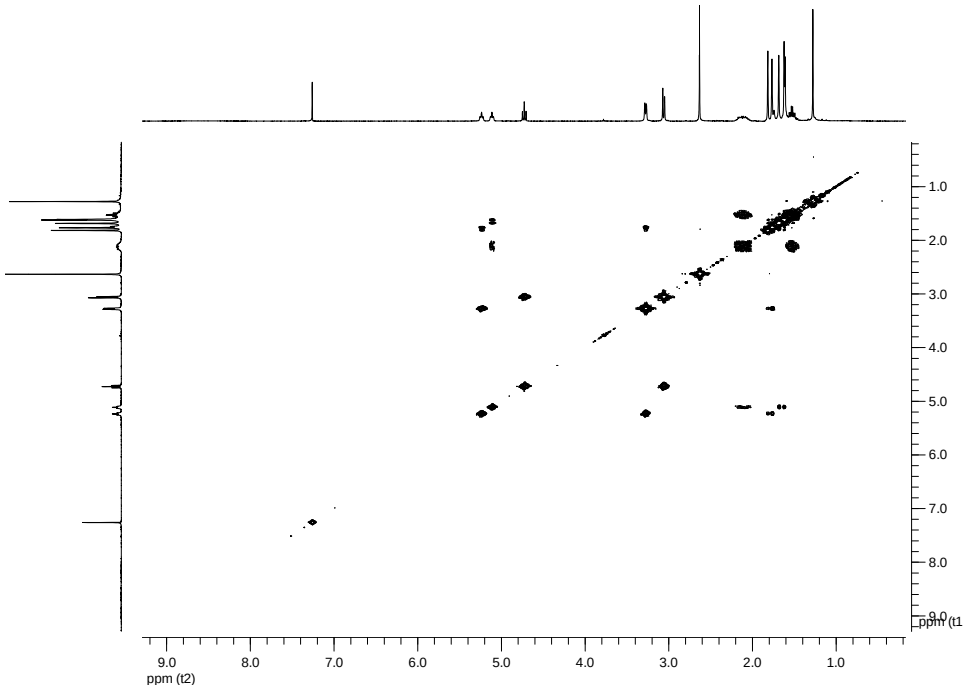

Figure A.35 COSY (400 MHz) spectrum of compound **6** ($CDCl_3$)

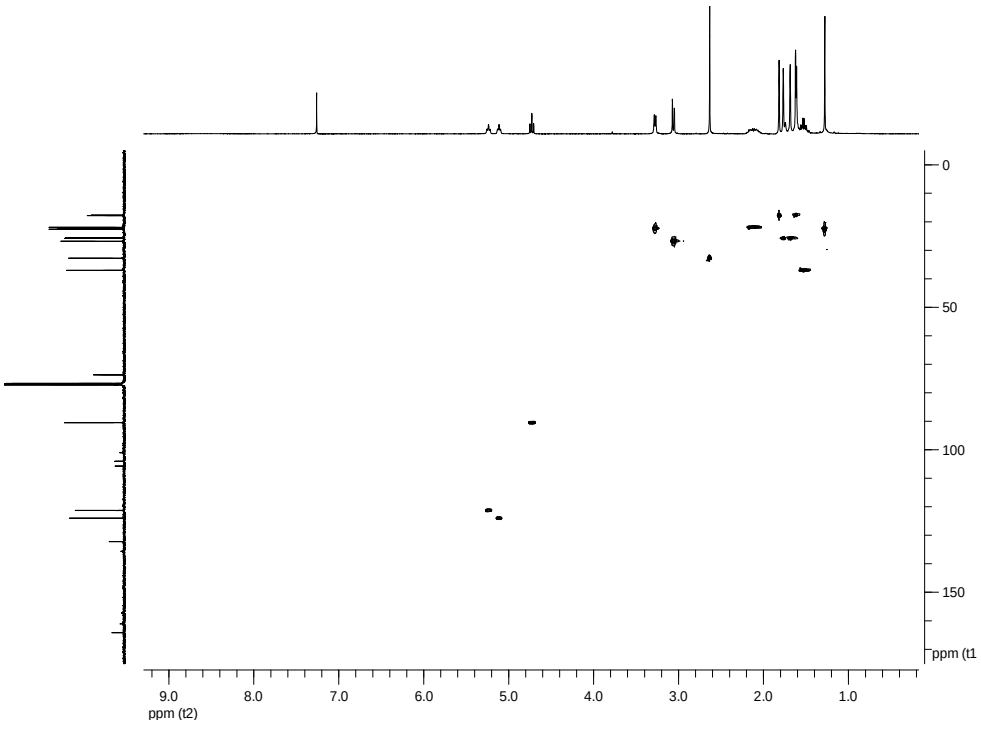

Figure A.36 HSQC (400 MHz) spectrum of compound **6** ($CDCl_3$)

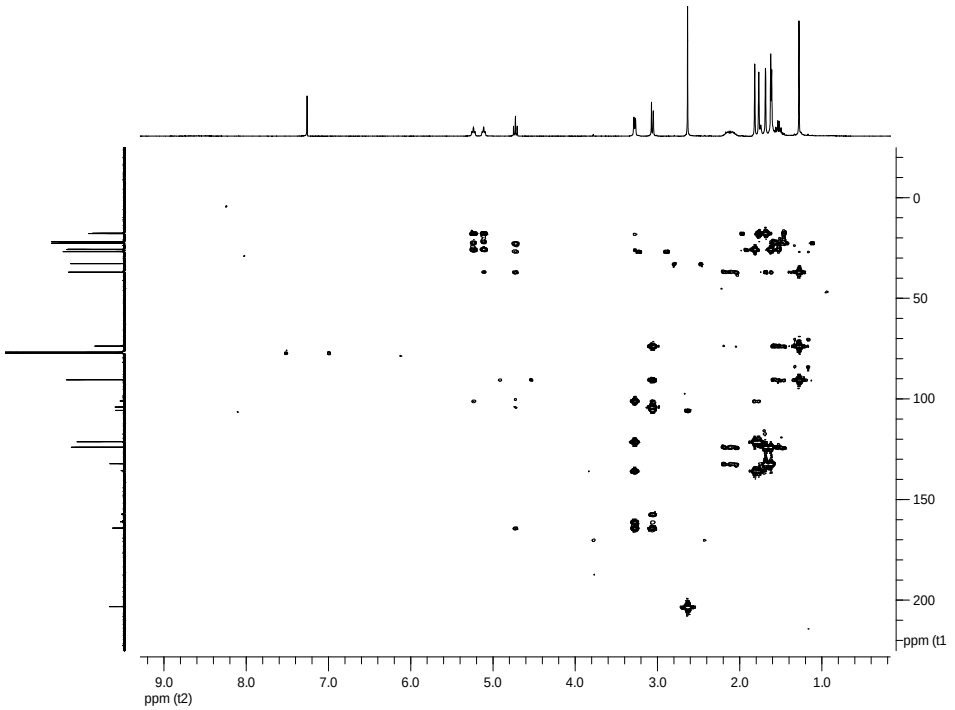

Figure A.37 HMBC (400 MHz) spectrum of compound **6** ($CDCl_3$)

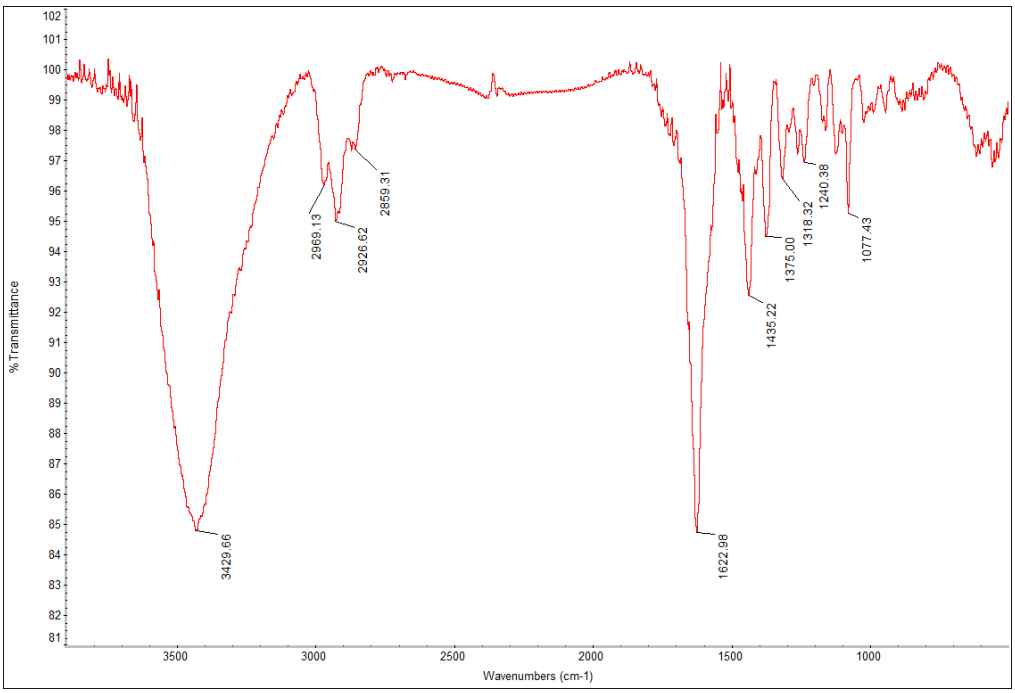

Figure A.38 IR spectrum of compound **6** (KBr)

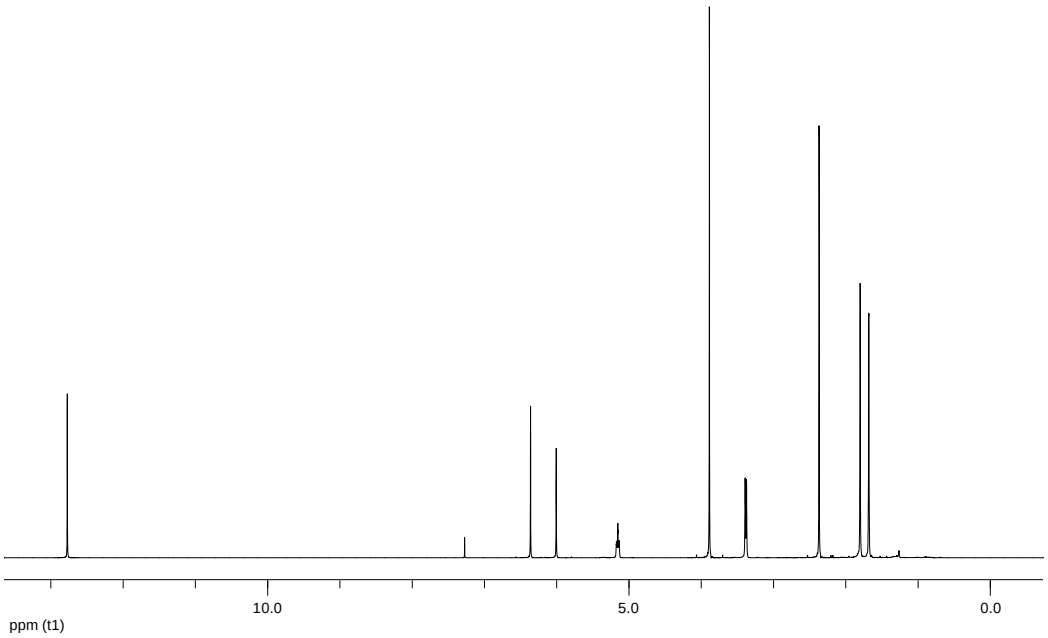

Figure A.39 ^{1}H NMR (400 MHz) spectrum of compound **7** ($CDCl_3$)

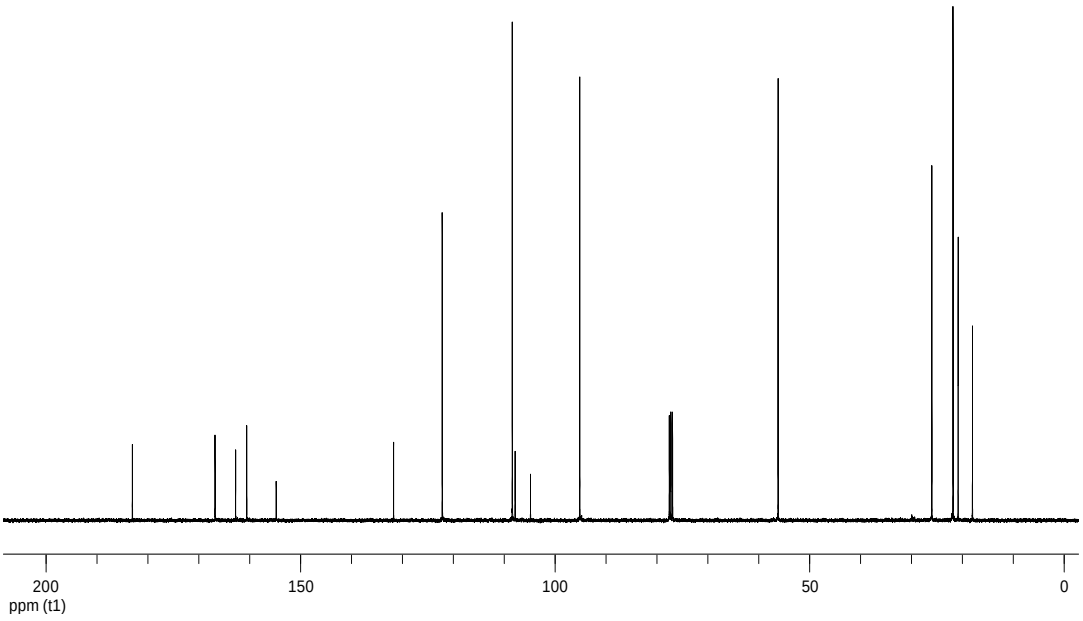

Figure A.40 ^{13}C NMR (400 MHz) spectrum of compound **7** ($CDCl_3$)

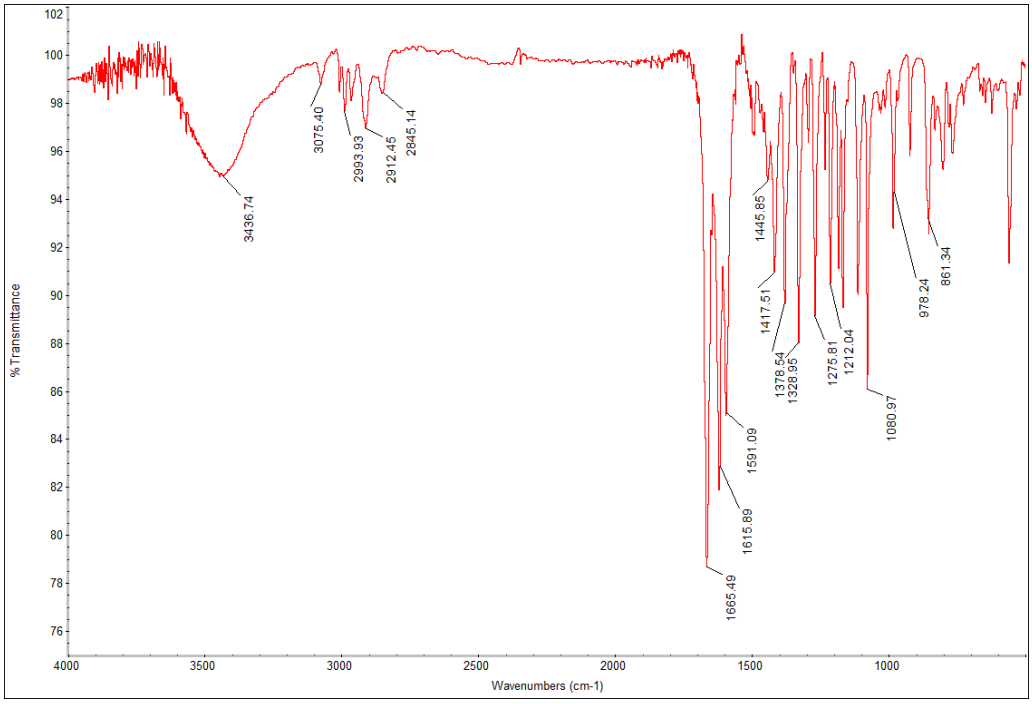

Figure A.41 IR spectrum of compound **7** (KBr)

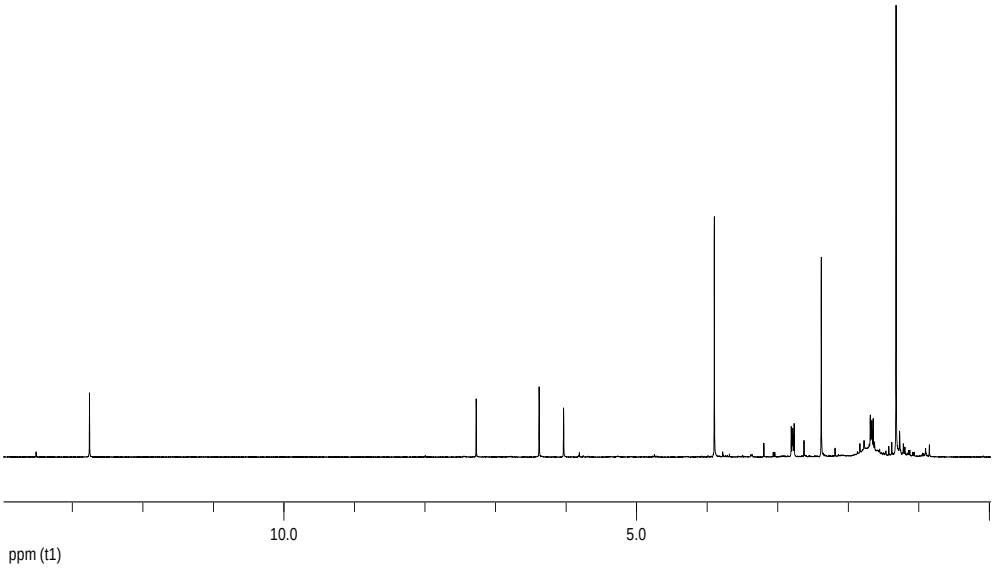

Figure A.42 ^{1}H NMR (400 MHz) spectrum of compound **8** ($CDCl_3$)

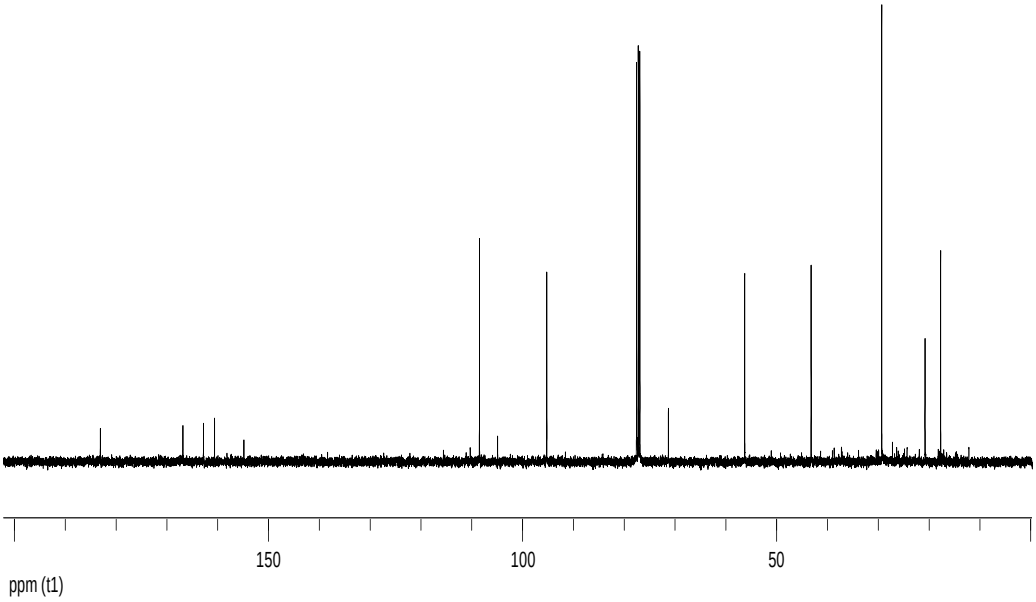

Figure A.43 ^{13}C NMR (400 MHz) spectrum of compound **8** ($CDCl_3$)

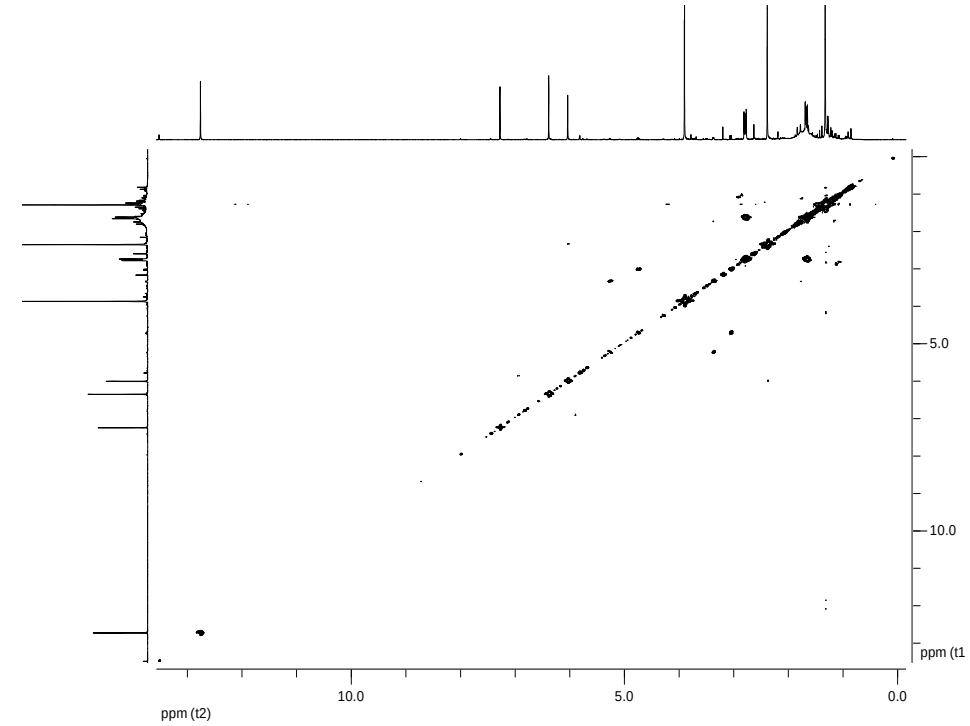

Figure A.44 COSY (400 MHz) spectrum of compound **8** ($CDCl_3$)

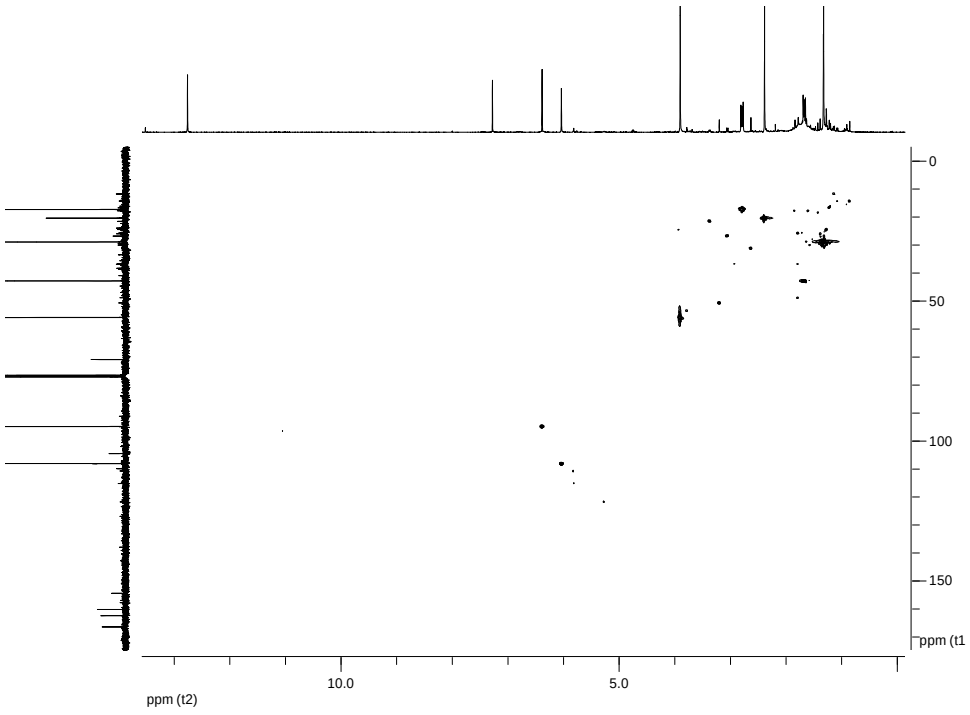

Figure A.45 HSQC (400 MHz) spectrum of compound **8** ($CDCl_3$)

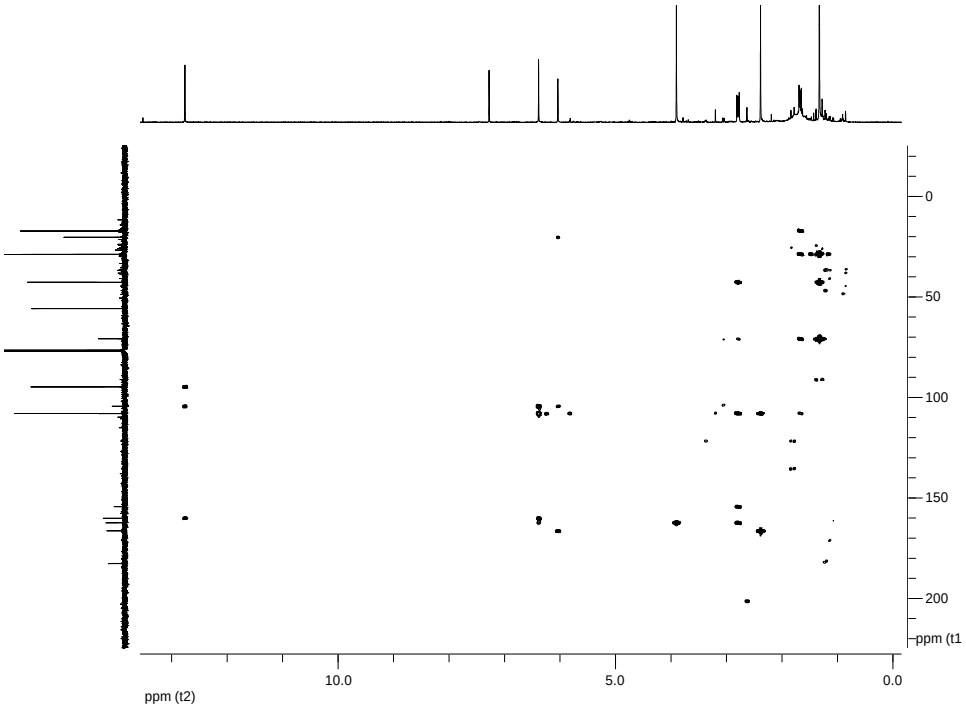

Figure A.46 HMBC (400 MHz) spectrum of compound **8** ($CDCl_3$)

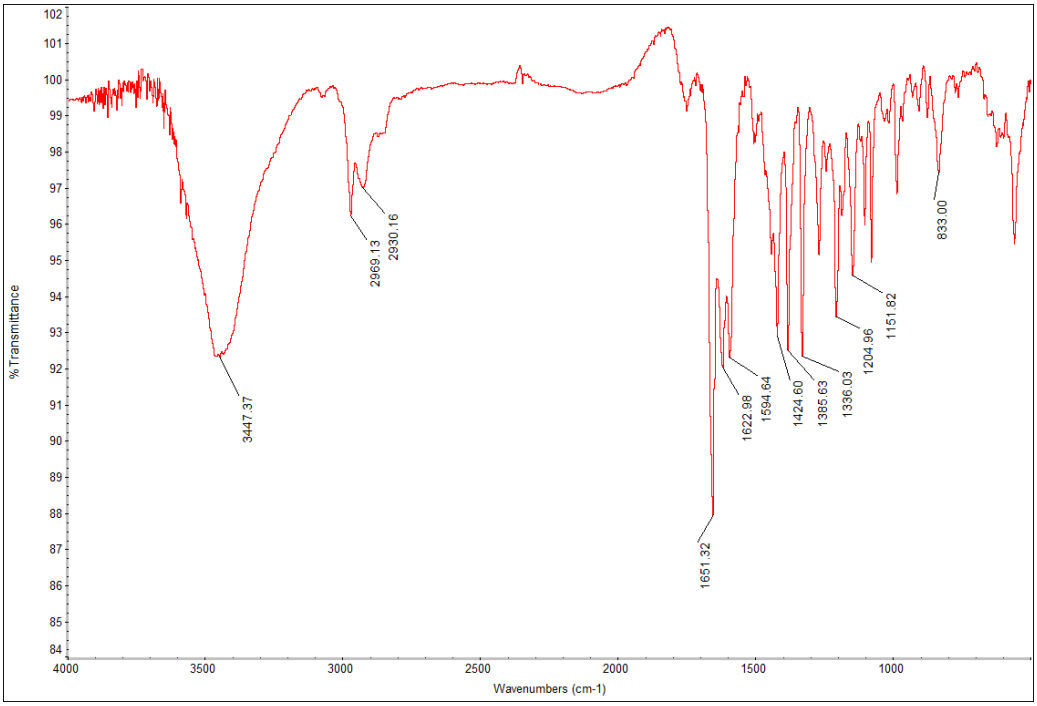

Figure A.47 IR spectrum of compound **8** (KBr)

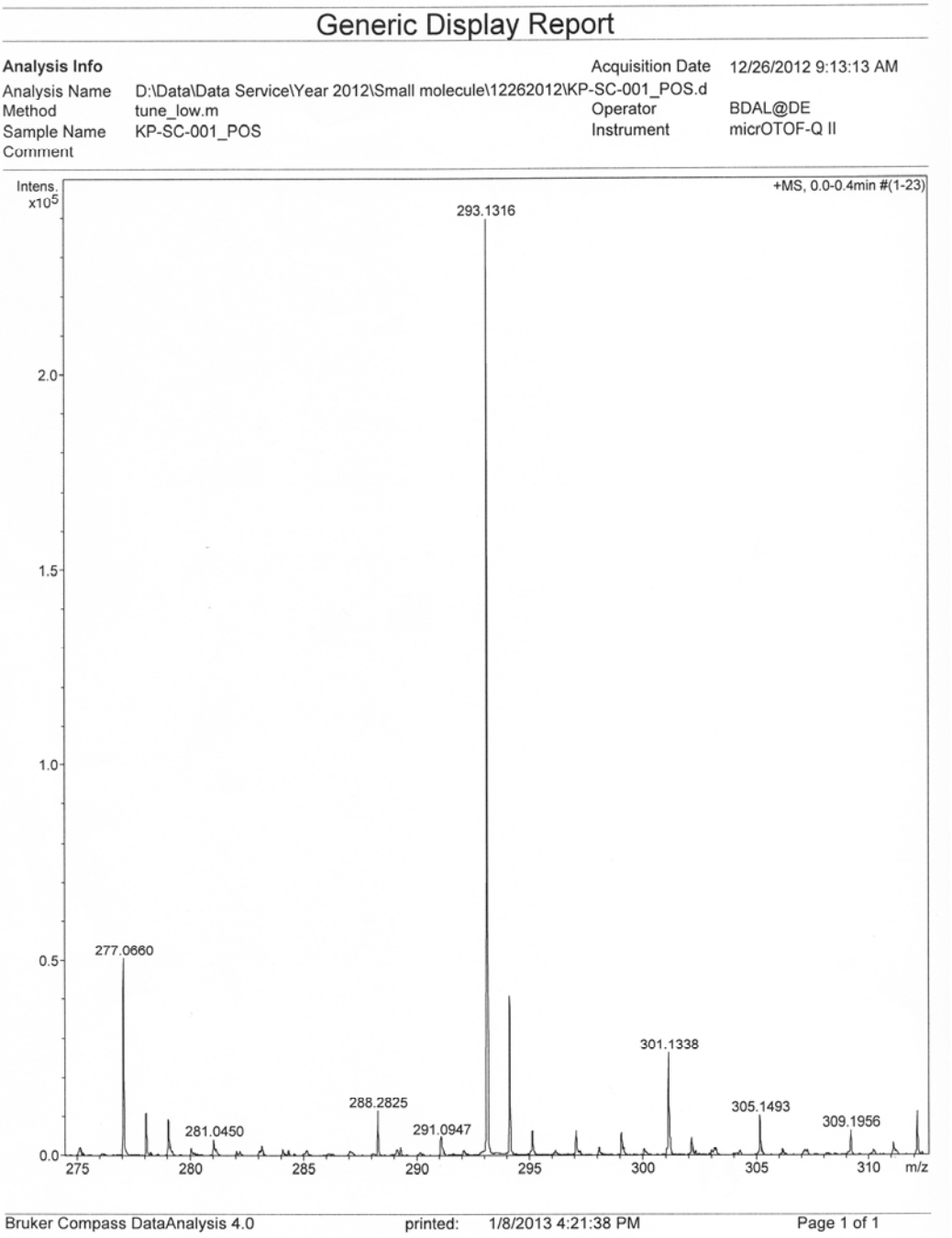

Figure A.48 HRESIMS Mass spectrum of compound **8**

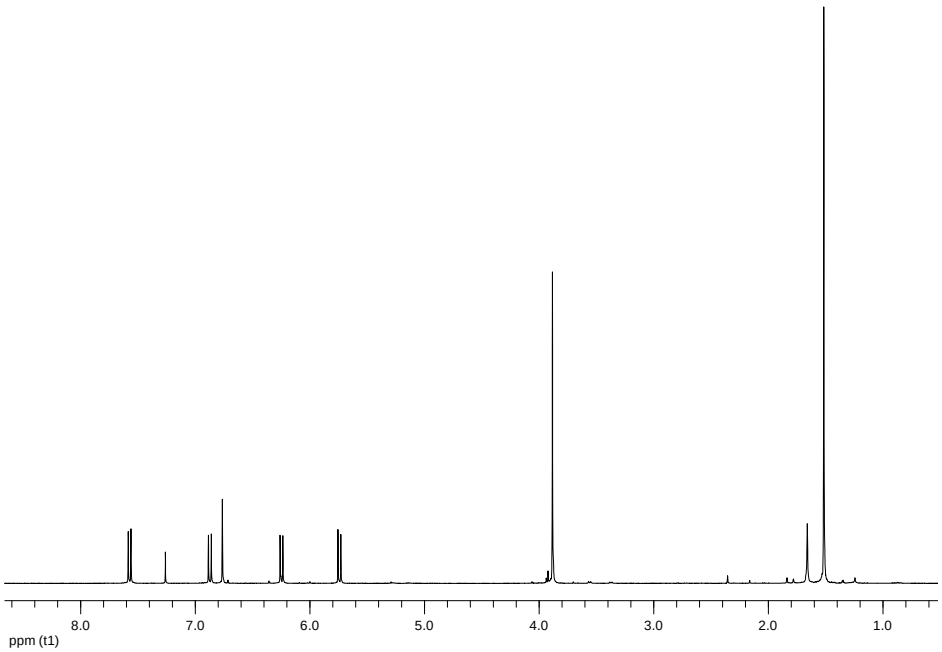

Figure A.49 ^{1}H NMR (400 MHz) spectrum of compound **9** ($CDCl_3$)

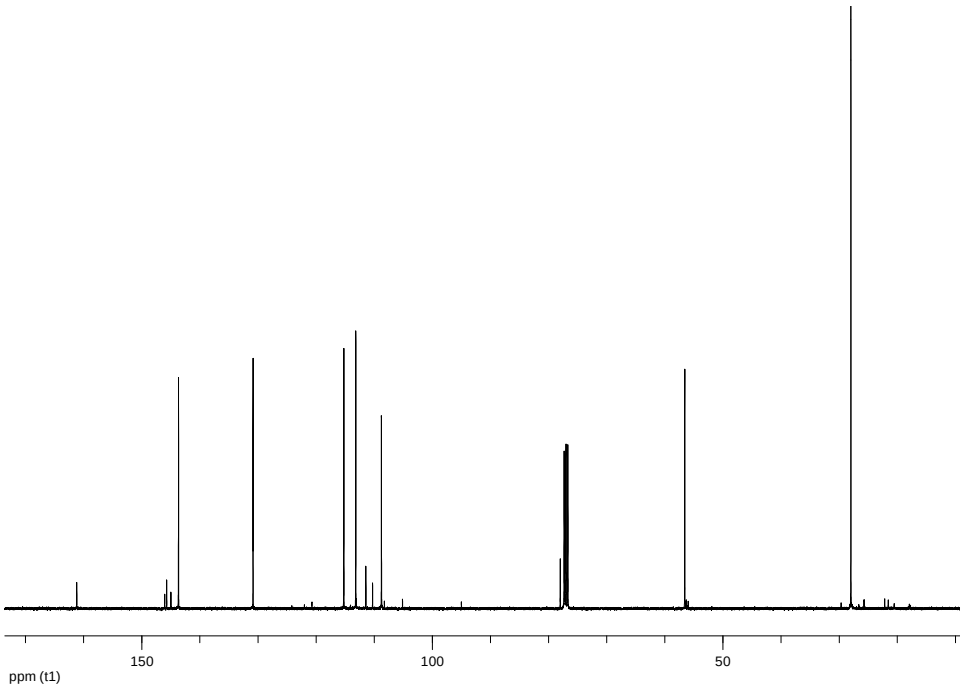

Figure A.50 ^{13}C NMR (400 MHz) spectrum of compound **9** ($CDCl_3$)

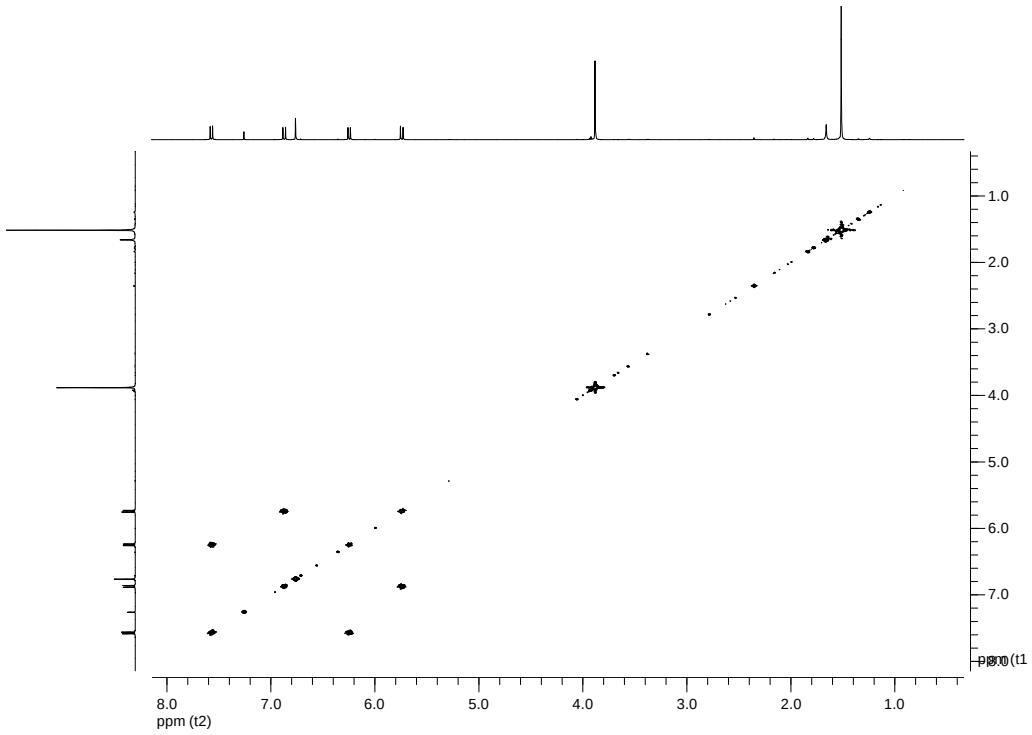

Figure A.51 COSY (400 MHz) spectrum of compound **9** ($CDCl_3$)

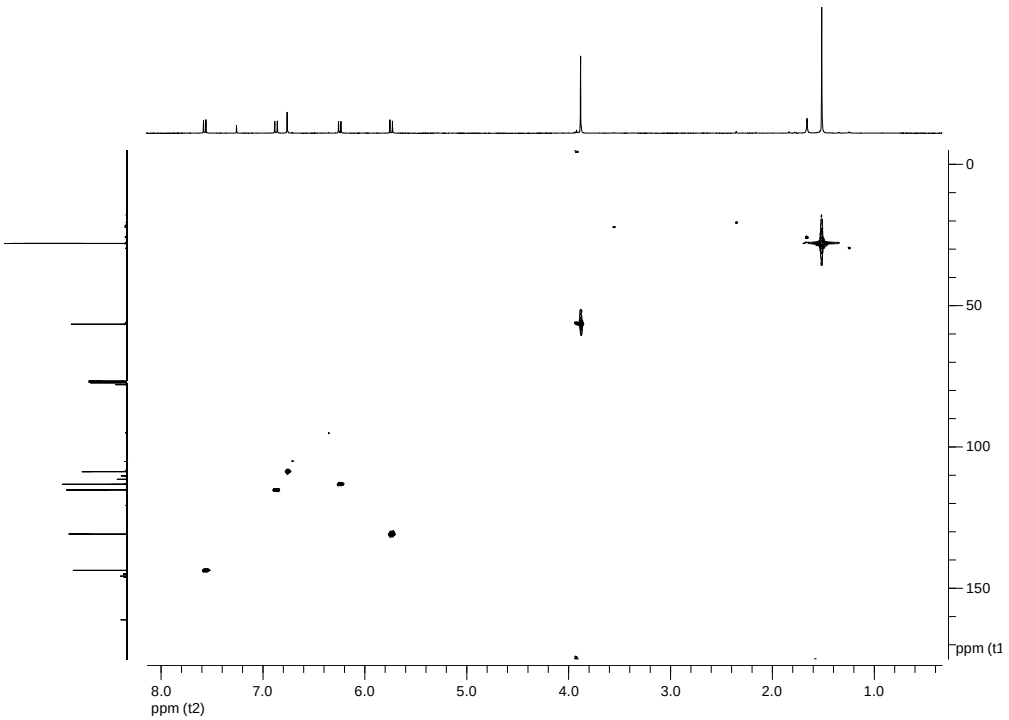

Figure A.52 HSQC (400 MHz) spectrum of compound **9** ($CDCl_3$)

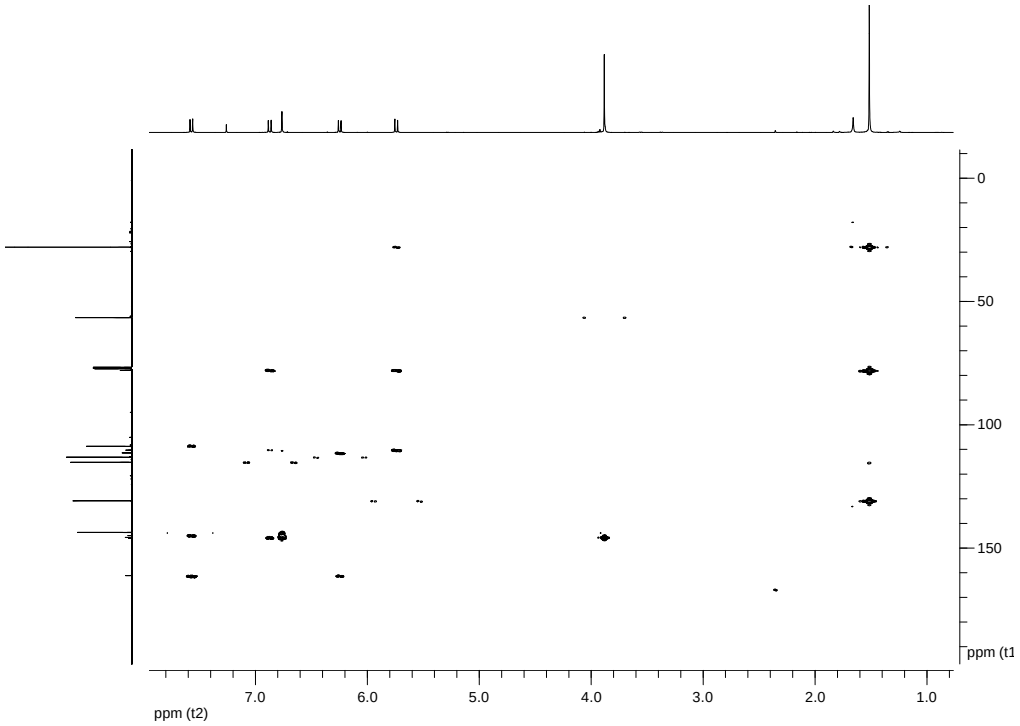

Figure A.53 HMBC (400 MHz) spectrum of compound **9** ($CDCl_3$)

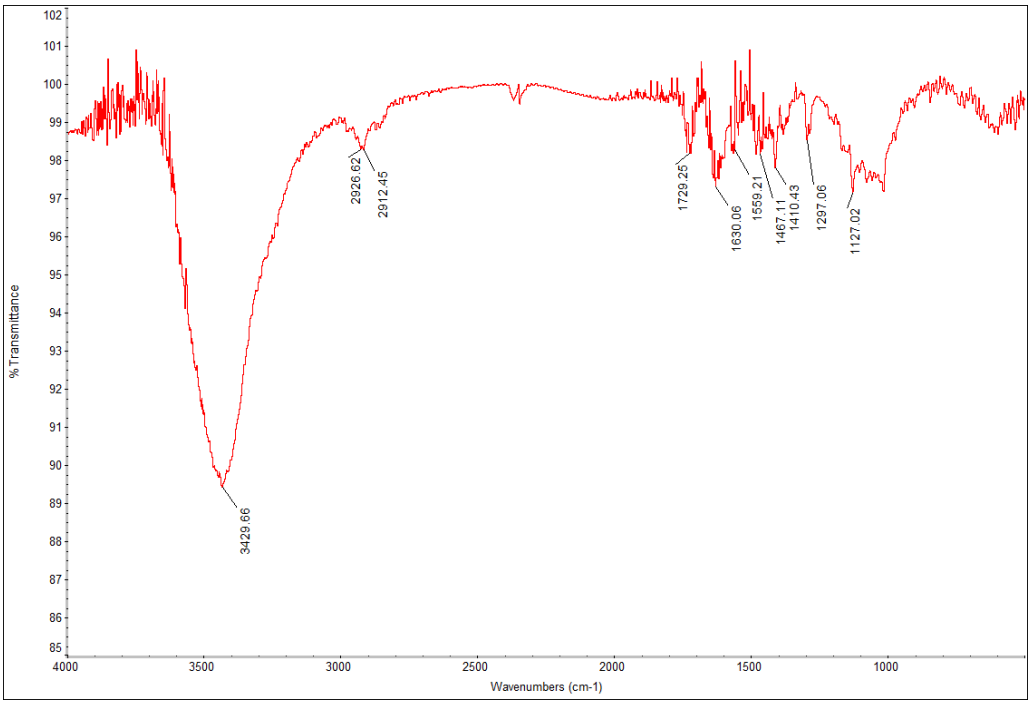

Figure A.54 IR spectrum of compound **9** (KBr)

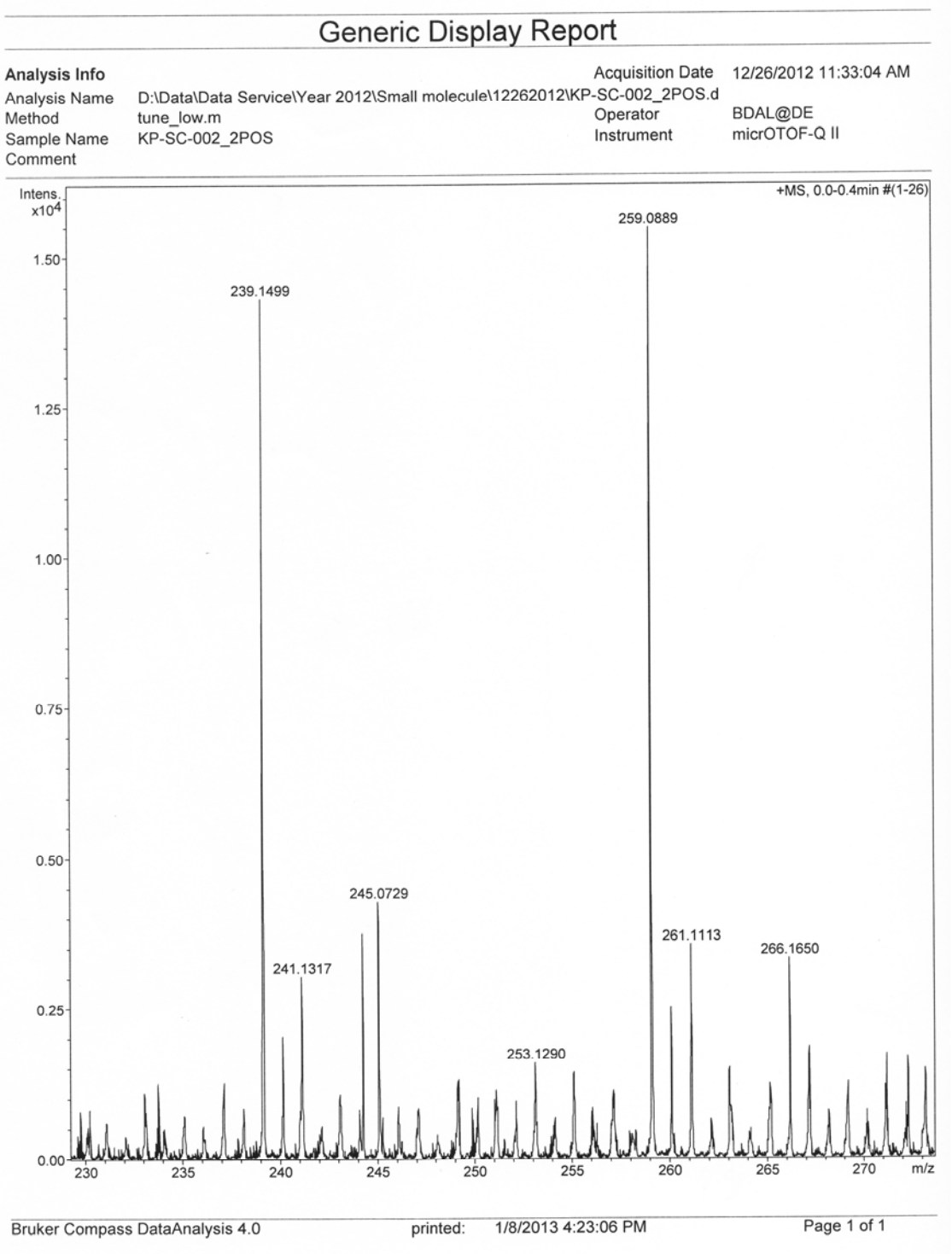

Figure A.55 HRESIMS Mass spectrum of compound **9**

VITA

Miss Siwattra Choodej was born on October 14, 1987 in Nongkhai, Thailand. I was graduated with Bachelor's Degree of Science in Chemistry from Faculty of Science, Chulalongkorn University, in 2009.

Present address is 100/484 Ramintra Rd., Khannayao, Bankok, Thailand, 10230, Tel: 090-9837496.